

# Realising the Artificial Chemical Cell with Vesicles

George Pasparakis, BSc

Thesis submitted to the University of Nottingham for  
the degree of Doctor of Philosophy

October 2008

*...to Maria*

## *Acknowledgments*

I feel truly indebted to my supervisor professor Cameron Alexander for all his guidance and inspiration throughout my studies. I would particularly like to thank Dr Sivanand Pennadam for his invaluable help during my first year in the lab and for all the initial training that enabled me to continue my studies more independently. Dr Alan Cockayne deserves a special mention for being ever so patient providing all the training in the microbiology lab. Also, I gratefully acknowledge Dr Wenxin Wang for generously sharing his knowledge in polymer synthesis.

Many thanks go to our lab technicians and especially to Christy for her help with my experimental work and her valuable assistance in solving everyday problems in the lab. Also, special thanks to my friends and colleagues in the advanced drug delivery group, Aram, Bow, Felicity, Mahmoud, Sabrina and Johannes for their company and useful discussions on a daily basis.

Professor Ben Davis and his student Paul Gardner are acknowledged for providing the AI-2 and for sharing their ideas regarding the formose reaction.

Most importantly, I would like to express my gratefulness to my family, my mother Akrivi and my sister Eva for their love and support and last but not least, my partner in life Maria.

# Contents

<i>Abstract</i>	i
<i>List of Tables and Figures</i>	ii-vi

## *Chapter 1. Polymeric Biomedical Materials – Polymer-Cell Interactions*

1. Introduction	1
1.1. Living Radical Polymerization	4
1.1.1. Atom transfer radical polymerization (ATRP)	4
1.1.2. Radical addition-fragmentation termination polymerization (RAFT)	6
1.1.3. Elements of the persistent radical effect	8
1.1.4. Polymer topology and architecture	9
1.2. Polymer design for bacterial detection	10
1.2.1. Protein engineering	17
1.2.2. Bacterial Detection	18
1.2.3. Bacterial capture and detection with imprinted polymers	19
1.2.4. Quantum Dots	21
1.3. Analysis	26
1.4. Polymer-cell interactions – Principles of bacterial adhesion	27
1.5. Aim of the PhD	32
1.6. References	34

## *Chapter 2. Control of bacterial aggregation by thermoresponsive polymers*

2. Introduction	41
2.1. Materials and Methods	47
2.1.1. Instrumentation	47
2.1.2. Polymers syntheses	49

2.1.3. a1, a2. Polymer synthesis (i)	49
2.1.4. b1. Sugar derivatisation (ii)	50
2.1.5. P2-1. Deprotection of AcGlc (iii)	50
2.1.6. P2-2. Derivatisation (iv)	50
2.1.7. Cloud point measurements	51
2.1.8. Anthrone assay	51
2.1.9. Alizarin Red S (AR) assay	51
2.1.10. AR assay for reversible Glc-PBA binding	52
2.1.11. Concanavalin A (Con A) assay	52
2.2. Results and Discussion	53
2.2.1. Synthesis of Polymer P2-1	53
2.2.2. Synthesis of Polymer P2-2	55
2.2.3. Polymer characterization	56
2.2.4. Lower critical solution temperature measurements	64
2.2.4.1. Effect of comonomers hydrophilicity on LCST	64
2.2.4.2. Effect of Salt presence on LCST	66
2.2.5. AR-Glc Reversible binding	68
2.2.6. Glycopolymer biorecognition using lectins	75
2.2.7. Polymer-bacteria interactions	78
2.3. Conclusions	85
2.4. References	86

### *Chapter 3. Sweet-talking block copolymer vesicles*

3. Introduction	92
3.1. Materials and Methods	96
3.1.1. Materials and Instrumentation	96
3.1.2. Polymer Synthesis	97

3.1.2.1. Synthesis of polymer P3-1	97
3.1.2.2. Synthesis of polymer P3-2	98
3.1.3. Bacteria-vesicles interactions	98
3.1.4. Critical micelle concentration	99
3.1.5. Dynamic light scattering	99
3.1.6. Microscopy	99
3.1.7. Con A assay	100
3.1.8. Bacteria-Vesicles interactions and competition experiments	100
3.1.9. Interactions of ethidium bromide loaded vesicles with bacteria	100
3.2. Results and Discussion	101
3.2.1. Polymers syntheses and characterization	101
3.2.2. LCST of polymers	108
3.2.3. Self assembly properties	111
3.2.4. Microscopy	113
3.2.5. Biorecognition properties (con A)	115
3.2.6. Interactions with E. coli	118
3.2.7. Molecular transport	121
3.3. Conclusions	124
3.4. References	124

## *Chapter 4. Quorum Quenching Polymers*

4. Introduction	131
4.1. Materials and methods	137
4.1.1. Materials and Instrumentation	137
4.1.2. Synthesis of acrylamidophenylboronic acid (AAPBA)	138
4.1.3. Synthesis of Poly(NIPAM-co-APBA)	139

4.1.4. Cloud point measurements	139
4.1.5. AR assay for reversible binding to Poly(NIPAM-co-APBA)	140
4.1.6. AR assay for reversible PBA binding to diol containing polymers (PVA, GEMA and GAL)	140
4.1.7. AB Medium	140
4.1.8. <i>Vibrio harveyi</i> BB170 and MM32 culture	140
4.2. Results and discussion	141
4.2.1. Synthesis and scavenging properties of poly(NIPAM-coAPBA)	141
4.2.2. Polyhydroxyl quorum quenchers	148
4.3. Conclusions	154
4.4. References	155

## *Chapter 5. Concluding Remarks – Future Prospects*

5.1. Introduction	160
5.2. References	170
<i>List of Publications</i>	172

## *Abstract*

Responsive biomedical materials span a plethora of applications in the biomedical field, from stents, hydrogels, degradable implants to drug delivery systems, and are in constant further development to give properties that ultimately improve the quality of life and prevent disease. In an effort to develop cell-interacting constructs we sought to synthesize polymers with bioresponsive and even “life-like” properties. By exploiting living polymerization techniques we aim to build self-assembled capsule-mimicking structures (i.e. vesicles) that can serve as prototype copycats of natural cell membranes. Also, we aim to establish a primitive communication platform of the artificial structures with their natural counterparts (i.e. bacterial cells) by using the “glyco-code” as a means of biochemical language.

First, model thermoresponsive polymers are utilized that bear carbohydrate moieties to study polymer-cell interactions via multivalency and ligand-receptor interactions. The glycopolymers were found to induce bacterial aggregation of a specific bacterial strain through specific molecular recognition effects.

In chapter three, block-copolymer vesicles are synthesized that comprise sugar groups on their coronae and also interact with bacteria through multiple specific ligand-receptor interactions. Also, molecular transport of a model from the vesicles to the bacterial cells is facilitated by discrete vesicle-bacteria complex formation.

Chapter four explores the communication networks employed by bacterial cells, that is quorum sensing, and simple polymers are tested as molecular quorum quenchers that modulate the quorum sensing response of bacteria through autoinducers scavenging.

Ultimately, we seek for an integrated platform to set up an “imitation game” where artificial entities, such as the polymer vesicles, can act as prototype cell-mimics that can actively intervene to the bacterial communication networks. Aspects of the principles and practical requirements to prove the concept are discussed in the final chapter.

# List of Tables and Figures

## Chapter 1

**Table 1-I** Some examples of polymers applications in the biomedical field.

**Figure 1-1.** The general mechanism of ATRP.

**Figure 1-2.** The general mechanism of RAFT polymerization.

**Figure 1-3.** a) Radical generation, the cross reaction between the transient (R) radical with the persistent one (Y) and the self-termination of the former and b) Dissociation of the R-Y to form the radical species and the possible reactions of the latter.

**Figure 1-4.** Advanced architectures accesible with modern polymerization methods.

**Table 1-II** Attachment sites for bacterial binding via ligand-receptor interactions.

**Figure 1-5.** Left - structures of poly-glyco-ene-yne materials prepared by Disney et al. Right, visualization of *E. coli* strains after incubation with mannosylated polymer 2a; mutant strain (left) and mannose-binding strain (right).

**Figure 1-6.** Amphiphilic polyphenylenes prepared by Kim et al. for interaction with *E. coli*. Micellar (a) and tubular (b) structures interacting with bacterial fimbrils.

**Figure 1-7.** Schematic of the imprinting process for spores used by Harvey et al..

**Figure 1-8.** Functionalised nanocrystals and magnetic beads for detection and binding of proteins and cells via surface-displayed glycopolymers.

**Figure 1-9.** Surface modification of bacteria through multivalent interactions with vancomycin-functionalised synthetic polymers. Incorporation of a fluorescent antigen on the synthetic polymer promotes antibody recognition and subsequent opsonisation and phagocytosis of the bacteria, while simultaneously allowing monitoring of detection and binding events.

## Chapter 2

**Figure 2-1.** Synthesis of Polymers. i. THF, AIBN, 65 °C, 18 h ii. CHCl<sub>3</sub>/CH<sub>2</sub>Cl<sub>2</sub> (3/2), BF<sub>3</sub>Et<sub>2</sub>O, β-AcGlc, 12 h iii. MeOH, MeONa (cat.) 90 min. iv. HEPES pH 4.5, GlcN, EDC, NHS (cat.) 12 h.

**Figure 2-2.** Reaction mechanism of the anomeric -OH with a nucleophile under acidic conditions.

**Figure 2-3.** Deacetylation mechanism of protected -OHs polymer-bound glucose.

**Figure 2-4.** Amide formation via carbodiimide coupling: carboxylate **1** attacks the diimide **3** that has an electrondeficient carbon and forms the highly reactive O-acylisourea **4**. Then addition of the amine **2** results in formation of the amide bond **6** and gives the stable R<sub>2</sub>-urea byproduct **5**.

**Figure 2-5.** <sup>1</sup>H NMR (in D<sub>2</sub>O) was used to determine the relative ratios of the monomers after polymerization and the degree of sugar derivatisation for **P2-1**. Assignments of characteristic resonances were based on analogous spectral data for glycopolymers [24].

**Figure 2-6.** FTIR spectra. **a1**, 3400 cm<sup>-1</sup> (O-H), 3000 cm<sup>-1</sup> (N-H, amide), 1648 cm<sup>-1</sup> (C=O, amide), 1535 cm<sup>-1</sup> (N-H, amide); **b1** 3400 cm<sup>-1</sup> (O-H), 3000 cm<sup>-1</sup> (N-H, amide), 1728 cm<sup>-1</sup> (C=O, acetate), 1648 cm<sup>-1</sup> (C=O, amide), 1535 cm<sup>-1</sup> (N-H, amide) 1056 cm<sup>-1</sup> (C-O-C); **P2-1** as in **b1** negligible acetate peak (1728 cm<sup>-1</sup>).

**Figure 2-7.** <sup>1</sup>H NMR of **P2-2** and its precursor polymer.

**Figure 2-8.** FTIR spectra: **a2**, 3400 cm<sup>-1</sup> (O-H), 3000 cm<sup>-1</sup> (N-H, amide), 1728 cm<sup>-1</sup> (C=O, carboxyl), 1648 cm<sup>-1</sup> (C=O, amide), 1535 cm<sup>-1</sup> (N-H, amide); **P2-2**, as in **a2** without carboxyl (1728 cm<sup>-1</sup>).

**Table 2-I** Summary of degree of sugar derivatization of **P2-1** and **P2-2**.

**Figure 2-9.** LCST curves of **P2-1** and **P2-2** with their precursors.

**Figure 2-10.** Intermolecular association of pendant carboxylate groups that influence the LCST onset.

**Figure 2-11.** Effect of PBS (salt-rich saline) on the LCST behaviour of the polymers and their precursors.

**Figure 2-12.** The salt effect on poly(N-isopropylacrylamide), (retrieved from reference [31]).

**Figure 2-13.** The three component assay comprising AR, PBA and diol moieties of the polymer-pendant glucose.

**Figure 2-14.** Fluorescence spectra of P2-1 and P2-2 using AR and PBA in glycine buffer (0.1 M, pH 9.3)

**Figure 2-15.** Left, Absorbance curve of **P2-1** below and above LCST and on the right, visual inspection of diol binding and release below and above LCST.

**Figure 2-16.** The dynamic equilibria of phenylboronic acid with a diol molecule (adapted from reference [28]).

**Figure 2-17.** Reversible binding assay of **P2-1** and **P2-2** with AR and PBA in PBS pH 7.4.

**Figure 2-18.** Control fluorescence experiments showing negligible increase in fluorescence maxima of alizarin red (AR) at 578 nm with and without thermoresponsive polymers over assays of varying temperature (AR excitation energy, 460 nm - PBA = phenylboronic acid).

**Figure 2-19.** Schematic showing the complex formation between the tetrameric lectin with the polymer bound ligand, that is glucose.

**Figure 2-20.** Polymer interaction with Con A. Gradual increase in turbidity due to polymer-Con A complexation, as measured by UV/Vis spectrometry at 550 nm.

**Figure 2-21.** Quantitative estimation of protein “scavenging” by polymers **P2-1** and **P2-2**.

**Figure 2-22.** Polymer-bacteria aggregates using polymers **P2-1** and **P2-2** as tested with E. coli MG1655pGFP (scale is 10  $\mu\text{m}$ , O.D. 0.7-0.8).

**Figure 2-23.** Typical images of bacterial aggregates in presence of **P2-1** or **P2-2** at room temperature. Extensive bacterial aggregation of fimH expressing E. coli upon addition of thermoresponsive glycopolymers at temperatures below polymer LCST (white bar: 25  $\mu\text{m}$  O.D 0.7-0.8).

**Figure 2-24.** Polymer (10 mg/mL)-glucose competition assay; gradual reduction of cluster size due to glucose increase (white bar is 10 $\mu\text{m}$ , O.D. 0.8)

**Figure 2-25.** Reduction in size of polymer-bacteria aggregates with increasing amounts of glucose.

**Figure 2-26.** Retention of polymer-bacteria aggregates in presence of sucrose (non-competing ligand for fimH).

**Figure 2-27.** Control experiments using a mutant E. Coli strain without fimH and polymers **P2-1** and **P2-2**. Additional control assays with precursor polymers lacking sugar segment and MG1655pGFP strain also showed negligible bacterial aggregation at room conditions (white bar: 10  $\mu$ m).

**Figure 2-28.** Control of bacterial aggregation formation by thermal oscillation across LCST in presence of **P2-1** and **P2-2**.

**Figure 2-29.** Reversible bacterial cluster assembly/disassembly in presence of **P2-1** and **P2-2** by temperature oscillation.

## *Chapter 3*

**Figure 3-1.** Syntheses of polymers (see Materials and Methods section).

**Figure 3-2.**  $^1\text{H}$  NMR allows determination of  $M_n$  values for **P3-1** and its precursor polymers. Deacetylation of the sugar moieties and subsequent growth of the DEGMA block can both be monitored.

**Figure 3-3.** GPC trace of **P3-1** and its precursor poly(AcGEMA)<sub>ATRP</sub>.

**Figure 3-4.**  $^1\text{H}$  NMR of **P3-2** and its starting polymers. The PDEGMA block is present in the spectra but it was not possible to quantify growth since the signals overlap with those of the sugars on the first GEMA block [29].

**Figure 3-5.** GPC trace of **P3-2** and its precursor poly(AcGEMA)<sub>RAFT</sub>.

**Table 3-I** Properties of polymers.

**Figure 3-6.** LCST of **P3-1** and **P3-2**. Comparison with a PDEGMA homopolymer.

**Figure 3-7.** Dynamic light scattering data below and above the LCST of **P3-1** and **P3-2** [polymer=0.5mg/mL].

**Figure 3-8.** DLS data on size reduction of vesicles above the LCST of pDEGMA.

**Figure 3-9.** CMC graphs of P3-1 and P3-2 below and above LCST. Note the slight decrease in CMC values above LCST which is attributed to the complete collapsing of the PEGMA block.

**Figure 3-10.** Optical microscopy images of **P3-1** and **P3-2** (scale is 10  $\mu\text{m}$ ).

**Figure 3-11.** TEM micrographs of **P3-1** and **P3-2**. Images on the right side are digitally expanded for detail clarification (scale is 1  $\mu\text{m}$ ).

**Figure 3-12.** Interaction of glycopolymers with FITC-Con A. Images a, b depict **P3-1** and **P3-2** respectively, in phase contrast, showing the relative sizes of the vesicles, while c,d depict the same structures in confocal mode, with green fluorescence indicative of FITC-Con A (scale bars 1  $\mu\text{m}$ ).

**Figure 3-13.** The turbidity assay of **P3-1**, **P3-2** and pGEMA homopolymer with con A at the same concentrations (3 mg/mL).

**Figure 3-14.** Competition assay of con A with glucose. A) vesicles in phase contrast, b) green vesicles in fluorescence mode indicative of FITC-Con A accommodation on the coronae and c) diminishing of green colour due to addition of glucose and dissociation of the polymer bound lectin (scale is 1  $\mu\text{m}$ ).

**Figure 3-15.** Association of vesicles with bacteria: Large (>1  $\mu\text{m}$ ) P3-2 vesicles bind but do not aggregate with E. coli MG1655pGFP as shown in images (a-c) in fluorescence mode; d) no binding of E. coli Top 10 to **P3-2** vesicles is observed in phase-contrast mode.

**Figure 3-16.** Polymer-glucose competition assay. **P3-1**-E. coli aggregates before (a) and after addition of 0.05 (b), 0.5 (c), and 5 mM glucose (d).

**Figure 3-17.** Molecular transport from **P3-2** vesicles to E. coli. Image (a) shows vesicles and cells in phase-contrast mode, (b) shows the same cells in fluorescence mode; bacteria fluoresce green (GFP) and vesicles containing ethidium bromide fluoresce orange-red. Image (c) shows the same vesicle-cell partners after 30 min with bacteria now fluorescing orange-red owing to transfer of ethidium bromide. Insets in (b) and (c) show vesicles at higher image contrast and magnification for clarity. Scale bars in main figure are 1  $\mu\text{m}$ .

**Figure 3-18.** In (a) E. coli MG1655pGFP (green) and red **P3-2** vesicles loaded with ethidium bromide are seen to associate in discrete complexes. Image (b) shows the same vesicle captured after 30 minutes. Bacterium in close proximity with the vesicle turns red due to ethidium bromide transfer. Scale bars are 10  $\mu\text{m}$ .

## Chapter 4

**Table 4-I** Various autoinducers found in gram negative (left) and positive bacteria.

**Figure 4-1.** *Vibrio harveyi* quorum sensing network comprised by three autoinducers, CAI-1, HAI-1 and AI-2 [1].

**Figure 4-2.** The AI-2 originates from the precursor molecule DPD that exists in equilibrium with other rearranged forms that are also active in the biological context. The upper pathway shows the biosynthesis route for *Vibrio harveyi* whereas in the lower pathway the R-THMF is produced in *Salmonella enterica* [6, 13, 14].

**Figure 4-3.** <sup>1</sup>H NMR of poly(NIPAM-co-APBA).

**Figure 4-4.** QS control concept by smart polymers. The QS response of the bacteria is governed by the polymers activation through a temperature stimulus.

**Figure 4-5.** The structure of AI-2 and its glucose analogue.

**Figure 4-6.** LCST control experiment without addition of sugar. Effect of pH on the LCST of the polymer.

**Figure 4-7.** Cloud point curves of Poly(NIPAM-co-APBA) at varying pH (a), and in presence of glucose analogues at different pH at a, b, and c.

**Figure 4-8.** Schematic of the alizarin assay developed to probe the diol capturing/release at different temperatures around LCST.

**Figure 4-9.** Alizarin fluorescence spectra at varying temperatures in presence of the polymer (a) and visual inspection of the colorimetric change above (b) and below (c) LCST.

**Figure 4-10.** Structures of QS-capture polymers.

**Figure 4-11.** QS scavenging network (a) in comparison with Alizarin Red S (AR) and QS- analogue phenylboronic acid (PBA).

**Figure 4-12.** Left, fluorescence intensity of AR (0.01 mM) in presence of PBA (control, 1 $\mu$ M) and after addition of the polymers (2 mg/mL). Right, the same experiment but with borate instead of PBA.

**Figure 4-13.** Light production with time for *Vibrio harveyi* in the absence and presence of PVA (a), GAL (b) and GEMA (c). Bioluminescence curves in the absence of polymer are shown in red - insets show expansions of the delay time of luminescence onset.

**Figure 4-14.** Comparison of light production maxima in presence of PVA, GAL and GEMA polymers for *Vibrio harveyi* strains BB170 (a) and MM32 (b). Controls refer to light production in absence of polymers without (a) and with (b) added AI-2.

**Figure 4-15.** Growth curves for *V. harveyi* BB170. Increased O.D. is observed in the case of GAL as the latter exists as micellar dispersion.

**Figure 4-16.** Growth curves for *V. harveyi* MM32. Increased O.D. is observed in the case of GAL as the latter exists as micellar dispersion.

**Figure 4-17.** A model triblock copolymer that could act as a smart AI-2 scavenger. The NIPAM moiety acts as the thermoresponsive unit whereas the acrylamide shifts the LCST at suitable levels. The tris-hydroxy moiety acts as the scavenger.

## Chapter 5

**Figure 5-1.** The Turing test concept. The interrogator attempts to distinguish the man from the machine by querying the subjects [2].

**Figure 5-2.** The biological version of the Turing Test. The interrogator cells attempt to distinguish other cells of their own kind and artificial chemical cells through chemical exchange of small molecules that comprise the cellular language [1].

**Table 5-I** Comparison of the Turing test with its biological counterpart.

**Figure 5-3.** The basic requirements that a primitive CHELL must fulfill to pass successfully the imitation game.

**Figure 5-4.** Cell-CHELL interactions. Schematic representation of an ideal conversation loop between bacterial cells with their artificial counterparts.

**Figure 5-5.** The formose reaction and its products. Formation of the AI-2 upon addition of borate in the reaction mixture.

# Chapter 1

## *Polymeric Biomedical Materials – Polymer-Cell Interactions*

### **1. Introduction**

Responsive biomedical materials span a plethora of applications in the biomedical field and are in constant further development to give properties that ultimately improve the quality of life and prevent disease [1, 2]. Polymers are used in stents, hydrogels, degradable implants and in non-structural biomaterials such as drug delivery systems. There is now an increasing focus on materials design at the molecular level in order that new polymers can be designed to function in a biomimetic way (table 1-I). For example, polymers are designed for specific interactions with biological substrates so that biological function can be put under external control. There is now a real need to develop understanding of how mammalian/bacterial cells interact not only at the cell-to-cell communication level but also at the cell-substrate interface. The substrate in this context can be any surface of interest, that is an implant, a non-degradable biomaterial or a cell-culture surface. An example of cell-substrate interface control is provided by cell-responsive hydrogels, which have been designed that respond/degrade proportionally to cell proliferation due to the selection of specific chemical ligands which alter the matrix as cells grow [3]. Other biological responses that modify a synthetic substrate include enzyme activity and enzyme responsive hydrogels have been synthesized [4-6] that degrade only on the selected specific biological stimulus (that is the enzyme substrate) rather than a chemical or physical one.

Stimulus-responsive polymer vehicles for delivery of anticancer drugs or other bioactive substances such as proteins are also under intense investigation. There are already some pharmaceutical products in which polymers are an essential component of the final formulation such as polyethylene glycol (PEG) containing drugs. Researchers have started to focus on ligand-receptor interactions that occur in biology and try to embed these groupings in artificial entities to induce biomimetic behaviour but without the drawbacks of purely natural recognition macromolecules. This could potentially lead to better therapies, with fewer side-effects, yet with substrate specificities and an inherent elegance found in natural systems.

**Table 1-I**

Some examples of polymers applications in the biomedical field.

Degradable biomaterials	Hydrogels
Phase-change injectable polymers	pH/thermo responsive polymers, colloid gels
Protein repellent surfaces/materials	PEG-coated implants
Microfluidic devices/Microelectromechanical devices	polymethylmethacrylates , polydimethylsiloxanes
stiff/elastic biomaterials, elastomers	polymer composites
Wound healing bandages	Polysaccharides (i.e. alginates, hyaluronates)
Smart/degradable sutures, polymer meshes	“Smart” fibres
Biom mineralization	polyacrylic acids
Micro/nano particles for DDSs and MRI contrast agents	Polymer coated nanoparticles, microgels
Artificial tissues and organs (skin, blood etc.), cell mimics	dendrimers, hydrogels, micelle formulations
Protein/gene therapy	polymer-protein conjugates, polyethyleneimine, cationic polymers
Microbial/bactericidal action	quaternary ammonium polymers
Analytical applications (i.e. sensors and actuators)	fluorescent, conductive polymers, composites
Drug delivery vehicles	self-assembled polymers
2 and 3d scaffolds for cell culture and tissue regeneration	hydrogels, engineered polymer surfaces, sol-gel transition polymers

The chemist's toolbox is thus greatly inspired by natural structures found at the molecular level of the biological organelles. In an inspiring review by Professor S. Mann [7], a nanoscale perspective of molecular processes fundamental in life is given. The near-perfect realisation of function in natural biomolecules (i.e. proteins) has not surprisingly led to intense efforts from synthetic chemists and molecular biologists in order to achieve biomacromolecule-like robustness and uniformity in synthetic materials.

Recent progress in polymer chemistry and technology is now enabling synthetic macromolecules to resemble complex biopolymers. There are methods developed that allow for complex architectures and topologies to be made in a robust and highly reproducible manner that were not possible to synthesize with conventional polymerization methods. Also, functionalization of these materials is possible by coupling on natural ligand-receptor systems leading to highly active bioconjugates. Chemical moieties that have been the focus of researchers include carbohydrates (known for their biochemical versatility in stereoselectivity), nucleic acids (high specificity due to base complementarity), proteins and peptides (strong and highly specific ligand-receptor motifs).

The need for well-defined polymers however does not occur due to an intellectual challenge but rather from actual clinical needs. For example, there are already protein-based drugs in the market where polymers are used in the final drug formulation (in the form of polymer-protein conjugates or protein chimeras) as a protective means to increase the regulation of the drug in the bloodstream by reducing the denaturation rate. In order to obtain a well-characterized pharmacological profile of these drugs, well-defined architecture and homogeneity of the polymers is absolutely critical. Also, degradation products during or after elimination of these drugs must be known as a subtle heterogeneity in the

drug formulation could cause side effects or reduce the pharmacological potency. It is also crucial to have homogeneous polymer materials when the latter are used in drug delivery systems. For example, polymer-based micellar drug delivery systems (DDS) must have nearly monodisperse size distributions in order to achieve accurate dosage formulation for drug potency maximization. Finally, in the case of degradable hydrogels/implants, a uniform polymeric mesh will provide controlled degradation profiles which will also influence the drug release profiles from the polymer matrices.

It is therefore critical to develop methods to produce uniform and well defined polymers that can be used in the biomedical field. Modern polymerization techniques that have been developed in the 90s will be briefly discussed in the following paragraphs. It will be shown that these methods allow for superior control over topology and architecture on polymeric materials, not accessible with conventional polymerization processes.

## 1.2. Living Radical Polymerization

### 1.2.1. Atom transfer radical polymerization (ATRP)

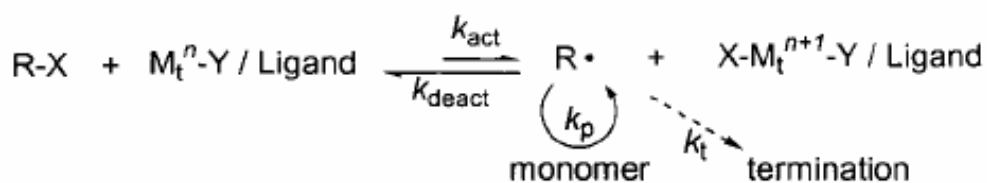


**Figure 1-1.** The general mechanism of ATRP [8,9].

A transition metal such as copper is required to generate radicals via redox reactions. The transition metal exists as a complex  $\text{M}_t^{n\text{-Y}}/\text{Ligand}$  with Y being a ligand or the counterion. The transition metal is prone to a one-electron oxidation reaction which abstracts a halogen atom from

dormant species compounds such as R-X. This redox reaction generates radicals ( $R\bullet$ ) that in turn attack the monomers and induce polymerization in a known radical fashion (figure 1-1). The equilibrium constant  $K_{eq}$  is determined from the ratio of the activation ( $k_{act}$ ) to deactivation constant ( $k_{deact}$ ).  $K_{eq}$  must always be optimized as a low equilibrium constant will lead to a slow polymerization process whereas high  $K_{eq}$  results in fast termination process and ultimately loss of control during the polymer growth. The rate of polymerization is much slower than the activation/deactivation process and hence the concentration of the active radicals remains low compared to the R-X radicals. Also, the fast deactivation rate will lead to polymers of low polydispersity.

The livingness of the process derives from the rate of deactivation and therefore leads to a uniform polymer growth with minimum termination in the reaction mixture which usually does not exceed 5% of the growing polymer chains.

Most vinyl based monomers can be polymerized by ATRP, especially styrenes, acrylates and methacrylates and to lesser extent (meth)acrylamides (although these are known to disproportionate the catalyst complex [10]). The molecular weight of the polymers is determined by the concentration of the initiator (R-X with X being a halide such as Cl or Br). At the correct conditions the concentration of the polymer chains should be equal to the initial concentration of the initiator in the reaction mixture. Therefore, since ATRP is a living process we can predetermine the M.W. of the final polymer via the degree of polymerization (DP) which is set by the initiator concentration. Also, in a typical ATRP the molecular weight increases linearly with conversion and it is therefore possible to terminate the polymerization at any point of time in order to achieve the desired molecular weight.



First, radicals are generated by the initiator similarly to a conventional radical process. Then the radicals are added to the transfer agent and homolytic fragmentation of the R group occurs (14). The R• is capable to reinitiate by the formation of a new propagating radical P<sub>m</sub>•. In essence, at each radical addition to the initial transfer agent, a new macro-transfer agent is produced at the propagation step and hence equal probability of all polymer chains to grow is established. Both addition and fragmentation steps should be fast enough and optimized to achieve efficient re-initiation. At the end of the polymerization, almost all polymer chains are terminated with the thiocarbonylthio transfer agent which allows for synthesis of block copolymer synthesis even in one-step synthesis (assuming that all initial monomers are consumed before addition of the second). Termination also occurs by chain-chain coupling but to a lesser extent than radical polymerization. Careful consideration should be paid in the design of the RAFT agents as each monomer has a different propagating capacity. The effect of a RAFT agent is greatly determined by the Z and R groups. Generally, dithiobenzoates and other aromatic dithioesters, aromatic dithiocarbamates, trithiocarbonates are regarded as very efficient RAFT agents whereas for R groups, cyanoalkyl or cumyl moieties are the most common particularly for methacrylate based monomers due to their good captodative character [15].

The living polymerizations briefly described above are subject to the persistent radical effect which is briefly described in the following paragraphs. The versatility of these methods allows for complex architectures to be accessed that are not possible with other conventional polymerization methods. Most importantly, these advanced polymer structures can be obtained at highly uniform and homogeneous populations as living polymerizations allow for low polydispersities to be achieved (PD<1.5) [13, 14].

### 1.2.3. Elements of the persistent radical effect

Let us consider two sources that generate free radicals, R which is a transient radical and Y which is a persistent one. If the radicals are formed simultaneously and at the same ratio one would expect that due to the radical-radical reactions the products R-Y and R-R will be formed at a 2:1 ratio (figure 1-3a). However what we observe in reality, the R-Y is the dominant product. This is happening because the transient radicals disappear by the cross-reaction and through self-termination and hence soon an excess of the Y radical will be established which in turn will favor formation of the R-Y product which will be the dominant one.

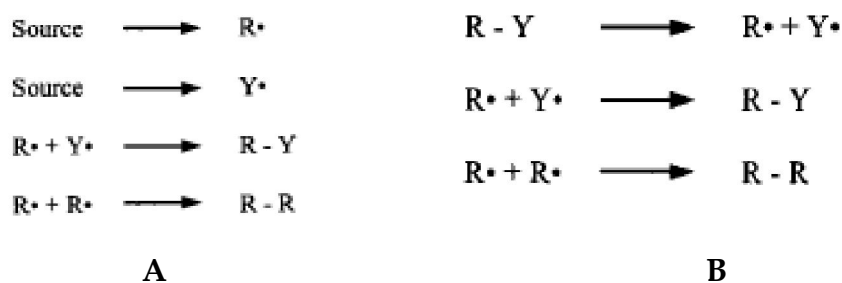


**Figure 1-3.** a) Radical generation, the cross reaction between the transient (R) radical with the persistent one (Y) and the self-termination of the former and b) Dissociation of the R-Y to form the radical species and the possible reactions of the latter [16].

In another situation where the radicals are formed by the dissociation of the R-Y precursor (consider all other conditions as before), the lifetime of the R-Y will be considerable higher as it is permanently regenerated from the cross-reaction (figure 1-3b). Therefore it is the presence of the persistent radicals that lead to the increased formation/prolongation of the R-Y product, as in reality the self-termination of the transient radicals never stops. Considering the case one could add a substance such as a monomer that could lead to formation of the R-M• at each dissociation cycle of the R-Y precursor. This is the basic concept of the effect of the persistent radicals and explains the reason we obtain the dormant species (R<sub>n</sub>-Y) as the main products in the polymerization mixture. Both RAFT and ATRP obey the PRE rules as studied by Fischer [16] and Fukuda [17].

### 1.2.4. Polymer topology and architecture

The LRP methods described above, allow for complex architectures to be produced that cannot be accessed with other conventional polymerization methods (i.e. free radical polymerization). The living nature of these polymerizations allows for sequential addition of different monomers even in one-pot reaction to obtain block-copolymers of linear, star or comb-like topologies of low polydispersity. Also, the polymer chains produced are terminated with active chemical groups that can either be used to further grow more blocks or to functionalize with other (bio-)chemical ligands to obtain (semi-)telechelic polymers (figure 1-4). In addition, controlled polymerization of well-defined networks allows for uniform mesh size distribution of polymer networks, which is highly desired when it comes to biodegradable materials that must be uniformly eliminated from the human body.

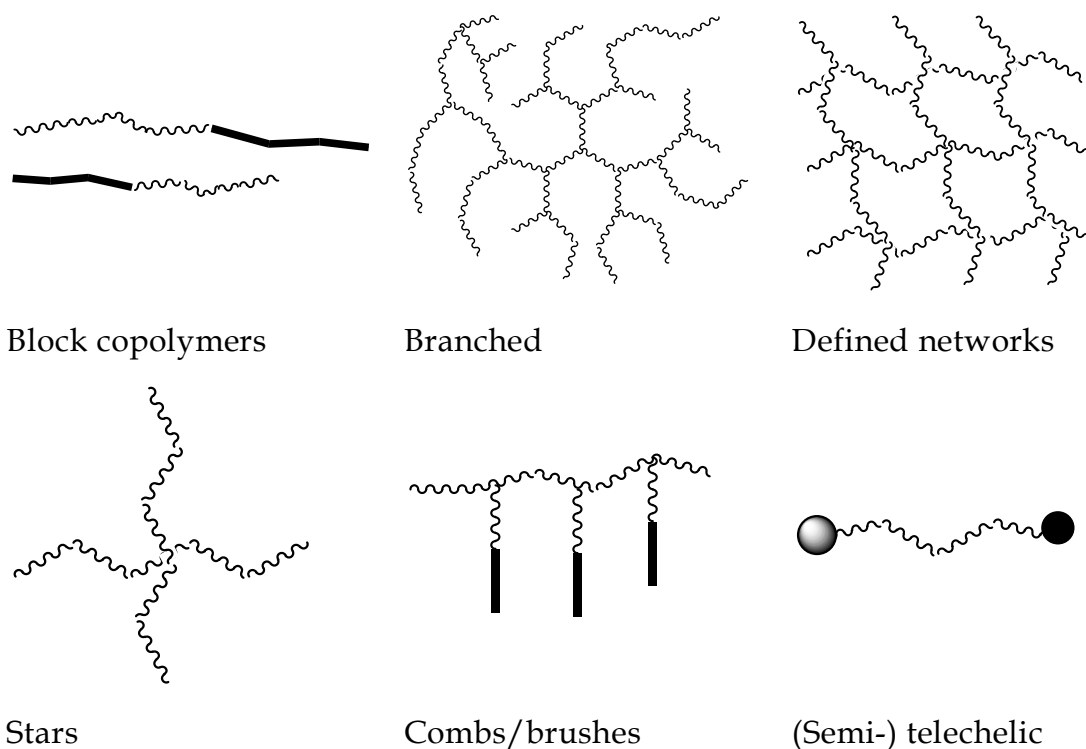


**Figure 1-4.** Advanced architectures accessible with modern polymerization methods.

Another interesting topology that has relatively recently emerged is the hyperbranched structure which resembles the dendritic architecture found

in dendrimers (figure 1-4). With LRP methods, one can synthesize uniform hyperbranched materials at considerably lower costs compared to dendrimers which are known to be laborious and expensive to produce. Hyperbranched polymers exhibit lower hydrodynamic radii and can accommodate large amounts of bioactive substances (i.e. drug molecules) in their dendritic network and hence are superior candidates for drug delivery applications.

As an example of the sophistication of new polymer systems we first consider polymers that have been designed to interact with bacteria, a relatively simple but immensely important class of cells.

### **1.3. Polymer design for bacterial detection**

Polymeric materials can be used to interact with microorganisms in a variety of analytical contexts and these are growing in importance for medical, food and defence applications. The reasons for using polymer-based systems in micro-organism sensing and detection are many-fold, but primarily because the polymer 'platform' is so varied and thus the functionality can be adapted as required. With recent advances in macromolecule synthesis and materials fabrication techniques as mentioned above it is possible to produce polymers with a wide range of functional chemistries and apply these to many device formats.

New detection methods are being developed that can be used in conjunction with the novel polymer chemistries for application to the analysis of many other microorganisms (viruses, yeasts, fungi). In all cases however, there is the need to develop materials that can interact selectively with the analyte to ensure a correct signal free from false positive and negative responses. Synthetic and modified natural polymers are thus a good choice for a microorganism recognition system due to multifunctionality and polyvalency.

The combination of multiple weak interactions of individual sugars to generate high affinity binding modes of carbohydrates with their receptors is well known in glycoscience and microbiology as polyvalency. Many bacteria have receptor sites for sugars that can act cooperatively to induce surface- and cell-binding interactions (table 1-II) [18, 19].

**Table 1-II**

Attachment sites for bacterial binding via ligand-receptor interactions.

<b>Organism</b>	<b>Attachment site</b>
<i>Chlamydia trachomatis</i>	mannose-binding proteins
<i>Enteroaggregative E. coli</i> (EA <sub>g</sub> EC)	sialic acid
<i>Enterococcus faecalis</i>	galactose, fucose, and mannosamine, but not mannose
<i>Uropathogenic E. coli</i>	Gal(a1,4)Gal on glycolipid uroplakins Ia and Ib
<i>Haemophilus influenzae</i>	[NeuAc(α2-3)] <sub>0,1</sub> Galβ4GlcNAcβ3Galβ4GlcNAc
<i>Helicobacter pylori</i>	NeuAc(α2-3)Galβ4GlcNAc
<i>Pseudomonas aeruginosa</i>	GalNAc(b1,4) in asialo-GM1 and asialo-GM2 or GM1 salivary mucin glycopeptides (sialic acid) lactose of glycolipids
<i>Staphylococcus saprophyticus</i>	blood group A (terminal GalNAc)
<i>Staphylococcus aureus</i>	N-terminal fragment (29 kDa) of fibronectin (Fn <sub>29</sub> K); Fibronectin bone sialoprotein (BSP) (small, ca. 80 kDa) integrin-binding, RGD-containing bone matrix glycoprotein, collagen of cartilage; collagen; N-terminal region (heparin-binding domain) of fibronectin
<i>Streptococcus pneumoniae</i>	laminin; collagen types I, II, and IV; fibronectin; and vitronectin

This phenomenon has been exploited by Disney et al. to produce lectin- and bacteria-recognition materials [20]. Specifically, water soluble fluorescent glycopolymers prepared from poly(p-phenylene ethylene) were derivatised with carbohydrate moieties using a post-polymerization method. Coupling of sugar species with the polymer backbone was accomplished by using standard carbodiimide chemistry which resulted in polymers with 25% sugar functionalisation of the reactive sites. Several polymer batches were synthesized varying the saccharide attached on the backbone (figure 1-5).

Mannosylated polymers strongly interacted with Concanavalin A (Con A) whereas the galactosylated counterparts did not show any binding with the lectin demonstrating the specific binding-character of the polymers. This group were also able to observe bacteria clustering, following polymer addition due to the polyvalent nature of the binding process. The intrinsic fluorescent character of the synthesized glycopolymers in combination with the bacteria clustering induction, made the bacteria-polymer interactions visible even with the naked eye (figure 1-5). The coupling of these types of polymers with the techniques for fluorescence-based sensing and detection renders this method potentially very useful in quantitative microbiology.

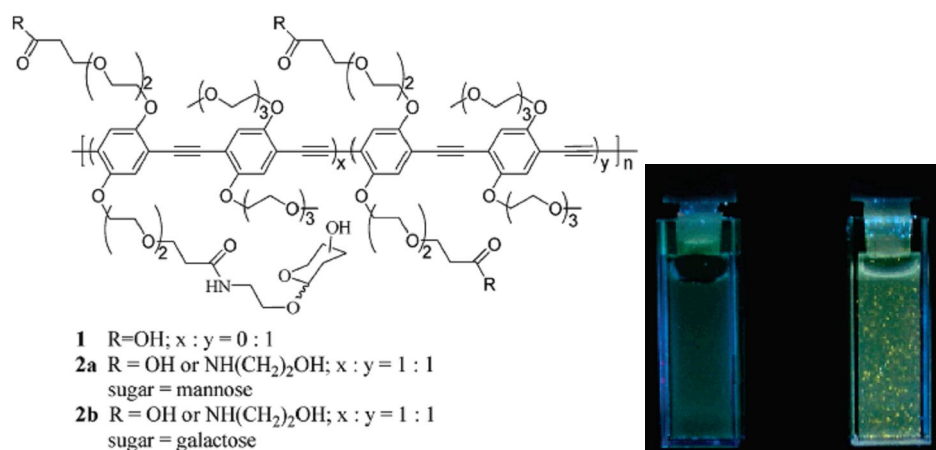


**Figure 1-5.** Left – structures of poly-glyco-ene-yne materials prepared by Disney et al. Right, visualization of *E. coli* strains after incubation with mannosylated polymer 2a; mutant strain (left) and mannose-binding strain (right).

The presence of carbohydrate recognition sites (CRSs) on certain bacteria has been used by Kim et al. who synthesised supramolecular objects that could interact with CRSs found on bacteria [21, 22]. The recognition targets adopted for this study were the FimH sites found on the pili of type I *E. coli*. By rationally designing materials at the molecular level, in this case by embedding information for their supramolecular self-assembly at the macromolecular scale in a protein-like folding fashion, this group were able to obtain micellar, vesicular or tubular structures by subtly changing the composition of the starting materials (figure 1-6). The rod-coil amphiphiles used in this study consisted of tetra (p-phenylene) or di[tetra(p-phenylene)], as the hydrophobic moiety and oligo(ethylene oxide) decorated with mannose as the hydrophilic segments. The coexistence of incompatible hydrophobic/hydrophilic moieties drove the supramolecular self-assembly of these materials in aqueous environments such that carbohydrate molecules at the outer surface were exposed ready to bind with CRSs. These materials were found to interact with *E. coli* in a strong multivalent manner and the supramolecular structure was also found to play a key role in the binding process. Spherical micellar structures could bind more strongly with Con A compared to cylindrical micelles. Although this observation has not

been fully understood, the findings clearly signify the importance of supramolecular architecture when designing biofunctional materials using bottom-up approaches (i.e. self-assembly).

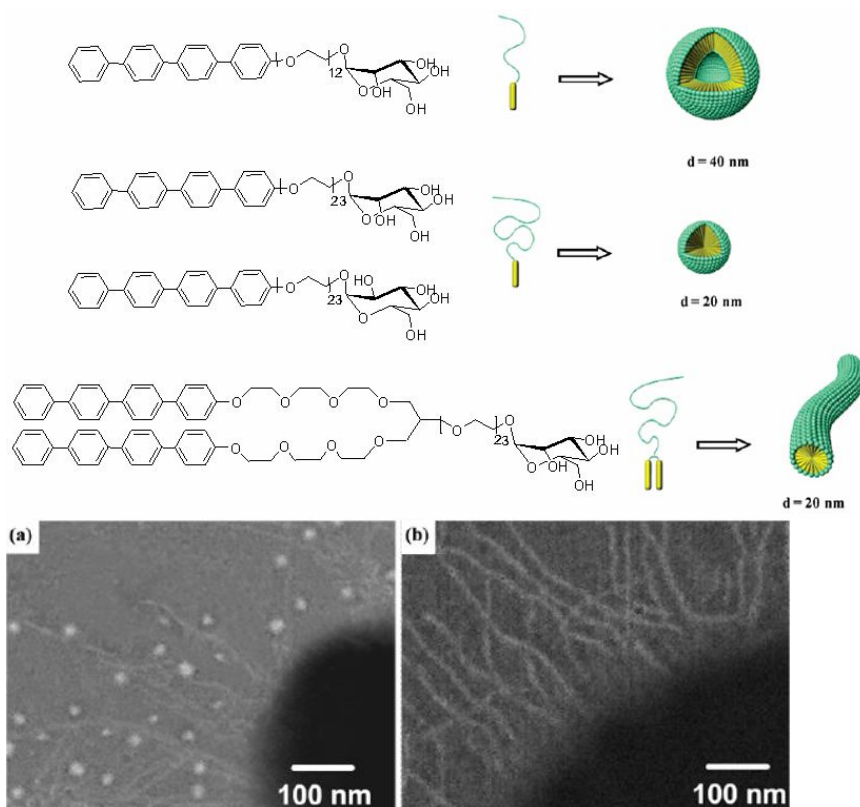


**Figure 1-6.** Amphiphilic polyphenylenes prepared by Kim et al. for interaction with *E. coli*. Micellar (a) and tubular (b) structures interacting with bacterial fimbrils.

The ubiquity of sugar-receptor interactions in eukaryotic systems is harnessed by certain microorganisms to invade host defences. Mannose receptors are present on many other cell surfaces as well as those of bacteria, and a case of particular medical relevance is the presence of mannose receptors on macrophages. Park and co-workers prepared styrene based polymers decorated with glucose or mannose moieties and examined their binding with macrophage cell surface mannose receptors [23]. The polymers were also fluorescently labelled and the increased binding of the mannose-derivatised polymers on the cell surfaces was observed by using confocal microscopy.

One important aspect in biological recognition is the presentation of the ligand to its receptor (and vice versa). Thus it is not always sufficient to tag sugar moieties to the side chains or termini of synthetic polymers in order to effect a biological recognition event. In addition, efficient and selective carbohydrate synthesis remains a challenge for the preparative organic chemist. As a consequence, new methods for producing selectively functionalised and correctly architected glycopolymers continue to be a focus. Miura et al. used chemoenzymatic methods to produce glycopolymers from nonreducing disaccharides [24]. Specifically, they reacted divinyl sebacate with trehalose or galactose-type trehalose in the presence of various lipases. The enzymatic esterification was highly chemoselective, mediating ester formation at the Glc 6-OH for trehalose and Gal 6-OH for galactose-type trehalose. The resulting monomers were polymerized with a  $\text{H}_2\text{O}_2$ /(ascorbic acid) system to yield vinyl-alcohol-backbone glycopolymers. Lectin-inhibition assays showed selective binding (Con A and RCA<sub>120</sub> for  $\alpha$ -D-Glc and  $\beta$ -D-Gal specificity respectively) and increased affinity compared to monovalent counterparts attributed to polyvalency. The method is attractive due to the high chemoselectivity and the environmentally friendly character of enzyme-based chemistry since esterification reactions can also be completed in aqueous systems; chemoenzymatic methods though still lack high yield conversions and hence are not yet suitable for bulk production of polymeric materials.

ATRP has several advantages over more “traditional” polymerization methods when designing biologically active materials; it can be done in relatively mild conditions and the living character provides versatility and fine control of the designed polymers. In an effort to achieve control of polymer structure and biological functionality Ladmiral et al. introduced a novel method of polymer synthesis based on ATRP and ‘click’ chemistry [25]. Starting from trimethylsilyl methacrylate and using CuBr/ N-(n-

ethyl)-2-pyridylmethanimine as the catalyst system, low dispersity polymers were produced (PDI<1.15). Quantitative deprotection of the polymers with a TBAF/acetic acid system, yielded alkyne terminated polymers readily reactive with sugar azides via triazole bridge formation.

Huisgen 1,3-cycloaddition combined with ATRP has also found application in virus-polymer conjugates [26]. Methacryloxy ethyl glucoside was polymerised using an azide functional initiator and the resulting azide-capped polymers were conjugated to azide-containing virus particles via a bifunctional fluorescein with alkyne groups. The resulting particles were found to have higher hydrodynamic volume compared with the unmodified ones and could agglutinate con A. The apparent advantage of this method is that polymer libraries of varying sugar species can be easily constructed simply by adding appropriate ratios of sugar derivatives. "Click" chemistry in combination with ATRP proved to be a powerful method towards tailored made synthesis of complicated polymeric structures without sacrificing structural integrity.

Cuihua Xue et al. employed Suzuki coupling reactions or Sonogashira polymerization methods to synthesize fluorene based polymers with pendant bromoalkyl groups [27]. They explored both pre- and post-polymerization methods to attach glucose moieties on the polymers via reaction of the bromoalkyl group with 1-thio- $\alpha$ -D-glucose tetraacetate. However, the materials synthesized exhibited poor water solubility unless oligo (ethylene glycol) had been used as a tethering spacer between the polymer backbone and the carbohydrate species. Although the biological activity of these glycopolymers has yet to be fully tested, the blue-light emitting nature of the fluorenyl moieties suggests the approach could have important value for analytical detection of microorganisms.

### 1.3.1. Protein engineering

Wang and Kiick employed methods from protein engineering to synthesize a glycopolymer of controlled supramolecular conformation [28]. Bacterial expression of the sequence (AAAQAAQAQAAAEAAAQAAQAQ)<sub>6</sub> produced a protein-like structure with the intrinsic property of adopting a helical conformation at room conditions. The structure was purposely enriched with glutamic acid residues at predefined positions that could further be derivatised with amine-containing carbohydrates. The resulting monodisperse material preserved its helical conformation and when tested for biological activity with cholera toxin, a 200-fold increased inhibitory effect was observed compared to galactose. This approach of tailor-made synthesis of protein-based materials offers several advantages over more traditional routes in that a) it is bio-friendly in the sense that it solely relied on natural reagents (that is, amino acids) and hence is potentially more biocompatible than materials made by synthetic building blocks; b) both final composition and higher structural conformation can be precisely controlled from the very beginning; and c) it produces nearly monodisperse materials compared with other conventional techniques (i.e. free radical polymerization).

Related studies by the Kiick group involved the synthesis of glycopolymers by using commercially available poly(glutamic acid) as backbone coupled with galactosylamine derivatives of different linker size [29]. The researchers explored the role of sugar spacing along the polymer backbone in respect with the polymers binding capability to the cholera toxin, and concluded -in accordance with previous studies- that the sugar concentrations on the polymer backbone required for optimum binding, are not the highest possible but rather those that coincide to the precise spacing of the toxin's binding sites. In addition, the linker that connects the sugar with the polymeric backbone plays a key role to the accessibility

of the sugar to the binding site. Overall, the strategy explores facile routes of studying carbohydrate-lectin interactions by varying parameters such as the sugar moiety, degree of substitution and linker length based on polypeptides.

### 1.3.2. Bacterial Detection

The selectivity of the binding interactions of polymers with bacteria requires coupling to a detection system in order to be useful analytically. Chunayan Sun *et al.* used an interesting method to detect bacteria and their binding properties with synthetic materials [30]. They synthesised liposomes consisting of polydiacetylene (PDA) and mannose-glycolipids. Because of the presence of an -ene -yne on the backbone of the polymer, PDAs have the intrinsic property of changing colour (blue to red shift) in response to external factors such as pH, temperature etc. When the liposomes were mixed with bacteria populations they changed colour from blue to red indicative of the binding of the *E. coli* FimH binding site (present on the pili of wild-type *E. coli*) with the mannose binding sites on the liposomes membrane and disruption of the latter. The colorimetric transition was attributed to the change of the electronic properties of the backbone of the polymer resulting from relative conformation alternations of the side chains of the polymer. This colour transition with bacteria was also examined when several metal ions (i.e.  $\text{Ca}^{+2}$ ,  $\text{Mg}^{+2}$ ,  $\text{Ba}^{+2}$ ) were present in the cell culture media and it was found to be considerably faster, thus confirming previous studies supporting the fact that divalent cations often promote binding of carbohydrates with FimH sites via bridge bond formation.

In a similar context Su and co-workers synthesised vesicular structures based on 10,12-pentacosadiynoic acid as the sensor moiety and 1,2-dihexadecanoyl-3-o- $\beta$ -maltotriosyl-glycerol as the bacteria recognition molecule [31]. When the vesicles were tested for their ability to 'sense'

type I *E. coli*, a rapid colorimetric response was observed in less than two minutes.

These methods can be regarded as useful qualitative observations of bacterial sensing i.e. the colour change can be detected with the naked eye.

### 1.3.3. Bacterial capture and detection with imprinted polymers

For some microbiological assays, especially when sterilisation protocols need to be followed, more robust materials than vesicles and soluble glycopolymers are required. In such cases, molecularly imprinted polymers (MIPs) are of interest, as these materials are typically highly cross-linked and resistant to harsh environmental conditions [32].

MIPs are prepared by polymerisation in the presence of template species, using functional groups in the imprinting mixture such that when the templates are removed, 'negatives', complementary to the templates, are embossed in the polymer. These negative copies can act as binding sites for the templates, and such a process has been very widely used as a means to sense/capture low molecular weight analytes [33, 34]. However, although the imprinting protocol is conceptually very powerful and generic in its scope, little work has been carried out in the imprinting of higher molecular weight systems or at the micron scale, as is required for microorganisms. Initial work in the binding of bacteria at imprinted surfaces [35, 36] demonstrated modest recognition of *S. aureus* and *L. monocytogenes*. More recently, Harvey and co-workers were able to extend this method to bind *Bacillus thuringiensis* and *Bacillus subtilis* spores, as mimics of the pathogen *Bacillus anthracis* (figure 1-7) [37].

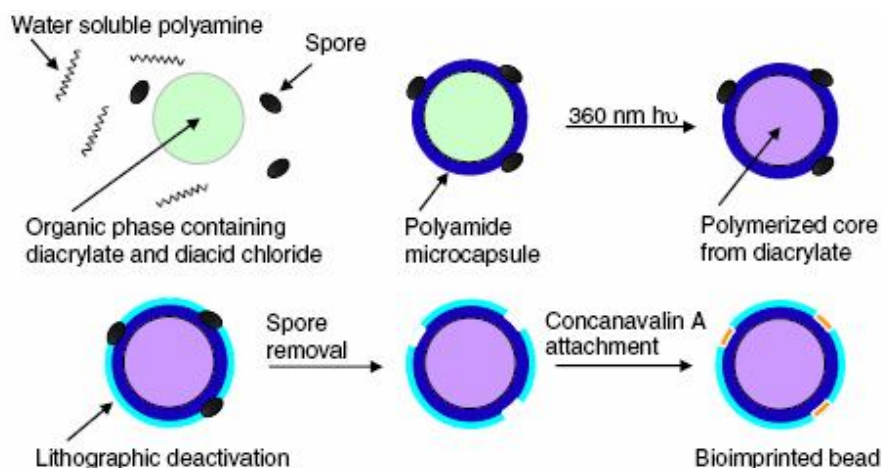


**Figure 1-7.** Schematic of the imprinting process for spores used by Harvey et al. [37].

A clear enhancement of spore recognition by the imprinting process was demonstrated in this work, as well as enhanced capture of the biological agent, which is important for food microbiology and defence/security applications.

The Dickert group have been very active in developing imprinting approaches to capture and detection of microorganisms. Imprinting of cells as varied as erythrocytes, yeasts and bacteria has been carried out by soft lithographic procedures combined with *in situ* polymerisation at quartz crystal microbalance surfaces. The method typically has involved preparing a thin polymer layer on a QCM surface and bringing a second layer with adsorbed biotemplate in close proximity to the first surface followed by UV polymerisation of a monomer layer or sol-gel encapsulation of the template. Removal of the outer surface has generated imprints ranging from the nanometre to micron scale. Selective detection of different blood cell types, virus serotypes and yeast concentrations over 5 orders of magnitude have been demonstrated, indicating the versatility as well as the selectivity of detection possible with MIP analysis.

The MIP approach has also been used to imprint certain viruses, which although generally less complex than bacteria, can in some cases share

common surface properties, primarily excess negative charge. Bolisay and co-researchers synthesized MIPs capable of capturing tobacco mosaic virus (TMV) in relatively large quantities [38]. TMV has the requisite negative charge on its surface, and thus crosslinked MIPs derived from polyallylamine - which initially formed charge-charge interactions with TMV - were used to mediate non-covalent association of the MIP with the cylindrical viral template. When MIPs and non-imprinted polymers were tested for their virus-capturing ability it was found that TMV imprinted polymers were able to detect and capture considerably higher amounts of cylindrical TMV than the control polymers. The results suggest the formation of cylindrical-like cavities in the polymer network complementary to the virus cylindrical shape.

#### 1.3.4. Quantum Dots

Over the last 10-15 years, many research groups have sought to use quantum dots (qdots) for applications in biomedical analysis [39, 40]. Qdots have the advantages of sustained light-emission, large quantum yields, excellent photostability, a very wide range of emitter wavelengths and the ability to fine-tune the emission bands. These properties enable qdot systems to be used to “follow” long-lasting biological processes - which classic fluorescence strategies cannot do. This is a very active field of research and bacterial detection is a key goal for many working in this area.

Glyco-qdots decorated with carbohydrate antigens were prepared by Fuente et al. [41]. This group first synthesized neoglycoconjugates of maltose or the trisaccharide Le<sup>x</sup> antigen (Gal $\beta$ 1-4[Fuc $\alpha$ 1-3]GlcNAc) from their protected derivatives by reaction with 11-thioacetate undecanol. The neoglycoconjugates were then attached to CdS nanocrystals to obtain glyco-qdots which were stable for several months.

A related approach involved derivatising disaccharides using 2-aminoethanethiol by imine reduction with  $\text{NaCNBH}_3$  [42]. The thiol-functionalized neoglycoconjugates were readily attached to CdSe-ZnS qdots. The resulting glyco-qdots were water soluble which prevented self-aggregation when in aqueous environments. Sugar derivatization mediated specific binding with lectins which resulted in formation of aggregates due to the formation of large lectin-qdots complexes. To date these qdot bioconjugates have not been tested for their biological activity but it is likely that glyco-qdots of this type will become important materials in mimicking and/or monitoring biological events as they are relatively easy to prepare and have the stability lifetimes (days to months) required for analysis of bacterial processes, including, for example, biofilm formation.

In what can be considered as an analogous strategy, Sun and co-researchers used the well-known biotin-streptavidin couple to decorate light emitting nanocrystals or magnetic beads with glycopolymers [43]. A glycopolymer with galactose units and a biotin end-capped acrylamide backbone was synthesised which could selectively bind with commercially available streptavidin functionalised qdots or magnetic beads to generate high-density functionalised surfaces (figure 1-8). The specific binding nature of the synthesised materials was confirmed via lectin-binding assays. The biotin-streptavidin system has been used extensively in the past for similar bio-recognition/conjugation applications due to the high selectivity and hence high conjugation capacity that this system offers.

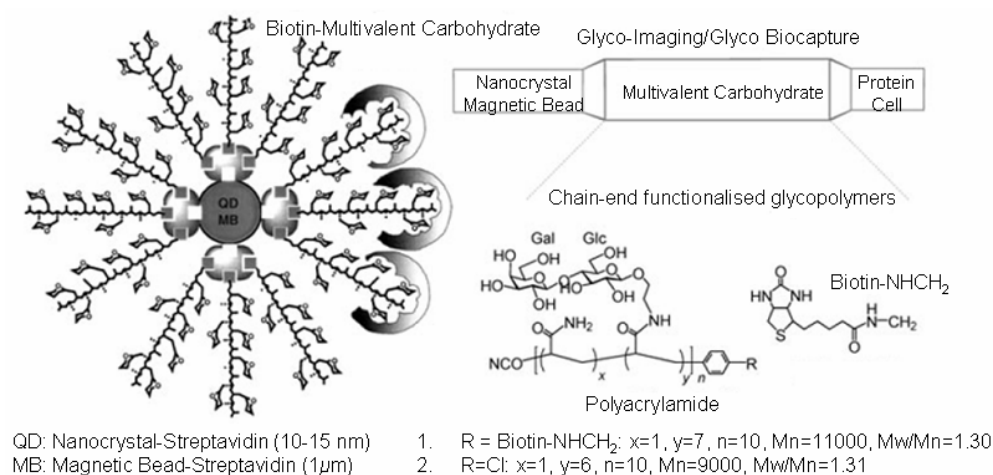


**Figure 1-8.** Functionalised nanocrystals and magnetic beads for detection and binding of proteins and cells via surface-displayed glycopolymers.

Molecularly assembled nano- probes, contrast agents and biomarkers could thus be relatively easily synthesised by following this readily accessible route.

Two final examples indicate some innovative strategies and some future directions in controlling polymer-bacteria interactions.

Krishnamurthy et al. proposed an ingenious strategy for the *in vivo* elimination of gram-positive bacteria from the immune system assisted by a bifunctional polymer [44]. Their concept involved the surface modification of gram-positive bacteria that are normally difficult for the immune system to recognize, such that their capture by antibodies was promoted, leading to subsequent elimination by macrophages (figure 1-9). This approach, which can be considered partly analogous to the ‘cellular painting’ (cell surface remodelling) approaches to cell-specific drug targeting [45-48] involved the generation of polymers that would both specifically interact with the desired bacteria while displaying a “tag” that would be recognised by the natural opsonization pathways.

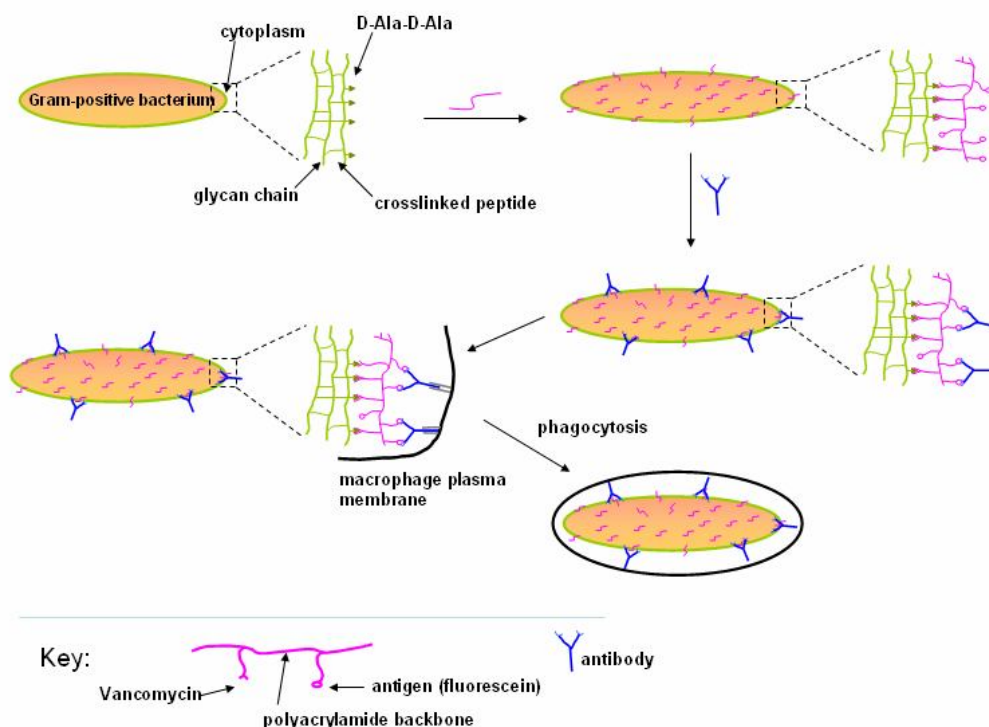


**Figure 1-9.** Surface modification of bacteria through multivalent interactions with vancomycin-functionalised synthetic polymers. Incorporation of a fluorescent antigen on the synthetic polymer promotes antibody recognition and subsequent opsonisation and phagocytosis of the bacteria, while simultaneously allowing monitoring of detection and binding events [44].

This required the design of an acrylamide polymer with dual-purpose functionality. The starting material poly(N-acryloylsuccinimide) was reacted with fluorescein cadaverine and then with amino-functional vancomycin derivative to yielded a multivalent polymer, which was quenched with ammonium hydroxide to ring-open reactive anhydride groups in the final acrylamide polymer. The vancomycin groups on the polymer served only as recognition sites -rather than as antibiotics- of the D-Ala-D-Ala peptides on the bacteria. Therefore the derivatization ratio of the polymer with vancomycin was kept low (5%) whereas the fluorescein groups served as haptens recognized by specific antibodies. The polymer was bound to the bacterial surface in a multivalent manner and strongly promoted opsonization of the bacteria by monoclonal IgG (antifluor)

when tested with flow cytometry. Subsequently, the polymer-bacteria complexes could be ingested by macrophage cells twice as efficiently as the non-polymer treated bacteria. This particular strategy is likely to find a number of applications in the biomedical field since it exploits multivalency and therefore can accommodate weak-interacting therapeutic species by amplification of the host-receptor interactions. In addition, this amplification can be used as a signal intensity enhancer for *in situ* bacterial analysis. The real power of such a system would therefore lie in the ability to detect pathogens *in vivo* with very high sensitivities or to detect and deactivate the pathogen with the same multivalent polymer. Such combined therapeutic-diagnostic systems (occasionally but not elegantly described as “theranostics”) are perhaps the ultimate medicines – being able to detect and treat disease exactly when and where required.

Another inventive method uses Nature’s own *in situ* diagnostic and communication systems to interact with, detect or deactivate bacteria. Amongst many bacterial species, cell-cell communication networks known as quorum sensing (QS) have evolved to maintain and control bacterial population behaviour [49, 50]. QS is mediated by low molecular weight compounds, principally (but not exclusively) of the N-acyl-homoserine lactone (AHL) family, which can be produced and sensed by bacteria. It has been found that the concentration of AHLs in the bacterial microenvironment is proportional to the population density of the bacteria population and the latter use them as a means to sense their population density. Upon a certain concentration of AHLs, bacteria start to show single-organism-like behaviour and often increase their infectivity or pathogenicity. Kato et al. explored the possibility of QS-interference by using cyclodextrins [51]. It was hypothesized that the hydrophobic acyl chain of the AHLs could be included in the interior cavity of cyclodextrins via hydrophobic interactions and hence exclude them from the bacterial sensing network. The researchers tested *Serratia marcescens*, an

opportunistic pathogen that produces prodigiosin via QS mediated mechanism at the stationary growth phase. When the bacteria were grown in presence of optimum concentration of cyclodextrins in the growth medium, it was observed that the production of prodigiosin was reduced approximately 40% suggesting the reduction of AHLs available to be detected by the bacteria. This is one of the very first studies in which a QS system has been targeted by a synthetic material and can interfere with the bacterial language. It is expected that even more advanced materials will be synthesized for QS interference since AHLs exist in relatively high concentrations in the bacterial microenvironment and hence are potential molecular targets for future therapeutics.

#### **1.4. Analysis**

The section on bacterial detection serves to cover a brief selection of the many exciting new methods being developed to prepare synthetic polymers and to use them in biomedical application. Increases in the specificity of interactions are occurring as polymer chemists exert better control over the polydispersity of the materials that are synthesised which in turn leads to more precise display of cell-binding ligands from the resulting polymers. The use of bio-inspired approaches, such as the decoration of polypeptides that adopt specific conformations, but using the flexible arsenal of the modern synthetic chemist is also allowing the preparation of 'cell-complementary' structures that can bind to target analytes. Finally, improvements in the sensitivity of analytical devices, for example using techniques such as surface-enhanced resonance Raman scattering (SERRS), are enabling detection of biopolymers at the attomole level and below. These are all very encouraging developments when considering detection of many biological species, not only microorganisms. However, it should still be borne in mind that a single pathogenic cell can, if conditions are favourable, undergo replication and give rise to a population capable of causing harm. In

addition, if mutations occur in a bacterial or viral strain, any detection system designed to be specific to that strain may be rendered ineffective. As a consequence, there is increasingly a need to develop “self-evolving” or “smart” detection systems, that will respond to the local environment in order to be able to detect changes in the analyte species. Polymers and sensor systems of this type will form the next generation of analytical devices.

### **1.5. Polymer-cell interactions - Principles of bacterial adhesion**

The first examples considered for polymer-cell interactions are those of bacterial adhesion. Although bacteria, and especially their colonies are in fact highly complex, they are still inherently simpler than eukaryotic cells, and hence are considered first here.

The mechanisms of bacteria adhesion are of paramount importance in biotechnological applications and are central to biosensors technology, and development of antimicrobials and infection-resistant surfaces. Adhesion can be considered a phenomenon where bacteria attach to a surface by active physicochemical interactions. The broad definition implies that there are numerous mechanisms involved which make cell/surface interactions a rather complicated field of study.

Generally, adhesion is driven by long and short range interactions. In the former case, can be regarded van der Waals, gravitational forces, hydrophobicity and electrostatic charge which are all non-specific and take place in distances greater than 150 nm and can be expressed as functions of free energy and distance. Short range interactions are effective at distances less than 3 nm and involve specific chemical bonding, and ionic interactions. Therefore, long range interactions occur first, and make it feasible for bacteria to be in a position subsequently to interact with the surface via short range interactions and achieve adhesion in a more selective manner.

Hydrophobicity is a relative description and provides a scale of order for the water molecules in the first tens of molecular layers. Intermolecular interactions (i.e. hydrogen bonds) are apparent near hydrophilic surfaces whereas water molecules are less structured on hydrophobic surfaces. The hydrophobicity/hydrophilicity of a surface is usually determined by contact angle measurements. The hydrophobicity of bacteria varies according to the species and the bacterial surface properties. In general, hydrophobic bacteria prefer hydrophobic substrates. Similarly, hydrophilic bacteria adhere to hydrophilic surfaces.

Bacteria in aqueous media are negatively charged. In addition, high surface charge is usually correlated with hydrophilic character of the bacterial surface. It has been found that electrostatic interactions of bacteria with surfaces may have an initial role to the initial phase of adhesion but they are not crucial when specific interactions start to dominate.

Roughness is defined as the average distance between peaks and valleys present on a surface and is expressed as an arithmetic mean value. It has been found that rough surfaces promote bacterial adhesion and this is attributed to the increment of the surface area and the presence of more favorable sites for bacteria to adhere [52, 53].

Varying levels of roughness, hydrophobicity and charge-charge interactions tend to be present in all cell-material interfaces and are thus present for all bacteria-polymer interactions – however, of greater importance in biomedical surfaces are the more specific interactions at the lower length scales.

Specific interactions of particular interest are those that involve lectins. Lectins are carbohydrate binding proteins found in most living organisms. They are involved in numerous biological processes such as cell

interactions in the immune system, malignancy and metastasis of cancerous cells, and virus infection. According to the way by which binding with carbohydrates occurs, lectins have been categorized into two families; The group I lectins that completely envelop ligands in deep pocket-like domains and the group II where binding occurs in shallow pockets on the protein surface. The pocket-like domains are preformed since no significant change in conformation has been observed upon binding. Lectins interact with carbohydrates by forming non-covalent bonds which are reversible and highly specific. The binding that occurs in the carbohydrate recognition domain (CRD) of lectins is mainly attributed to hydrogen bonding of the carbonyl groups of the protein and the hydroxyl groups of the sugar molecules [54, 55].

The characteristic of lectin-carbohydrate binding is that the hydroxyl groups act both as electron donors and acceptors. This is because the oxygen of the OH group is  $sp^3$  hybridized thus having two lone pair of electrons and one proton. Therefore, the OH can act both as an acceptor of two hydrogen bonds and as a donor of a single hydrogen bond. In most cases of lectin-carbohydrate systems, hydrogen bonding has a cooperative character. For example, periplasmic transporter proteins bind with all hydroxyl groups of the bound carbohydrate in a cooperative manner. Conversely, other systems have been shown to interact with specific hydroxyls such as the Con A-glucose system where the hydroxyl at the C2 position is completely solvent exposed and does not contribute to the binding with the CRD [56].

Van der Waals forces have also been found to contribute to the overall binding despite their weak nature. The presence of calcium cations (or transition metals) also play a role in fixing the amino acids to find the optimum position to bind ligands effectively but they are not directly involved in the binding process. Only in C-type lectins,  $Ca^{2+}$  forms

coordination bonds with the sugar ligand. One lone pair of electrons from two vicinal hydroxyl groups coordinate with the  $\text{Ca}^{2+}$ , whereas the other two lone pairs form hydrogen bonds with amide groups. The only other direct carbohydrate-metal interaction is that of xylose isomerase where two  $\text{Mg}^{2+}$  coordinate with sugars.

Also water seems to play a role in the lectin-sugar binding. Water molecules act as interstitial compounds by forming bridges between the lectin and the sugar and further stabilize the protein-sugar complexes. Molecular dynamics simulations have shown that water molecules are in constant motion and that only few of them have long lifetime upon complexation [56].

One of the most interesting characteristics of lectins-monosaccharide interactions is that they are of weak affinity in nature especially when compared with enzyme-substrate specific associations; in most cases the dissociation constants range in the millimolar order of magnitude. But then how can lectins act as recognition molecules and mediate crucial biological processes? The pioneering work of Reiko Lee in the 90s elucidated how nature employs multivalency in order to overcome weak affinity between lectins and monosaccharides. Y. C. Lee and R. T. Lee used chicken and rat hepatic lectins which bind to N-acetylgalactosamine (GalNAc) and N-acetylglucosamine (GlcNAc) respectively. They observed that when using neoglycoproteins bearing large number of sugars as ligands, the binding affinity was increased geometrically (fell to the nanomolar range) whereas the monosaccharide counterparts had an affinity in the range 0.1-1.0 mM. The term cluster glycoside effect was coined to describe the increment of the degree of dependency of affinity towards valency [57].

Since then, many lectin-sugar systems have been studied in an effort to relate the structure of a ligand to the interaction with the receptor. There are four widely used methods that have been employed for these studies, the hemagglutination inhibition assay (HIA), the enzyme linked lectin assay (ELLA), isothermal titration microcalorimetry (ITC) and surface plasmon resonance (SPR) which are explained in basic detail in review [58].

There are many lectin-sugar systems that have been studied thus far. Research in the field is intense because carbohydrates have been recognised as molecules of paramount importance that mediate numerous biological processes.

Recently, arrays initially developed for cDNA were modified for carbohydrate-carbohydrate and carbohydrate-protein interactions. Microarrays have been developed by several research groups mainly by exploiting tools developed by miniaturization technologies [59-61]; this technology is likely to be very useful for future studies since it provides high throughput screening which is considered a prerequisite for systematic analysis of the vast number of protein-sugar combinations that exist.

A convenient way to study the interactions of lectins with carbohydrates, and multivalency in principle, is by introducing sugar groups to polymers in a sequential and/or selective way. Perhaps the most convenient means to achieve this is via glycopolymers which are defined as polymers with pendant carbohydrate molecules. The definition differentiates them from biopolymers where the polymer chains consist of carbohydrates. Synthetic polymers have already started to dominate the research in biomedical applications mainly because they are soft in nature and can be tailored to resemble human tissue properties and structure [62]. Now it is possible to

design polymers exclusively for biomedical purposes rather than modifying existing materials made for other applications [63].

### 1.6. Aim of the PhD

The aim of this PhD is to probe polymer-cell interactions by rational polymer design with the ultimate goal to set a very first platform design for future smart therapeutics that can exhibit bioresponsive and even “life-like” characteristics. By exploiting modern polymerization techniques we aim to build self-assembled capsule-mimicking structures (i.e. vesicles) that can serve as prototype copycats of natural cell membranes. Also, we aim to establish a primitive communication of the artificial structures with their natural counterparts (i.e. bacterial cells) by using the “glyco-code” as a means of biochemical language. Finally, coupling of these communication events with naturally occurring prebiotic reactions in a dynamic context should lead to the establishment of a biological version of the well-known Turing test in order to set the platform to start questioning how much alive an artificial structure can be. Ultimately, the knowledge acquired by this exercise should be expected to contribute to the realization of novel intelligent therapeutics that truly resemble the function of natural cells and lead to more effective albeit less invasive therapies.

In the second chapter, we explore the possibility of embedding the high specificity of the ligand-receptor interactions found in the area of carbohydrates to polymeric materials. We introduce simple carbohydrate molecules in a well studied thermoresponsive polymer poly(N-isopropylacrylamide) in order to synthesize copolymers with dual functionality. We aim to reversibly control the bacterial adhesion by these novel polymers via multivalency and thermoresponsiveness and therefore set the grounds for primitive polymer-cell communication networks.

In chapter three we extend this strategy by introducing block copolymers that can self-assemble in spherical glycoobjects of comparable size to bacterial cells. Bacterial adhesion/clustering is again aimed to be mediated by the specific interaction of the sugar units presented on the vesicular coroneae with the carbohydrate recognition sites on the bacterial fibrils. We also aim to make distinct vesicle-bacteria complexes that only form under certain specific conditions. Then, we aim to establish a very first step towards vesicle-bacteria communication.

If we can achieve transport from the vesicles to the cells, we plan to explore whether this strategy is applicable with real “linguistic molecules” commonly used in microbiological networks. The communication among bacteria is known to be mediated by signalling networks that involve diffusion/transport of small molecules, known as quorum sensing. We will then start to explore this communication platform in order to incorporate elements of these processes to our primitive cell mimics using the quorum sensing network of *Vibrio harveyi* as it is well studied and easily monitored with bioluminescence assays.

As a very first model we plan to test this hypothesis by using simple thermoresponsive polymers that can capture and release these “linguistic molecules” reversibly via thermal stimuli. We regard these polymers as precursors of the vesicular cell-mimics that will provide us with enough evidence on the bacterial response to the signalling perturbation induced by the presence of the former. Proof of the concept, if successful, will set the grounds towards achieving dynamic intervention on the bacterial communication network and achieve multiple communication cycles according to the polymers conformation.

We therefore discuss in the final chapter the principles of this very integration and the prerequisites needed in order to fully implement a

meaningful and bidirectional communication cycle for all the entities involved (bacteria and their artificial counterparts). Successful compilation of this “imitation game” could potentially lead to artificial structures that can act as smart cell-mimics with “life-like” characteristics as a novel approach towards less invasive therapies of high potency and perhaps, as Ehrlich dreamt in the 1910s, bring us closer to the holy grail of the “magic bullet that cures all diseases”.

### 1.7. References

1. Kumar, A., A. Srivastava, I.Y. Galaev, and B. Mattiasson, *Smart polymers: Physical forms and bioengineering applications*. Progress in Polymer Science, 2007. **32**(10): p. 1205-1237.
2. Galaev, I.Y. and B. Mattiasson, *'Smart' polymers and what they could do in biotechnology and medicine*. Trends in Biotechnology, 1999. **17**(8): p. 335-340.
3. Lutolf, M.P., G.P. Raeber, A.H. Zisch, N. Tirelli, and J.A. Hubbell, *Cell-responsive synthetic hydrogels*. Advanced Materials, 2003. **15**(11): p. 888-892.
4. Ulijn, R.V. and A.M. Smith, *Designing peptide based nanomaterials*. Chemical Society Reviews, 2008. **37**(4): p. 664-675.
5. Ulijn, R.V., N. Bibi, V. Jayawarna, P.D. Thornton, S.J. Todd, R.J. Mart, A.M. Smith, and J.E. Gough, *Bioresponsive hydrogels*. Materials Today, 2007. **10**(4): p. 40-48.
6. Ulijn, R.V., *Enzyme-responsive materials: a new class of smart biomaterials*. Journal of Materials Chemistry, 2006. **16**(23): p. 2217-2225.
7. Mann, S., *Life as a nanoscale phenomenon*. Angewandte Chemie-International Edition, 2008. **47**(29): p. 5306-5320.
8. Braunecker, W.A. and K. Matyjaszewski, *Controlled/living radical polymerization: Features, developments and perspectives (vol 32, pg 93, 2007)*. Progress in Polymer Science, 2008. **33**(1): p. 93-146.

9. Matyjaszewski, K. and J.H. Xia, *Atom transfer radical polymerization*. Chemical Reviews, 2001. **101**(9): p. 2921-2990.
10. Teodorescu, M. and K. Matyjaszewski, *Atom transfer radical polymerization of (meth)acrylamides*. Macromolecules, 1999. **32**(15): p. 4826-4831.
11. Patten, T.E. and K. Matyjaszewski, *Atom transfer radical polymerization and the synthesis of polymeric materials*. Advanced Materials, 1998. **10**(12): p. 901-915.
12. Patten, T.E., J.H. Xia, T. Abernathy, and K. Matyjaszewski, *Polymers with very low polydispersities from atom transfer radical polymerization*. Science, 1996. **272**(5263): p. 866-868.
13. Moad, G., E. Rizzardo, and S.H. Thang, *Radical addition-fragmentation chemistry in polymer synthesis*. Polymer, 2008. **49**(5): p. 1079-1131.
14. Moad, G., E. Rizzardo, and S.H. Thang, *Toward Living Radical Polymerization*. Acc. Chem. Res., 2008. **41**(9): p. 1133-1142.
15. Tanaka, H., *Captodative modification in polymer science*. Progress in Polymer Science, 2003. **28**(7): p. 1171-1203.
16. Fischer, H., *The persistent radical effect: A principle for selective radical reactions and living radical polymerizations*. Chemical Reviews, 2001. **101**(12): p. 3581-3610.
17. Goto, A. and T. Fukuda, *Effects of radical initiator on polymerization rate and polydispersity in nitroxide-controlled free radical polymerization*. Macromolecules, 1997. **30**(15): p. 4272-4277.
18. Mammen, M., S.K. Choi, and G.M. Whitesides, *Polyvalent Interactions in Biological Systems: Implications for Design and Use of Multivalent Ligands and Inhibitors*. Angewandte Chemie-International Edition, 1998. **37**(20): p. 2755-2794.
19. Sharon, N., *Carbohydrates as future anti-adhesion drugs for infectious diseases*. Biochimica et Biophysica Acta (BBA) - General Subjects, 2006. **1760**(4): p. 527-537.

20. Disney, M.D., J. Zheng, T.M. Swager, and P.H. Seeberger, *Detection of bacteria with carbohydrate-functionalized fluorescent polymers*. Journal Of The American Chemical Society, 2004. **126**(41): p. 13343-13346.
21. Kim, B.S., D.J. Hong, J. Bae, and M. Lee, *Controlled self-assembly of carbohydrate conjugate rod-coil amphiphiles for supramolecular multivalent ligands*. Journal of the American Chemical Society, 2005. **127**(46): p. 16333-16337.
22. Kim, B.S., W.Y. Yang, J.H. Ryu, Y.S. Yoo, and M. Lee, *Carbohydrate-coated nanocapsules from amphiphilic rod-coil molecule: binding to bacterial type 1 pili*. Chemical Communications, 2005(15): p. 2035-2037.
23. Park, K.H., W.J. Sung, S.W. Kim, D.H. Kim, T. Akaike, and H.M. Chung, *Specific interaction of mannosylated glycopolymers with macrophage cells mediated by mannose receptor*. Journal Of Bioscience And Bioengineering, 2005. **99**(3): p. 285-289.
24. Miura, Y., N. Wada, Y. Nishida, H. Mori, and K. Kobayashi, *Chemoenzymatic synthesis of glycoconjugate polymers starting from nonreducing disaccharides*. Journal Of Polymer Science Part A-Polymer Chemistry, 2004. **42**(18): p. 4598-4606.
25. Ladmiral, V., G. Mantovani, G.J. Clarkson, S. Cauet, J.L. Irwin, and D.M. Haddleton, *Synthesis of neoglycopolymers by a combination of "click chemistry" and living radical polymerization*. Journal Of The American Chemical Society, 2006. **128**(14): p. 4823-4830.
26. Sen Gupta, S., K.S. Raja, E. Kaltgrad, E. Strable, and M.G. Finn, *Virus-glycopolymer conjugates by copper(I) catalysis of atom transfer radical polymerization and azide-alkyne cycloaddition*. Chemical Communications, 2005(34): p. 4315-4317.
27. Xue, C.H., V.R.R. Donuru, and H.Y. Liu, *Facile, versatile prepolymerization and postpolymerization functionalization approaches for well-defined fluorescent conjugated fluorene-based glycopolymers*. Macromolecules, 2006. **39**(17): p. 5747-5752.

28. Wang, Y. and K.L. Kiick, *Monodisperse protein-based glycopolymers via a combined biosynthetic and chemical approach*. Journal Of The American Chemical Society, 2005. **127**(47): p. 16392-16393.
29. Polizzotti, B.D. and K.L. Kiick, *Effects of polymer structure on the inhibition of cholera toxin by linear polypeptide-based glycopolymers*. Biomacromolecules, 2006. **7**(2): p. 483-490.
30. Sun, C.Y., Y.J. Zhang, Y. Fan, Y.J. Li, and J.H. Li, *Mannose-Escherichia coli interaction in the presence of metal cations studied in vitro by colorimetric polydiacetylene/glycolipid liposomes*. Journal Of Inorganic Biochemistry, 2004. **98**(6): p. 925-930.
31. Su, Y.L., J.R. Li, L. Jiang, and J. Cao, *Biosensor signal amplification of vesicles functionalized with glycolipid for colorimetric detection of Escherichia coli*. Journal Of Colloid And Interface Science, 2005. **284**(1): p. 114-119.
32. Alexander, C., H.S. Andersson, L.I. Andersson, R.J. Ansell, N. Kirsch, I.A. Nicholls, J. O'Mahony, and M.J. Whitcombe, *Molecular imprinting science and technology: a survey of the literature for the years up to and including 2003*. Journal Of Molecular Recognition, 2006. **19**(2): p. 106-180.
33. Haupt, K., *Imprinted Polymers - Tailor-Made Mimics of Antibodies and Receptors*. Chemical Communications, 2003(2): p. 171-178.
34. Piletsky, S.A. and A.P.F. Turner, *Electrochemical Sensors Based on Molecularly Imprinted Polymers*. Electroanalysis, 2002. **14**(5): p. 317-323.
35. Whitcombe, M.J., C. Alexander, and E.N. Vulfson, *Smart Polymers for the Food Industry*. Trends in Food Science & Technology, 1997. **8**(5): p. 140-145.
36. Aherne, A., C. Alexander, M.J. Payne, N. Perez, and E.N. Vulfson, *Bacteria-Mediated Lithography of Polymer Surfaces*. Journal of the American Chemical Society, 1996. **118**(36): p. 8771-8772.
37. Harvey, S.D., G.M. Mong, R.M. Ozanich, J.S. McLean, S.M. Goodwin, N.B. Valentine, and J.K. Fredrickson, *Preparation and evaluation of spore-*

- specific affinity-augmented bio-imprinted beads*. *Analytical And Bioanalytical Chemistry*, 2006. **386**(2): p. 211-219.
38. Bolisay, L.D., J.N. Culver, and P. Kofinas, *Molecularly imprinted polymers for tobacco mosaic virus recognition*. *Biomaterials*, 2006. **27**(22): p. 4165-4168.
39. Michalet, X., F.F. Pinaud, L.A. Bentolila, J.M. Tsay, S. Doose, J.J. Li, G. Sundaresan, A.M. Wu, S.S. Gambhir, and S. Weiss, *Quantum Dots for Live Cells, in Vivo Imaging, and Diagnostics*. *Science*, 2005. **307**(5709): p. 538-544.
40. de la Fuente, J.M. and S. Penades, *Glyconanoparticles: Types, synthesis and applications in glycoscience, biomedicine and material science*. *Biochimica et Biophysica Acta (BBA) - General Subjects*, 2006. **1760**(4): p. 636.
41. de la Fuente, J.M. and S. Penades, *Synthesis of Le(x)-neoglycoconjugate to study carbohydrate-carbohydrate associations and its intramolecular interaction*. *Tetrahedron-Asymmetry*, 2002. **13**(17): p. 1879-1888.
42. Babu, P., S. Sinha, and A. Surolia, *Sugar-quantum dot conjugates for a selective and sensitive detection of lectins*. *Bioconjugate Chemistry*, 2007. **18**(1): p. 146-151.
43. Sun, X.L., W.X. Cui, C. Haller, and E.L. Chaikof, *Site-specific multivalent carbohydrate labeling of quantum dots and magnetic beads*. *Chembiochem*, 2004. **5**(11): p. 1593-1596.
44. Krishnamurthy, V.M., L.J. Quinton, L.A. Estroff, S.J. Metallo, J.M. Isaacs, J.P. Mizgerd, and G.M. Whitesides, *Promotion of opsonization by antibodies and phagocytosis of Gram-positive bacteria by a bifunctional polyacrylamide*. *Biomaterials*, 2006. **27**(19): p. 3663-3674.
45. Chung, H.A., K. Tajima, K. Kato, N. Matsumoto, K. Yamamoto, and T. Nagamune, *Modulating the actions of NK cell-mediated cytotoxicity using lipid-PEG (n) and inhibitory receptor-specific antagonistic peptide conjugates*. *Biotechnology Progress*, 2005. **21**(4): p. 1226-1230.

46. Chung, H.A., K. Kato, C. Itoh, S. Ohhashi, and T. Nagamune, *Casual cell surface remodeling using biocompatible lipid-poly(ethylene glycol)(n): Development of stealth cells and monitoring of cell membrane behavior in serum-supplemented conditions*. *Journal Of Biomedical Materials Research Part A*, 2004. **70A**(2): p. 179-185.
47. Boonyarattanakalin, S., S. Athavankar, Q. Sun, and B.R. Peterson, *Synthesis of an artificial cell surface receptor that enables oligohistidine affinity tags to function as metal-dependent cell-penetrating peptides*. *Journal Of The American Chemical Society*, 2006. **128**(2): p. 386-387.
48. Peterson, B.R., *Synthetic mimics of mammalian cell surface receptors: prosthetic molecules that augment living cells*. *Organic & Biomolecular Chemistry*, 2005. **3**(20): p. 3607-3612.
49. Federle, M.J. and B.L. Bassler, *Interspecies Communication in Bacteria*. *Journal of Clinical Investigation*, 2003. **112**(9): p. 1291-1299.
50. Daniels, R., J. Vanderleyden, and J. Michiels, *Quorum sensing and swarming migration in bacteria*. *Fems Microbiology Reviews*, 2004. **28**(3): p. 261-289.
51. Kato, N., T. Morohoshi, T. Nozawa, H. Matsumoto, and T. Ikeda, *Control of gram-negative bacterial quorum sensing with cyclodextrin immobilized cellulose ether gel*. *Journal Of Inclusion Phenomena And Macrocyclic Chemistry*, 2006. **56**(1-2): p. 55-59.
52. An, Y.H. and R.J. Friedman, *Concise review of mechanisms of bacterial adhesion to biomaterial surfaces*. *Journal of Biomedical Materials Research*, 1998. **43**(3): p. 338-348.
53. Drotleff, S., U. Lungwitz, M. Breunig, A. Dennis, T. Blunk, J. Tessmar, and A. Gopferich, *Biomimetic polymers in pharmaceutical and biomedical sciences*. *European Journal of Pharmaceutics and Biopharmaceutics*, 2004. **58**(2): p. 385-407.
54. Zelensky, A.N. and J.E. Gready, *The C-type lectin-like domain superfamily*. *Febs Journal*, 2005. **272**(24): p. 6179-6217.

55. Cambi, A. and C.G. Figdor, *Levels of complexity in pathogen recognition by C-type lectins*. *Current Opinion in Immunology*, 2005. **17**(4): p. 345-351.
56. Rini, J.M., *Lectin Structure*. *Annual Review of Biophysics and Biomolecular Structure*, 1995. **24**: p. 551-577.
57. Lee, Y.C. and R.T. Lee, *Carbohydrate-Protein Interactions - Basis of Glycobiology*. *Accounts of Chemical Research*, 1995. **28**(8): p. 321-327.
58. Lundquist, J.J. and E.J. Toone, *The cluster glycoside effect*. *Chemical Reviews*, 2002. **102**(2): p. 555-578.
59. Ratner, D.M., E.W. Adams, M.D. Disney, and P.H. Seeberger, *Tools for glycomics: Mapping interactions of carbohydrates in biological systems*. *ChemBiochem*, 2004. **5**(10): p. 1375-1383.
60. Houseman, B.T. and M. Mrksich, *Carbohydrate arrays for the evaluation of protein binding and enzymatic modification*. *Chemistry & Biology*, 2002. **9**(4): p. 443-454.
61. Feizi, T., F. Fazio, W.C. Chai, and C.H. Wong, *Carbohydrate microarrays - a new set of technologies at the frontiers of glycomics*. *Current Opinion in Structural Biology*, 2003. **13**(5): p. 637-645.
62. Ladmiral, V., E. Melia, and D.M. Haddleton, *Synthetic glycopolymers: an overview*. *European Polymer Journal*, 2004. **40**(3): p. 431-449.
63. Cunliffe, D., S. Pennadam, and C. Alexander, *Synthetic and biological polymers-merging the interface*. *European Polymer Journal*, 2004. **40**(1): p. 5-25.

## Chapter 2

# *Control of bacterial aggregation by thermoresponsive glycopolymers*

### **2. Introduction**

The ability to control the interactions of bacteria with receptors and surfaces is fundamental to pathogen detection, anti-infection strategies and, ultimately, to public health [1, 2]. Many bacteria have evolved specific adhesion structures such as fimbriae that bind to host cell glycoconjugates, thus exploiting the recognition and signalling pathways of sugar-bearing biopolymers that constitute the “glycocode”. Oligosaccharides have been used to block bacteria-cell interactions as a means to combat infection, while artificial glycopolymers that agglutinate bacteria through multiple cooperative polymer-cell interactions have been described for detection and deactivation of pathogens [3-5].

Perhaps the most well studied system so far are polymer inhibitors of pathogens such as polyacrylamide polymers with pendant copies of the C-glycoside of sialic acid developed by the Whitesides group [6]. The particular system prevents the crosslinking of erythrocytes by virus (hemagglutination inhibition) at concentrations of 35 pM, whereas the monomeric  $\alpha$ -methylsialoside counterparts inhibit hemagglutination at 2 nM concentration. This  $10^8$  fold enhancement is the largest known to date [4, 6].

An elegant way to study cell signaling responses in presence of external stimuli is bacterial chemotaxis. One of the most profound examples of this kind is from the pioneering work of Dr. Kiessling; her group employed ring

opening polymerization (ROMP) to produce linear glycopolymers. ROMP has the advantage that is a living/controlled polymerization method and polymers of narrow polydispersities can derive [7]. Polymers bearing multiple copies of galactose, of varying valencies were synthesized, and chemotactic responses as a means of controlling the angular velocity of the bacteria in presence of chemoattractants were studied [8]. In a different study from the same group it was found that synthetic multivalent ligands showed 100-fold amplification of E. Coli response compared to monovalent ligands [9]. Neoglycopolymers substituted with sialyl Lewis x derivatives were also found to inhibit L-selectin mediated leukocytes rolling to the endothelium by blocking L-selectin contacts with the endothelium wall. These compounds are promising for designing novel anti-inflammatory medicines [10].

The polyvalent binding strategy has also been exploited by Disney et al. to produce lectin- and bacteria-recognition materials [11]. Specifically, water soluble fluorescent glycopolymers prepared from poly(p-phenylene ethylene) were derivatized with carbohydrate moieties using a post-polymerization method. Coupling of sugar species with the polymer backbone was accomplished by using standard carbodiimide chemistry which resulted in polymers with 25% sugar functionalization of the reactive sites. Several polymer batches were synthesized varying the saccharide attached to the backbone. Mannosylated polymers strongly interacted with Con A whereas the galactosylated counterparts did not show any binding with the lectin, demonstrating the specific binding character of the polymers. This group was also able to observe bacteria clustering, following polymer addition due to the polyvalent nature of the binding process. The images that the researchers provided resemble those of the present work (see Results and Discussion section) and to our knowledge, it is the only study that provides such results deriving from the interactions of carbohydrate-bearing polymers with living organisms, namely bacteria.

However, for practical use, reversibility in the material-cell-binding behaviour is often needed, i.e. that interactions with bacteria can be switched on for capturing the organism and switched off for removal of cells prior to the next assay. In addition, reversible cell binding could be used as a means for controlling biofilm formation. In the present work we attempt to elevate the complexity of action of polymeric materials by introducing thermoresponsive polymers as an additional “function” that would facilitate reversible ligand-host interaction governed by external stimulus. Such an approach would bring us closer to natural bioprocesses where dynamic responses of biological signalling are elegantly dependant by subtle changes of a variety of stimuli (i.e. a pH gradient, analyte concentration etc.).

Thermoresponsive polymers have been used extensively in the past for many of applications in the biotechnological arena. Notably, the keyword ‘N-isopropylacrylamide’ in the Web of Science (WoS) database results in more than 5000 papers directly related to NIPAM its physicochemical properties and its applications. Indeed PNIPAM is a very well studied polymer and is the polymer of choice in the majority of applications where responsive polymers are involved. As discussed previously, NIPAM exhibits sharp coil-to-globule transition above 32 °C known as the lower critical solution temperature (LCST). LCST can be directly tuned by copolymerization of NIPAM with a hydrophilic or lipophilic monomer. In fact, the change of the LCST is directly proportional to the monomer content in the final polymer. For example, copolymerization of 10% of the hydrophilic acrylamide monomer with NIPAM will produce a polymer with sharp LCST at 37 °C i.e. near physiological temperature (see reference [12] for example). Hence, one can relatively easily, synthesize polymers with desired thermoprecipitation properties. This very property is exploited for a variety of applications such as affinity separations, protein purification, drug delivery, polymer-protein bioconjugates and hydrogel design for tissue engineering applications [13]. However, in order to fully exploit this unique property of reversible phase

separation of these materials one must introduce some extra functionality to achieve a more complex activity in the biological context.

Indeed, there are studies where researchers have tried to copolymerize hydrophilic/lipophilic segments not only to fine tune the LCST of the final polymer but to achieve active reversible ligand display with the scope of achieving stimulus driven interaction of the polymer with the biological target. The limitation to this approach though is that it is difficult to incorporate sufficient amount of the secondary functional monomer without losing the LCST property or shifting it to irrelevant levels (i.e. way above physiological temperature). For this reason, most studies involving thermoresponsive polymers use the latter as actuators to regulate interactions that originate from an entity separate from the polymer backbone. Polymer-protein bioconjugates are a characteristic example of this approach as a NIPAM homopolymer is grafted near the receptor binding pocket of a protein and hence regulating the activity of the latter in a stimulus dependant manner. When the polymer is solvated below LCST the binding pocket of the protein is fully accessible to the protein substrate thus “switching on” the protein, whereas above the LCST the polymer collapses and interacts with the protein binding site which in turn renders the latter inaccessible [14].

Lee and Park have exploited this approach by conjugating a poly(N-isopropylacrylamide-co-glucosyloxyethyl methacrylate) P(NIPAM-co-GEMA) copolymer to trypsin in an attempt to regulate the enzymes activity in accordance to the thermoprecipitation properties of the polymer [15]. They coupled the carboxy terminated copolymer with the free amines on the surface of trypsin via standard carbodiimide coupling and found that there was a degree of correlation of the enzyme activity to the polymers LCST, albeit not a binary response at the polymers phase transition. Nevertheless, they managed to retain significant amount of the enzyme’s activity despite

the chemical modification with the polymer and prevented self-digestion to acceptable levels. To our knowledge, this is the only study that NIPAM is combined with a glycomonomer (GEMA) to produce a polymer that can thermally stabilize the enzyme in presence of the hydrophilic sugar moieties. It is also worth mentioning, that the LCSTs of these polymers were above physiological range but at acceptable levels for protein stability (40-45 °C for 5-10% GEMA content).

The concept of hide-and-reveal through temperature switch with concerted polymer activity deriving from the polymer itself has also been demonstrated by others.

Dizman et al. combined NIPAM with a novel pyridine methacrylamide monomer that can be further quaternized with various bromoalkanes to produce polymers with antibacterial activities [16]. The researchers found that the quaternized polymers had significant antibacterial action against common pathogens (tested with *E. coli* and *S. aureus*) when in a soluble state. On the contrary, collapsed polymers had no activity, implying the “hiding” of the charged pyridine segments due to temperature stimulus.

Fujimoto et al. synthesized a copolymer based on NIPAM and N-hydroxysuccinimide precursor which was then reacted with the arginine-glycine-aspartate-serine (RGDS) tetrapeptide [17]. RGDS is a known and widely used peptide motif that is used to selectively bind to integrins (cell-surface receptors). The peptide-rich polymers could form stable aggregates above LCST and form stable physical assemblies with the relatively lipophilic dolichyl phosphate or dolichol apoptosis factors. In solution, a decrease of temperature ( $T < \text{LCST}$ ), rendered the polymers soluble, RGD peptides were exposed to the cell surface and therefore could bring the apoptosis factors in close proximity to the cellular surface in order to facilitate cell apoptosis by this temperature switch. Retention of temperature

above LCST was found to continuously stabilise the polymer aggregates without significant leakage of the surface adsorbed apoptosis factors. It should be noted that it is the presence of the hydrophilic RGD motif that gives an amphiphilic character to the polymer backbone which in turn results in the formation of uniform polymer aggregates above LCST. Presumably, this implies that a small number of the RGD motifs should be exposed in solution even when the polymer is in a globular state.

This hypothesis was also investigated by Hopkins et al. [18], where they synthesized a highly branched polymer based on NIPAM as the thermosensitive segment copolymerized with the hydrophilic 1,2-propanediol-3-methacrylate terminated with imidazole groups. The polymer also contained anthracene methyl methacrylate groups that, upon polymer collapse above LCST, formed fluorescently traceable uniform micron-sized aggregates. These sub-micron-sized particles were taken up by dermal fibroblasts by phagocytosis and because of their fluorescent character, the researchers could conveniently monitor the particles' cellular internalization. Only particles above LCST were found to be internalized inside the cellular compartments, whereas free soluble polymer below LCST was not taken up. The same group also presented preliminary results on branched NIPAM decorated with vancomycin [19]. The latter is a strong antibiotic against gram-positive bacteria and it acts by strong binding to the D-alanyl-D-alanine present on the peptidoglycan matrix. Hence, the researchers exploited this binding capability of vancomycin and found that the polymer synthesized was forming large aggregates when mixed with *S. aureus* due to the polyvalent interactions between the bacteria receptors and the polymer-bound vancomycin. However, the polymers synthesized did not exhibit an LCST, presumably due to the relatively large size of the hydrophilic vancomycin. Nevertheless, these preliminary results resemble the interactions of the polymers we envision to synthesize in the current work with certain bacteria species in a similar fashion.

Thus far, no one has used thermoresponsive polymers to achieve reversible binding to any biological host in a multivalent manner, despite the fact that in the past several examples of synthetic linear polymers have been well celebrated for their multivalent mode of action against biological hosts.

Our goal therefore was to switch on and off the interaction of a polymer with a biological host via application of external thermal stimuli that will induce dramatic change in the physicochemical properties of the polymer in such a way that the interaction with the targeted host will be suppressed.

This chapter describes the reversible aggregation of a specific bacterial strain controlled by thermoresponsive glycopolymers as the first step toward robust and reusable cell-sensing materials. Furthermore, it is shown that polymer activity in bacterial agglutination is achievable with rather simple sugar functionality, employing multiple glucose residues able to control cell aggregation through a combination of the cluster glycoside effect and polymer conformation.

## **2.1. Materials and Methods**

### **2.1.1. Instrumentation**

All solvents and reagents were of analytical or HPLC grade and purchased from Sigma or Fisher Scientific unless otherwise stated. Deuterated solvents were from Sigma or Cambridge Isotopes. N-isopropylacrylamide (NIPAM, Sigma) was recrystallized from hexane. Azobis(isobutylnitrile) (AIBN, Fisher) was recrystallised from ethanol. N-hydroxyethyl methacrylamide (HEMide) and acrylamido N-hexanoic acid (AA<sub>6</sub>) were synthesised according to previously published procedures [20, 21]. Beta-D-glucose pentaacetate (AcGlc) and methyl alpha-D-glucopyranoside (MeGlc) were purchased from Alfa Aesar. D-(+)-Glucosamine HCl (GlcN) was purchased from Fluka. Dialysis membranes were from Spectrapor. Gel Permeation Chromatography was carried out using Polymer Laboratories GPC 50 and

120 instruments with RI detector. Molecular weights were calculated based on universal calibration method using polystyrene standards. Tetrahydrofuran (THF) was used as the mobile phase with toluene trace as marker.  $^1\text{H}$  NMR spectra were recorded on a Bruker 400 MHz spectrometer. Cloud point measurements were measured by using a Beckman DU 640 UV/Vis spectrophotometer equipped with a thermostat unit. Fluorescence spectrometry was carried out using a Varian Cary Eclipse fluorescence spectrophotometer equipped with a peltier apparatus for temperature control. The KBr method was used for FTIR samples preparation, which were examined on a Perkin Elmer Paragon 1000 FTIR instrument. A Nikon optical microscope equipped with a camera connected to a personal computer was used for optical microscopy studies. Adobe Photoshop CS2 version 9.0 software was used for image analysis and bacteria aggregation quantification studies.

### 2.1.2. Polymer syntheses

The chemical synthesis of the polymers used in this study is shown in figure 2-1.

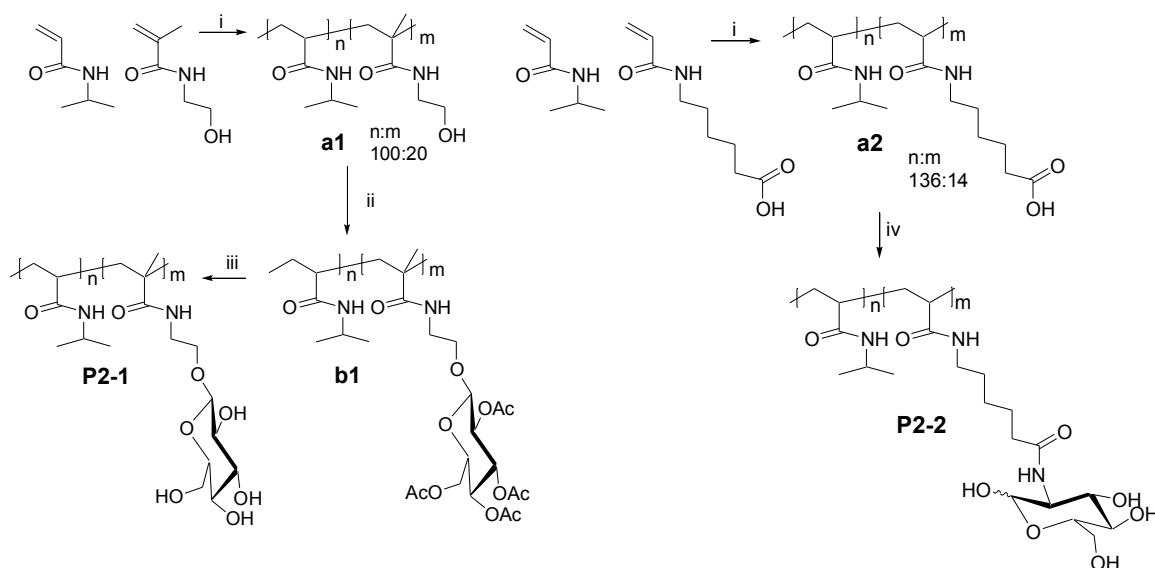


**Figure 2-1.** Synthesis of Polymers. i. THF, AIBN, 65 °C, 18 h ii. CHCl<sub>3</sub>/CH<sub>2</sub>Cl<sub>2</sub> (3/2), BF<sub>3</sub>Et<sub>2</sub>O, β-AcGlc, 12 h iii. MeOH, MeONa (cat.) 90 min. iv. HEPES pH 4.5, GlcN, EDC, NHS (cat.) 12 h.

### 2.1.3. a1, a2. Polymer synthesis (i)

Typical example of free radical polymerization for poly(NIPAM-st-HEMide) is given below. In a thick walled Schlenk flask, NIPAM and HEMide at molar ratios 80:20 were dissolved in THF (1 g/mL). 0.01 equivalent AIBN was added in the flask followed by three freeze thaw cycles using a vacuum line. The flask was placed in an oil bath at 65 °C for 18 hours. After cooling down to room temperature, the polymer was isolated by double precipitation in large excess of diethyl ether and dried under vacuum at 40 °C overnight (yield 91 %). The same procedure was followed for the preparation of a2 with relative monomer ratio NIPAM:AA<sub>6</sub> 90:10 (yield 83 %).

#### 2.1.4. b1. Sugar derivatisation (ii)

Polymer a1 (3.0 g) and AcGlc (2.0 g) were added to a round bottom flask, previously purged with N<sub>2</sub>, containing 60 mL anhydrous Chloroform/Dichloromethane (3:2 v:v, 60 mL) and molecular sieves (3A, 1.0 g). BF<sub>3</sub>Et<sub>2</sub>O (2 mL) in CH<sub>2</sub>Cl<sub>2</sub> (20mL) was then added dropwise via a glass syringe. The reaction was continued under nitrogen at 0 °C for 15 minutes and then left stirring at room temperature for 12 hours. Then, the reaction mixture was filtered and the solvent was removed by rotary evaporator. The residual material was then dissolved in a small amount of methanol and precipitated in excess diethyl ether twice to afford the polymer as a yellow powder (2.4 g, yield 80%).

#### 2.1.5. P2-1. Deprotection of AcGlc (iii)

Polymer b1 (2.0 g) was dissolved in anhydrous methanol (20 mL) and left stirring under a nitrogen atmosphere. A previously prepared solution of NaOMe in anhydrous methanol (5 mL, 0.1 M) was added through a syringe and the reaction mixture was left stirring for 90 minutes. Ion exchange resin (DOWEX® 50W2-200) was added to neutralise, followed by filtration. The polymer was recovered by precipitation in diethyl ether as a white powder which was finally dialysed against water for 2 days using a cellulose membrane with MWCO 1000 Da (yield 72%).

#### 2.1.6. P2-2. Derivatisation (iv)

Polymer a2 (500 mg) was dissolved in 4mL HEPES buffer (pH 4.5) containing EDC (400 mg) and NHS (100 mg). The reaction mixture was kept in an ice bath under vigorous stirring and a solution of GlcN (200 mg/mL, 3 mL) in HEPES buffer (pH 4.5) was added. The reaction was left stirring overnight with regular replenishing of EDC every 2-3 hours. Finally the polymer was recovered by freeze drying after being dialysed against water with a MWCO 1000 Da membrane for 3 days.

### 2.1.7. Cloud point measurements

LCST turbidity assays were performed by measuring the absorbance of polymer samples (PBS pH 7.4, 10 mg/mL) in respect to temperature (1 deg/min). The LCST was considered as the initial onset of a sharp increase in absorbance at 500 nm.

### 2.1.8. Anthrone assay

The anthrone-sulfuric acid method was used to quantify glucose attached on the polymers [22]. Anthrone (0.26 mmol, 50 mg) was first dissolved in absolute ethanol (1 mL) and then concentrated H<sub>2</sub>SO<sub>4</sub> (98 %) was added to bring the solution at 25 mL which was kept in the dark at 0 °C (solution I). Four standard glucose (or glucosamine, depending whether the assay concerns **P2-1** or **P2-2** respectively) solutions were prepared by dissolving increasing amounts of sugar in water (1 mM, 2 mM, 3 mM, 4 mM, solution II). Calibration standards were prepared by mixing 80 % H<sub>2</sub>SO<sub>4</sub>, (2 mL) with I (4 mL) and II (1 mL) in glass tubes, heating to 100 °C in the dark for exactly 15 minutes. After cooling to room temperature, absorbance was measured at 578 nm. A calibration curve of sugar concentration versus absorbance (A) was plotted and used for sugar detection on the polymers by measuring the absorbance of polymer samples (20 mg/L in water) as mentioned above.

### 2.1.9. Alizarin Red S (AR) assay

Alizarin Red S was also used to quantify the sugar content on the polymers according to the following protocol [23]. A stock solution of AR (0.1 mM) and PBA (1 mM) in glycine buffer (pH 9.3) was prepared (solution III). A calibration curve was constructed by preparing methyl-alpha-glucose standards of known concentration (0.1, 0.2, 0.3, 0.4, 0.5, 0.6, 0.7, 0.8 mM) using III. Fluorescence intensity was measured at 578 nm (excitation energy 460 nm). The sugar content on the polymers was measured similarly by preparing polymer solutions of 3 mg/mL in III and converting Fluorescence

Intensity (F.I.) to sugar mass based on the calibration curve from equation 2-1.

$$FI = -527.76 \log(\text{MeGlc} \cdot 10^3) + 1086.27, R^2=0.98 \quad (\text{eq. 2-1})$$

#### 2.1.10. AR assay for reversible Glc-PBA binding

To a freshly prepared glycine buffer (pH 9.3) AR (0.01 mM), phenylboronic acid (PBA, 0.05 nM) and polymer **P2-1** (or **P2-2**, 10 mg/mL) were dissolved. Immediate change in colour from burgundy to orange and subsequent slight colour fading was observed upon addition of PBA and polymer respectively. Sample (1 mL) was added in a quartz cuvette (1 cm path length) and the full fluorescence spectrum was recorded at temperatures above and below LCST. Various control experiments were conducted to eliminate factors influencing fluorescence intensity other than PBA-sugar binding; Diol release from PBA occurs in a time dependant manner<sup>5</sup> and hence 15 minutes were allowed for stability before recording each spectrum.

#### 2.1.11. Concanavalin A (Con A) assay

Con A (10 mg) was dissolved in freshly prepared assay buffer (0.1 M tris-HCl, 90  $\mu\text{M}$  NaCl, 1 mM  $\text{Ca}^{2+}$  and 1 mM  $\text{Mn}^{2+}$ , pH 7.5, 10 mL). **P2-1** (or **P2-2**) was dissolved using the same buffer (10 mg/mL). Equal volumes of Con A and polymer solutions (350  $\mu\text{L}$  of each) were mixed using a pipette for 5-10 seconds and transferred to a 1 mL quartz cuvette (1 cm path length); absorbance (A) at 550 nm was measured with time over 10 minutes. Then, the polymer-lectin complexes were centrifuged in order to isolate the polymer bound lectin from the polymer-protein complexes. The supernatant was decanted and replaced with a freshly prepared glucose solution (0.1 M glucose in buffer, 700  $\mu\text{L}$ ) to dissolve the polymer bound lectin. The latter was subsequently dissolved and was quantified by correlating the absorbance of each sample with a previously calibration lectin curve at 260

nm. Hence the absolute amount of lectin per standard polymer mass could be determined. The calibration curve used to quantify the lectin entrapment is given below:

$$[\text{Absorbance (A.U.)}] = 1.442[\text{ConA}(\mu\text{g})] + 0.0621, R^2=0.9995 \text{ (eq. 2-2)}$$

## 2.2. Results and Discussion

### 2.2.1. Synthesis of Polymer P2-1

The synthesis of P2-1 begins with the initial synthesis of a precursor polymer that was subsequently derivatized post-polymerization to produce the final material.

NIPAM was chosen as the thermoresponsive moiety as it gives polymers that exhibit sharp lower critical transition temperature at 32 °C which is near body temperature and its physicochemical properties in water have been studied extensively.

We then combined the monomer 2-hydroxyethyl methacrylamide (HEMide) as the sugar carrying moiety. This monomer is not readily available and was synthesised according to a previously published procedure [20].

The precursor polymer poly(NIPAM-co-HEMide) was first produced by means of free radical polymerization using AIBN as initiator. The resulting polymer was recovered in high yields which was then modified with peracetylated  $\beta$ -D-glucose under Lewis acid conditions. The mechanism of this reaction allows stereochemical control over the final product. The  $\text{BF}_3\text{Et}_2\text{O}$  activates the carbonyl at the anomeric position which acts as a leaving group. The cyclic oxonium ion which is formed by the involvement of the carbonyl protecting group at the 2 position is stabilised by cyclization. Then the hydroxyl nucleophile of the HEMAm monomer opens the cyclic

oxonium ion with such stereoselectivity that ensures formation of a  $\beta$ -glucoside [24]. The overall mechanism of this reaction is shown in figure 2-2.

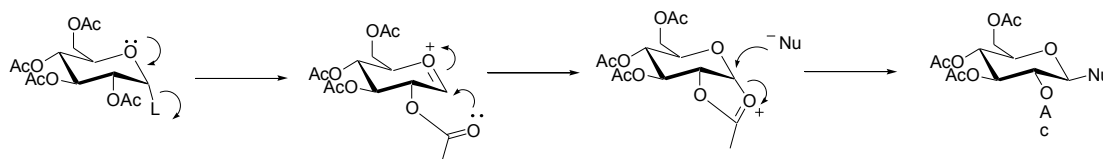


**Figure 2-2.** Reaction mechanism of the anomeric -OH with a nucleophile under acidic conditions.

It must be noted that generally this reaction exhibits high stereoselectivity and has been reported to give high yields (>80%). In this case though, glycosylation of the polymer precursor via this route gave around 32% yield. It is hypothesised that the polymer bound hydroxyl groups of the precursor are not sterically favored to freely react with the anomeric sites and hence the reaction is limited to low yields. Also, the relative hygroscopic character of the polymer precursor might have caused traces of moisture in the reaction conditions that contributed to the overall low yield.

The polymer bound protected sugars were then deacetylated under Zemplen conditions. The mechanism of the deprotection reaction is given below (figure 2-3).

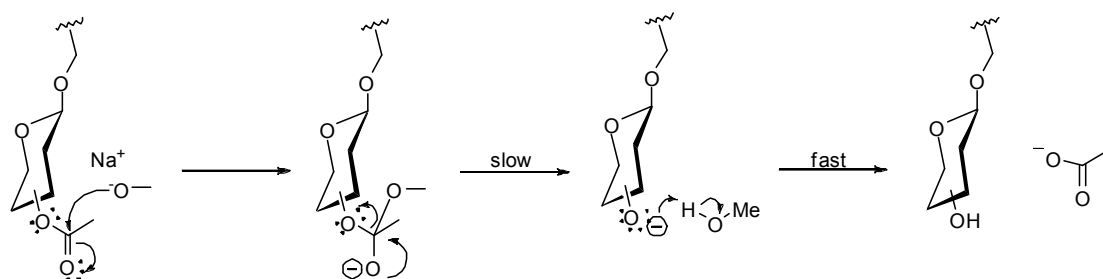


**Figure 2-3.** Deacetylation mechanism of protected -OHs polymer-bound glucose.

The deprotection reaction proceeds in a catalytic manner and affords complete deprotection of the sugars as evidenced by  $^1\text{H}$  NMR which showed complete removal of the acetate protecting groups.

Initial experiments involved the synthesis of the glucosyloxyethyl methacrylate monomer and its use as a co-monomer with NIPAM to produce thermoresponsive glycopolymers. The synthesis would involve similar conditions as those used for the glycosylation of the **P2-1** precursors in order to produce the desired monomer but was hampered due to partial hydrolysis of the monomer during the final deprotection step. In fear that this would also happen in case of deprotection of a methacrylate precursor polymer, synthesis of the HEMide instead of the commercially available hydroxyethyl methacrylate was judged as more desirable. The methacrylamide backbone of the polymer is stable under the deprotection step and also provides more consistent uniformity of the polymer backbone in combination with the NIPAM monomer. Finally, post-functionalization of the polymer precursors allowed for less laborious recovery of the products.

### 2.2.2. Synthesis of Polymer P2-2

The synthesis of **P2-2** involved the copolymerization of *n*-isopropylacrylamide with *N*-carboxylhexyl acrylamide. The monomer is not commercially available and was synthesised according to previously published method. It was envisaged that the long alkyl chain of the monomer would act as a spacer between the active sugar moiety and the polymer backbone [21]. The carboxyl group of the monomer can readily react with amino- sugars via standard carbodiimide chemistry as shown in figure 2-4.

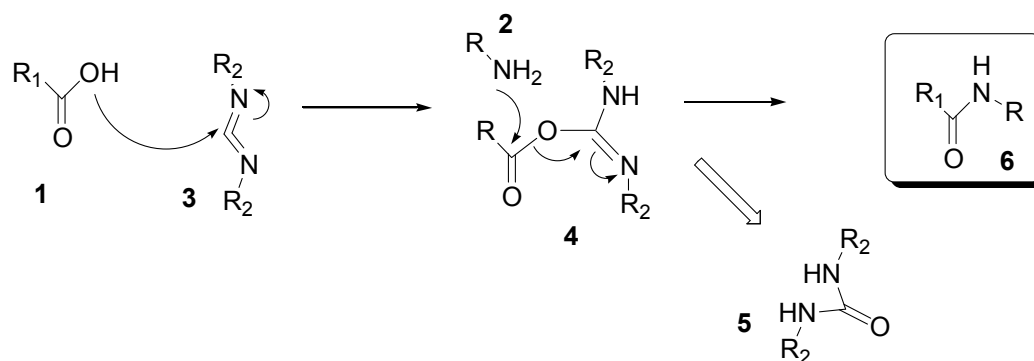


**Figure 2-4.** Amide formation via carbodiimide coupling: carboxylate **1** attacks the diimide **3** that has an electrondeficient carbon and forms the highly reactive O-acylisourea **4**. Then addition of the amine **2** results in formation of the amide bond **6** and gives the stable R<sub>2</sub>-urea byproduct **5**.

The reaction allows for specific attachment of the sugar via the amino group at the 2nd position of the sugar ring.

### 2.2.3. Polymer characterisation

The molecular weight and the polydispersity indices of the polymers were determined by GPC (summarized in table 2-I). The PDIs of both polymers are above 1.5 which is typical for polymers made by free radical polymerization since there is poor control over the polymer chain growth.

Perhaps more importantly for this study though was the accurate determination of the derivatization of the polymers with sugar molecules as previously described in the materials and methods section. <sup>1</sup>H NMR allowed absolute identification of the sugar derivatization for both polymers [25].

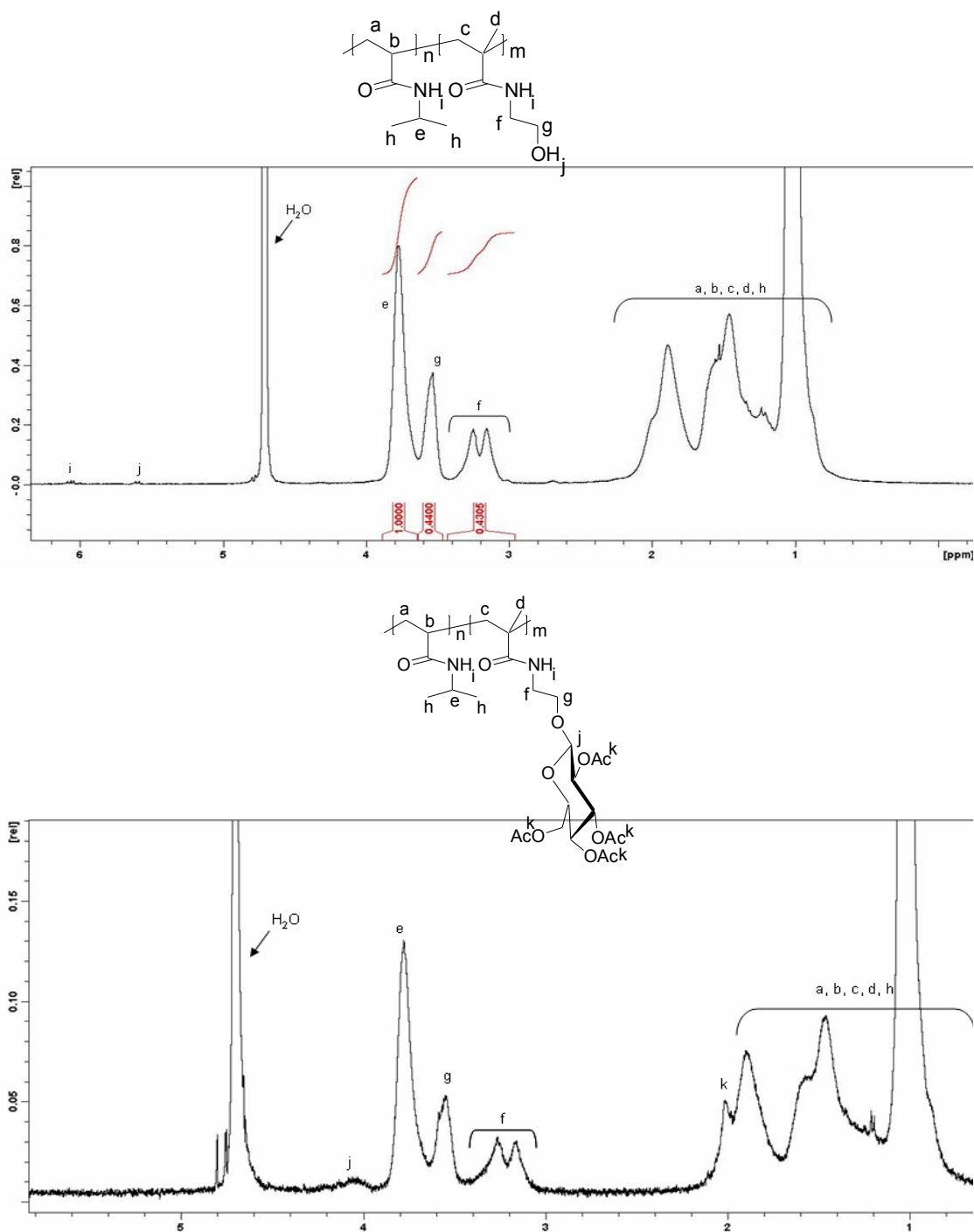


**Figure 2-5.**  $^1\text{H}$  NMR (in  $\text{D}_2\text{O}$ ) was used to determine the relative ratios of the monomers after polymerization and the degree of sugar derivatisation for **P2-1**. Assignments of characteristic resonances were based on analogous spectral data for glycopolymers [25] (continues on next page).

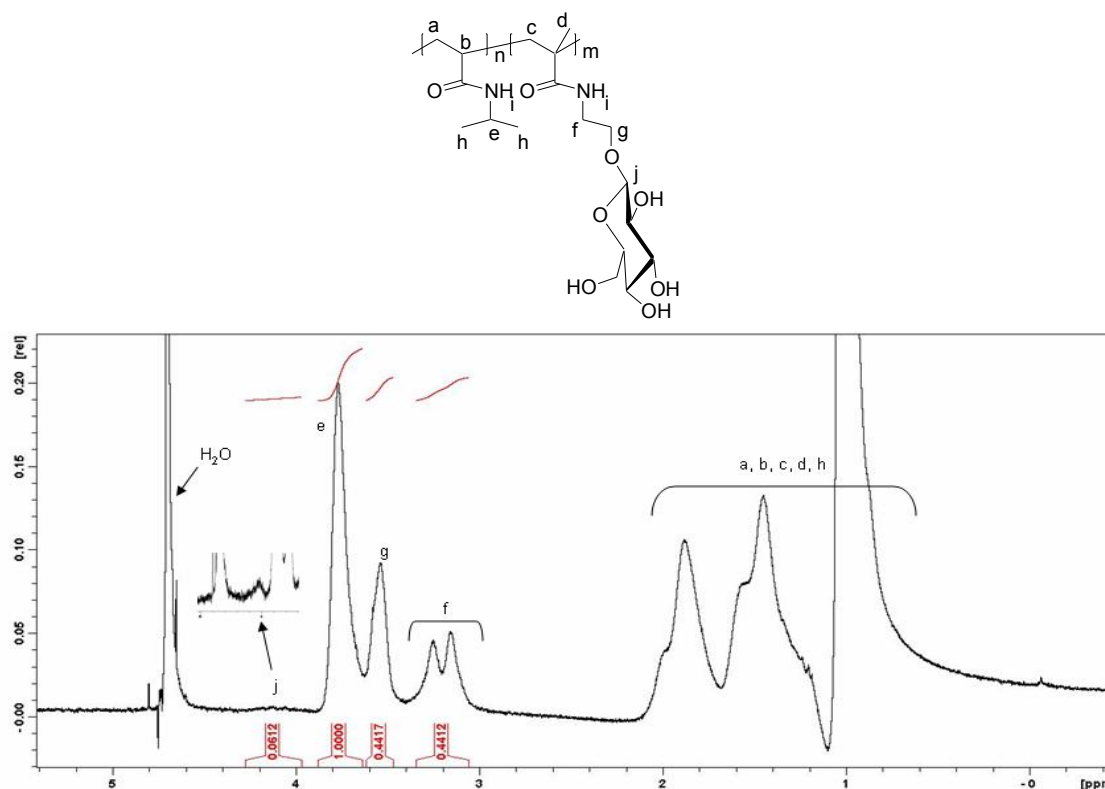


**Figure 2-5 (cont.).** <sup>1</sup>H NMR spectrum of P2-1.

<sup>1</sup>H NMR confirmed the initial ratios used in the polymerization mixture. Integration of the isopropyl proton peak (peak e) and the methylene protons of the HEMide (peaks f and g) monomer showed that there was no bias towards any of the polymers during polymerization. It was also possible to trace the strong signal of the acetate protecting groups of the sugar hydroxyls at 2.1 ppm which was absent in the final product thus ensuring the completion of the deprotection step. Also, it was possible to quantify the degree of sugar derivatization by integrating the signal peak of the anomeric proton at 4.2 ppm against the ethylene protons of the HEMide moiety or the isopropyl proton of NIPAM. However, limited accuracy could be achieved due to the low intensity of the anomeric peak.

Qualitative monitoring of the sugar derivatization was also conducted by FTIR. The appearance of the peak at 1728 cm<sup>-1</sup> corresponds to the stretching of the acetate C=O bond of the protecting sugar groups attached to the

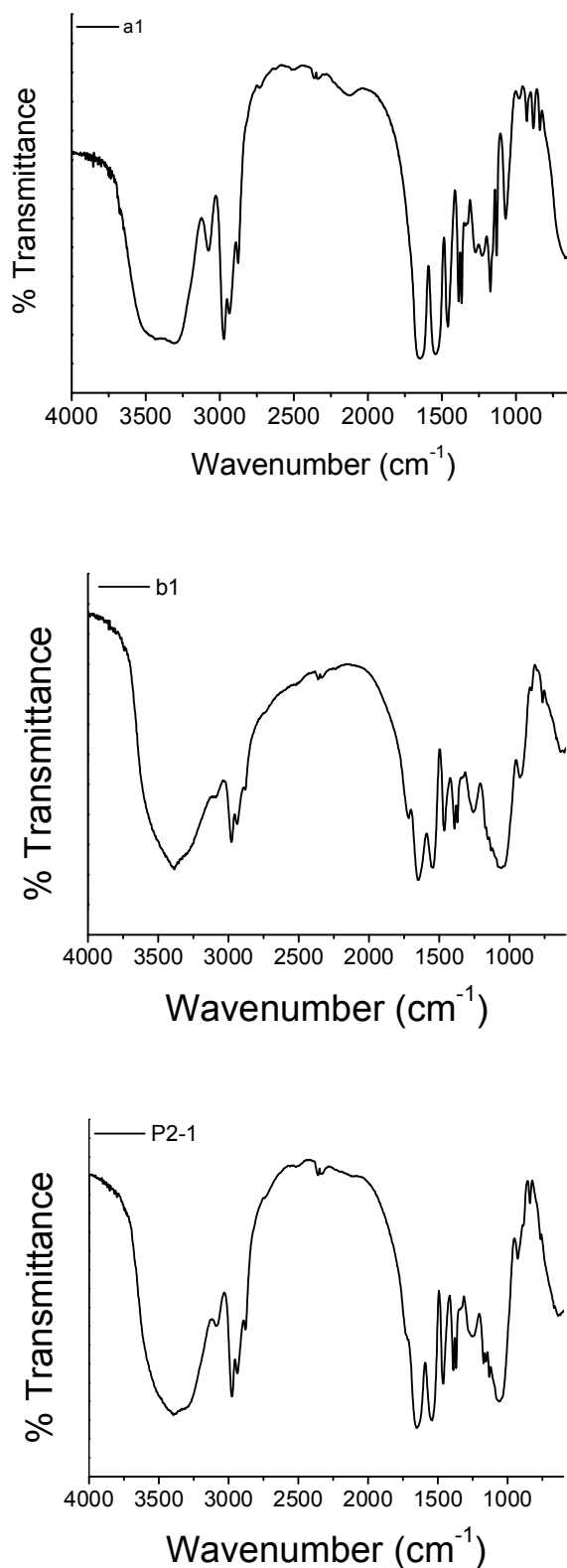


**Figure 2-6.** FTIR spectra. **a1**, 3400  $\text{cm}^{-1}$  (O-H), 3000  $\text{cm}^{-1}$  (N-H, amide), 1648  $\text{cm}^{-1}$  (C=O, amide), 1535  $\text{cm}^{-1}$  (N-H, amide); **b1** 3400  $\text{cm}^{-1}$  (O-H), 3000  $\text{cm}^{-1}$  (N-H, amide), 1728  $\text{cm}^{-1}$  (C=O, acetate), 1648  $\text{cm}^{-1}$  (C=O, amide), 1535  $\text{cm}^{-1}$  (N-H, amide) 1056  $\text{cm}^{-1}$  (C-O-C); **P2-1** as in **b1** negligible acetate peak (1728  $\text{cm}^{-1}$ ).

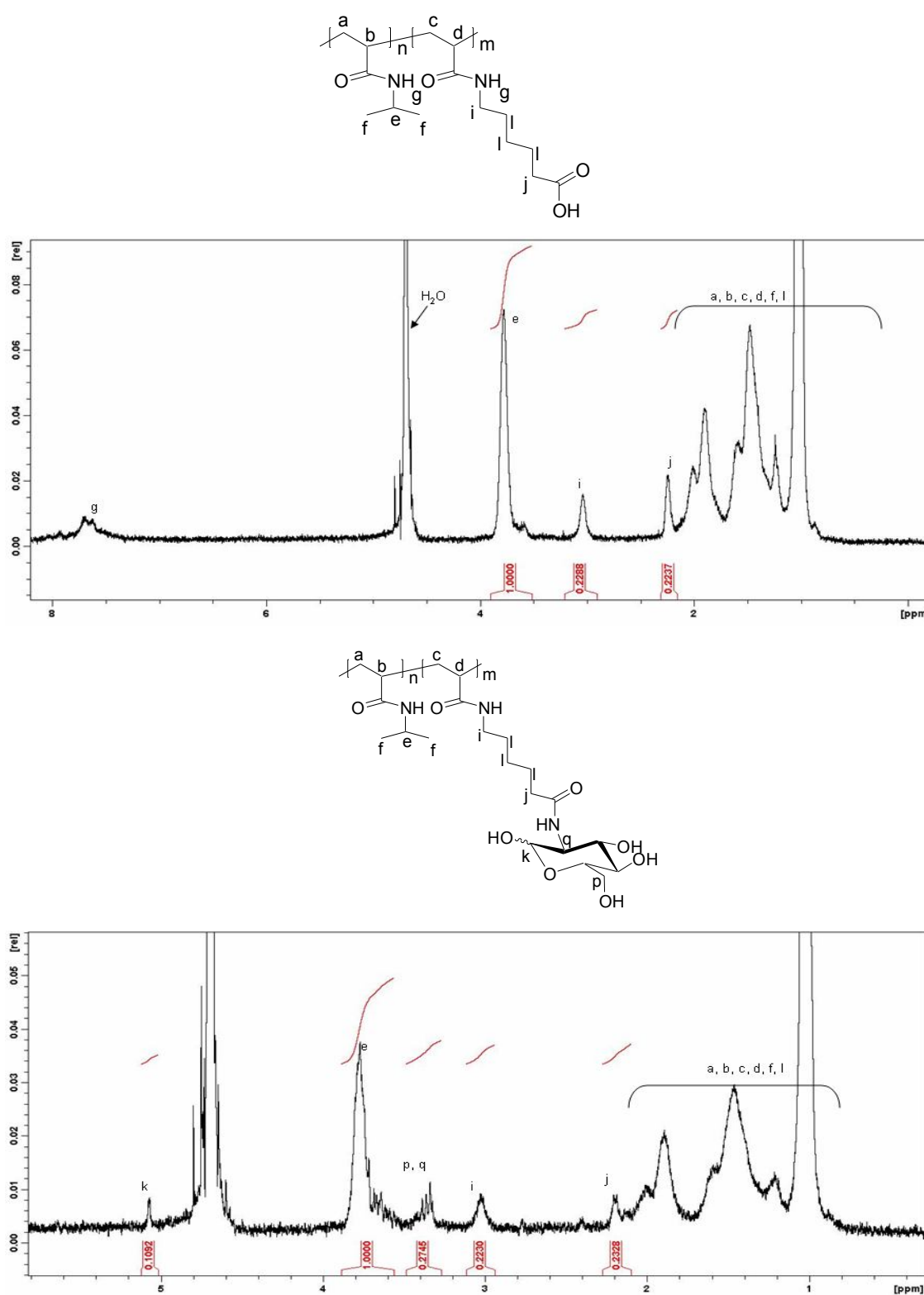


Figure 2-7.  $^1\text{H}$  NMR of P2-2 and its precursor polymer.

polymer. The fact that this peak is significantly reduced in the final polymer is indicative of deprotection as is apparent from figure 2-6.

Similarly for **P2-2**  $^1\text{H}$  NMR was used to determine the exact ratio between the two starting monomers (relative integration of peaks e, for NIPAM and I, for AA6). Again, the final monomer ratios coincided well with the starting monomer ratios used hence confirming absence of bias towards any of the monomers. We were also able to assign most of the protons of the amino sugar attached on the polymer and quantify it by integrating relative to the isopropyl proton of NIPAM too. Similar work by Polizzotti and Kiick [26] on poly(glutamic acid) polymers derivatized by aminosugars assisted to the accurate assignment of the sugar peaks on the  $^1\text{H}$  NMR spectrum of **P2-2** (peaks p, q and k).

FTIR of the derivatized product shows reduction of the C=O stretching peak of the carboxylate groups at  $1728\text{ cm}^{-1}$  which is apparent in the precursor polymer. This result implies that probably the degree of sugar derivatization is high and hence non-reacted carboxylates are negligible in order to appear in the FTIR spectrum.

The fact that for both polymers the sugar signals were relatively low, other methods had to be employed to support the quantification results that  $^1\text{H}$  NMR provided. We therefore used the anthrone assay which is a well known method to trace sugars accurately and with high sensitivity. The use of anthrone to detect sugars was firstly demonstrated by Roe in 1955 in an effort to measure sugar levels in blood and spinal fluid [27]. Reaction of sugars with a strong acid such as sulfuric acid and heating causes hydrolysis of the sugars to give furfuraldehyde products. The latter subsequently react with anthrone and give colored products which are easy to quantify by UV/Vis spectroscopy. It should be mentioned that the method is highly sensitive and consistency in protocol execution is essential for accurate and reproducible results.

First different calibration curves were constructed for **P2-1** and **P2-2** since the attached sugars differ at their linking position with the polymer backbone. Based on the calibration curves (equations 2-3 and 2-4) it was possible to trace the sugar content of each polymer.

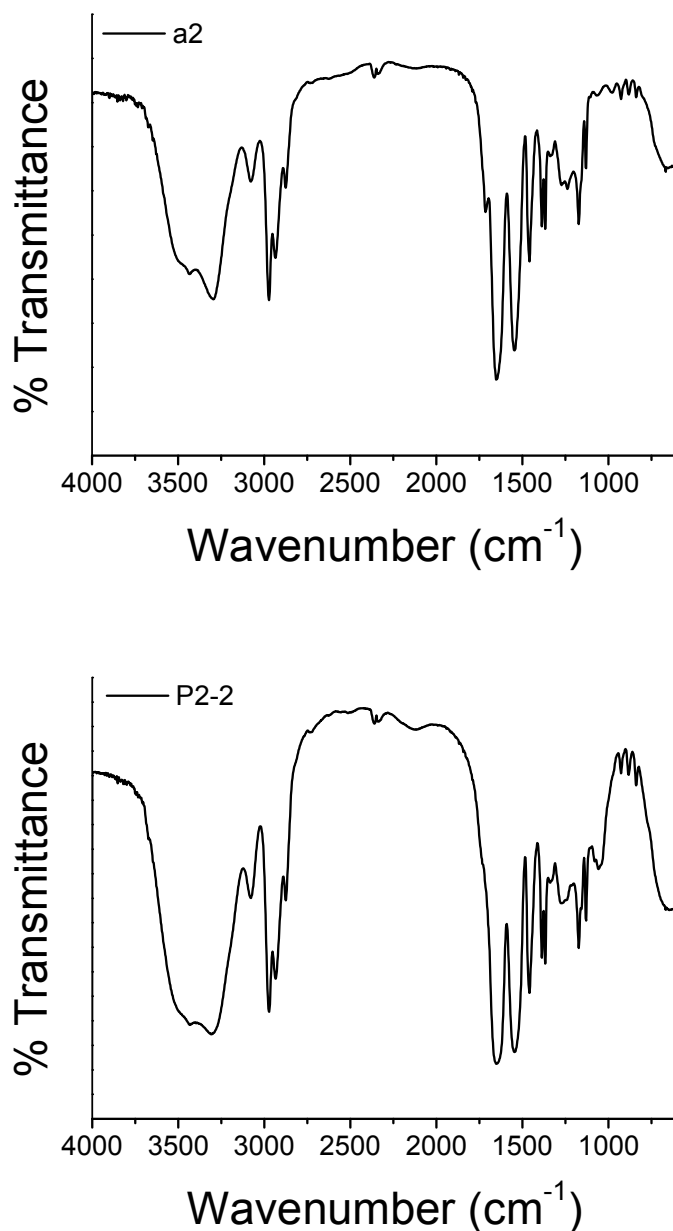


**Figure 2-8.** FTIR spectra: **a2**, 3400  $\text{cm}^{-1}$  (O-H), 3000  $\text{cm}^{-1}$  (N-H, amide), 1728  $\text{cm}^{-1}$  (C=O, carboxyl), 1648  $\text{cm}^{-1}$  (C=O, amide), 1535  $\text{cm}^{-1}$  (N-H, amide); **P2-2**, as in **a2** without carboxyl (1728  $\text{cm}^{-1}$ ).

$$A = 49.75[\text{Glc}] + 0.11467 \quad (R^2 = 0.98) \quad (\text{A for P2-1 was } 0.1823) \quad (\text{eq. 2-3})$$

$$A = 55.3258[\text{GlcN}] + 0.09868 \quad (R^2 = 0.98) \quad (\text{A for P2-2 was } 0.1788) \quad (\text{eq. 2-4})$$

A third assay to detect the degree of sugar derivatization which is based on a boronic acid and a diol-containing dye was used. Boronic acids are well known to bind covalently and reversibly to cis-diols and have been extensively used in the past as sugar sensors [28]. In solution, a boronic acid such as phenylboronic acid and a diol-containing molecule such as glucose establish an equilibrium and form the acidic boronate ester [29]. We exploited this principle in order to detect the diol-containing sugars on the polymers as follows. We establish an equilibrium that consists of phenylboronic acid, the polymer-bound sugars and Alizarin Red S. The latter is inherently a non-fluorescent dye that strongly fluoresces when a boronic acid binds to the catechol diol [23]. The fluorescence intensity of the non-quenched dye, that is sugar-bound dye, can be directly correlated to sugar concentrations in solution. Hence, we can construct calibration curves based on varying concentrations of sugars based on standard dye concentration. Subsequently, by establishing an equilibrium between a standard polymer concentration, the phenylboronic acid and the dye, it is possible to quantify the degree of sugar derivatization of the materials synthesised.

The results of all three methods used to determine the amounts of sugars attached to the polymers correlate well as shown in table 2-I.

**Table 2-I**  
Summary of degree of sugar derivatization of **P2-1** and **P2-2**.

<i>Polymer</i> ( $M_n$ , PDI)	% Degree of derivatisation (No of sugars attached per polymer chain)			
	<i>AR assay</i>	<i>Anthrone assay</i>	$^1\text{H NMR}$	<Mean>
<b>P2-1</b> (15800, 2.1)	31(6)	38(8)	27(5)	32(6)
<b>P2-2</b> (20100, 1.9)	88 (12)	81 (11)	87(12)	85(12)

## 2.2.4. Lower Critical solution temperature measurements

### 2.2.4.1. Effect of comonomers hydrophilicity on LCST

The poly(N-isopropylacrylamide) polymers are known to exhibit a globule-coil transition and phase separation at 32 °C [30]. Above the LCST the water molecules bound with the polymer chain are released as shown schematically at figure 3.3. The process is endothermic and driven by increase of entropy as water molecules escape to bulk solvent. At low temperatures, the hydrogen bonding between water molecules and the hydrophilic groups (i.e. amide group), outweighs the excess of free energy related to the exposure of the hydrophobic groups (i.e. isopropyl- moiety) to water leading to increased solubility of the polymer. Conversely, at higher temperatures, that is above LCST, hydrogen bonding weakens and the hydrophobic interactions are dominant leading to phase separation and polymer collapse.

The copolymerization of NIPAM with other hydrophilic and/or hydrophobic monomers has already been reported to alter the physicochemical behavior in aqueous environments [31]. It is well known that the presence of a hydrophobic unit in the polymer chain along with NIPAM promotes the decrease of the LCST whereas hydrophilic groups have the opposite effect. The mechanism for this is that the hydrophobic interactions, which are the driving forces for the phase separation as described previously, are amplified at high temperatures due to the less ordered water molecules around the hydrophobic domains. It has been proposed that LCST depends on the overall hydrophilicity of the polymer rather than the hydrophilicity of individual comonomers [29].

Both polymers exhibit LCSTs slightly above physiological temperature due to the introduction of the more hydrophilic sugar segments. Since the LCST is dependent on the hydrophilicity of the co-monomers used, we sought to use the LCST cloud point as a qualitative read-out of chemical modification

of the polymers due to sugar attachment. We therefore compared the LCST cloud points of **P2-1** and **P2-2** with their precursors. Broadening of LCST response of a1 was observed due to the introduction of the bulky AcGlc moiety (b1); a slight sharpening of LCST response was observed after deacetylation (**P2-1**). Since arithmetic ratios of the co-monomeric units of the backbone remained constant throughout the derivatization, no difference in LCST onset was observed. Broad LCST for a2 was mainly attributed to association of carboxyl groups (as shown in figures 2-9 and 2-10). It is worth mentioning that introduction of ionisable monomers such as AA<sub>6</sub> to the polymer chain will render the polymer pH-responsive. This means that the LCST of the polymer can be tuned by varying the pH of the aqueous solution however this effect was not investigated in detail in this study. Previous studies though have clarified the role of both the hydrophobic alkyl spacers (i.e. ethyl and hexyl groups on HEMide and AA<sub>6</sub> monomers) and the ionizable groups (i.e. carboxyl groups on AA<sub>6</sub>) on the overall phase-transition behaviour. Small spacers seem to have negligible effect on the LCST and slight increase of the latter is observed due to the dominant presence of the ionisable groups. On the other hand, long spacers dominate the overall hydrophobicity of the polymers and lower dramatically the LCST [21]. In the case of **P2-1**, the hydroxyl group of HEMide seems to have a more profound effect on the LCST than the short ethyl spacer and therefore slight increase of the LCST is observed. Interestingly, in the case of **P2-2** the long alkyl spacer of AA<sub>6</sub> (5 carbons), no decrease of LCST is observed and the LCST is rather higher than that of poly(NIPAM) homopolymer. The carboxyl groups therefore must be dominating the overall LCST of the polymer. At neutral pH, such that of water or the PBS used in this study (pH 7.4), most carboxyl groups are ionised and therefore render the AA<sub>6</sub> more hydrophilic which in turn shifts the LCST. Also, at these conditions a small number of the carboxyl moieties will still be in a non-ionized state (ca. 1%) and interchain hydrogen bonding occurs which is the reason of the significant broadening of the LCST onset. As expected, in **P2-2** where most of the carboxyl groups

have been capped with sugar molecules, broadening of the LCST onset is totally eliminated and sharp phase transition is also observed. Expected LCST shift was observed due to the hydrophilic nature of GlcN (figure 2-9).

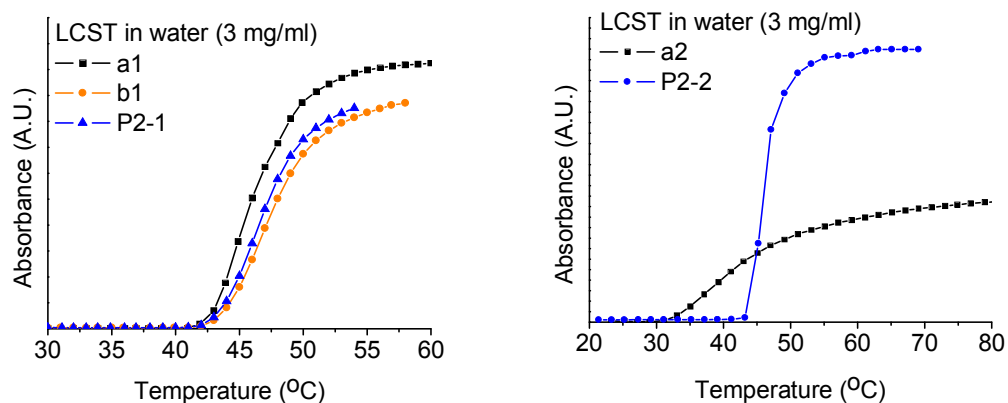


**Figure 2-9.** LCST curves of **P2-1** and **P2-2** with their precursors.

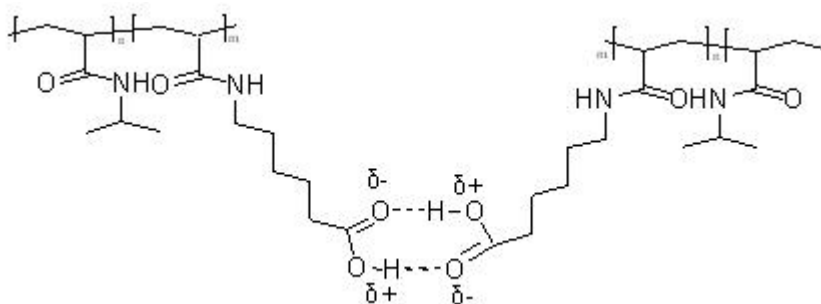


**Figure 2-10.** Intermolecular association of pendant carboxylate groups that influence the LCST onset.

#### 2.2.4.2. Effect of Salt presence on LCST

We also determined the LCST of the polymers in PBS since it is well known that salt-rich environments affect the overall behavior of thermoresponsive polymers [31].

In the PBS environment, the LCSTs of both polymers seem to decrease. This decrement is mainly attributed to the presence of anions that interact with the amide group of NIPAM via hydrogen bonding (figure 2-11).

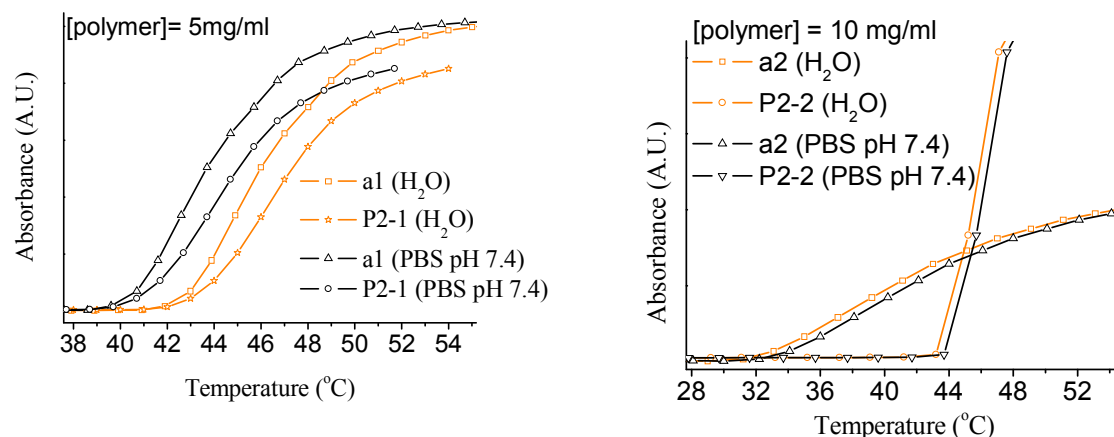


**Figure 2-11.** Effect of PBS (salt-rich saline) on the LCST behaviour of the polymers and their precursors.

Anions can also alter the hydrophobic interactions of the isopropyl group and the backbone by increasing the surface tension (figure 2-12). The presence of salt weakens the interaction of water molecules with the amide group and the carbonyl oxygen. Practically, this means that less heat needs to be transferred to the system to break the weakened hydrogen bonds formed between water molecules and the hydrophilic segments of the polymers, namely the amide group which is the reason of the lowering of the LCST. It should also be noted that the LCSTs observed represent the lower phase transition of the polymer in salt-rich environment since at higher salt concentrations two onsets (i.e. two-step phase separation) have been observed [32].

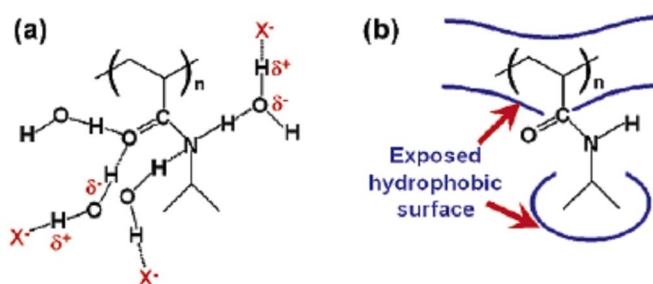


**Figure 2-12.** The salt effect on poly(N-isopropylacrylamide), (retrieved from reference [32]).

### 2.2.5. AR-Glc Reversible binding

We hypothesised that the reversible phase transition that occurs in the thermal-dependent manner could facilitate “on/off” like activity of the polymers. At temperatures lower than the LCST, the polymers exist as soluble coils in aqueous media and therefore expose their active ligands to potential biological hosts, that is, carbohydrate recognition sites, whereas at higher temperatures above the LCST the polymers collapse, eventually drop out of solution and hence “hide” their ligands from solution, rendering them inactive. Therefore, an assay had to be developed to demonstrate this principle of reversible activity of the polymers in aqueous solutions.

Since the alizarin assay to detect sugars attached on the polymers is insensitive to temperature but highly sensitive due to its fluorescence based analyte detection, it was used to probe the hide-and-reveal mode of action of the polymers above and below the LCST. We therefore employed the assay having in mind that the moiety mimicking the CRS would be phenylboronic acid which exhibits diol-specific binding properties with sugars. The three component equilibrium of the assay is altered according to temperature as shown in figure 2-13.

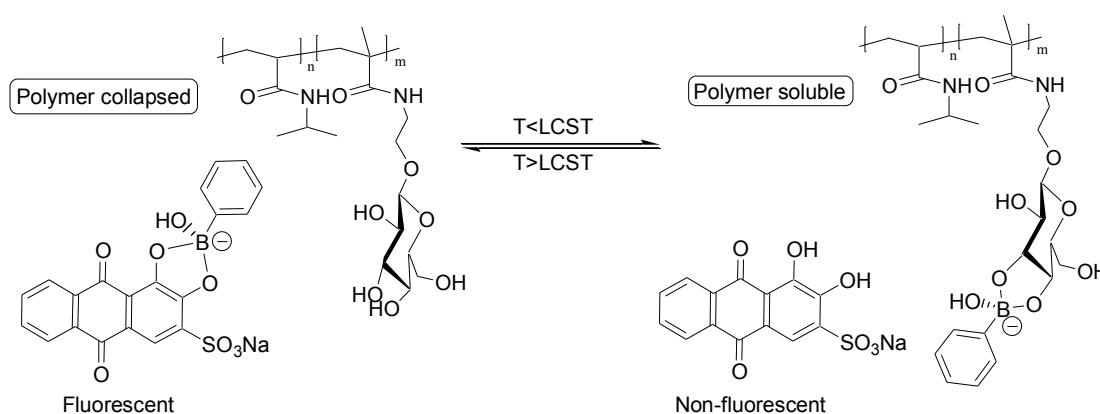


**Figure 2-13.** The three component assay comprising AR, PBA and diol moieties of the polymer-pendant glucose.

AR is inherently nonfluorescent but fluoresces strongly when bound to PBA in alkaline conditions. The covalent, but reversible (in response to pH [29] and temperature [33]), binding of PBA with the catechol diol groups induces emission at 578 nm. The introduction of glucose, which has high affinity to PBA, in the polymer results in competition for diol-binding sites on PBA between AR and polymer-bound glucose. Binding of glucose to PBA was thus monitored by variations in the AR-PBA complex fluorescence intensity as the concentration of glucose from the glycopolymer changed. The polymer-bound glucose reacted with PBA when the polymer was in a soluble phase ( $T < \text{LCST}$ ) as shown by reduction in AR-PBA complex fluorescence intensity. By contrast, an increased fluorescence intensity of the AR-PBA complex was observed at  $T > \text{LCST}$ , when the polymer was in a globular state and the glucose residues were not available for competitive binding with AR for PBA.

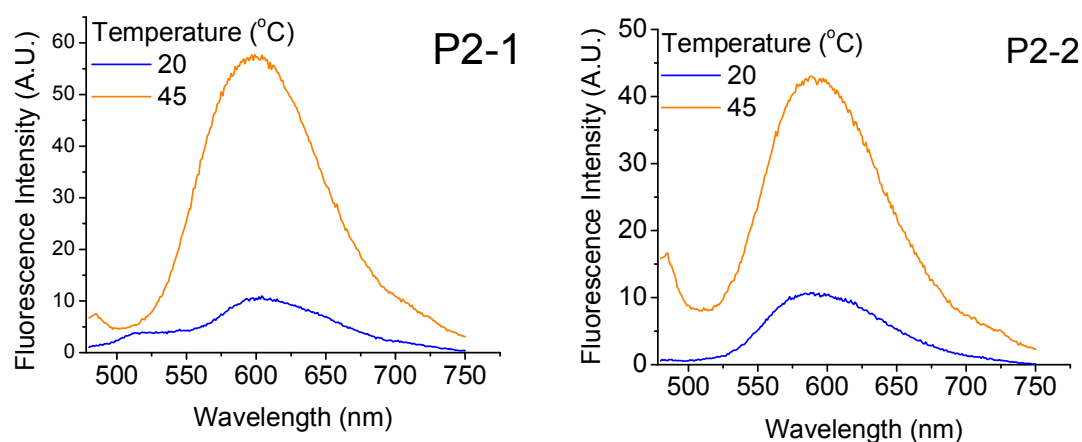


**Figure 2-14.** Fluorescence spectra of P2-1 and P2-2 using AR and PBA in glycine buffer (0.1 M, pH 9.3)

The effect was apparent to the naked eye, with the color change of a vial containing all three components (AR, PBA, and **P2-1** or **P2-2**) from burgundy to orange at low and high temperatures, respectively (figure 2-15).

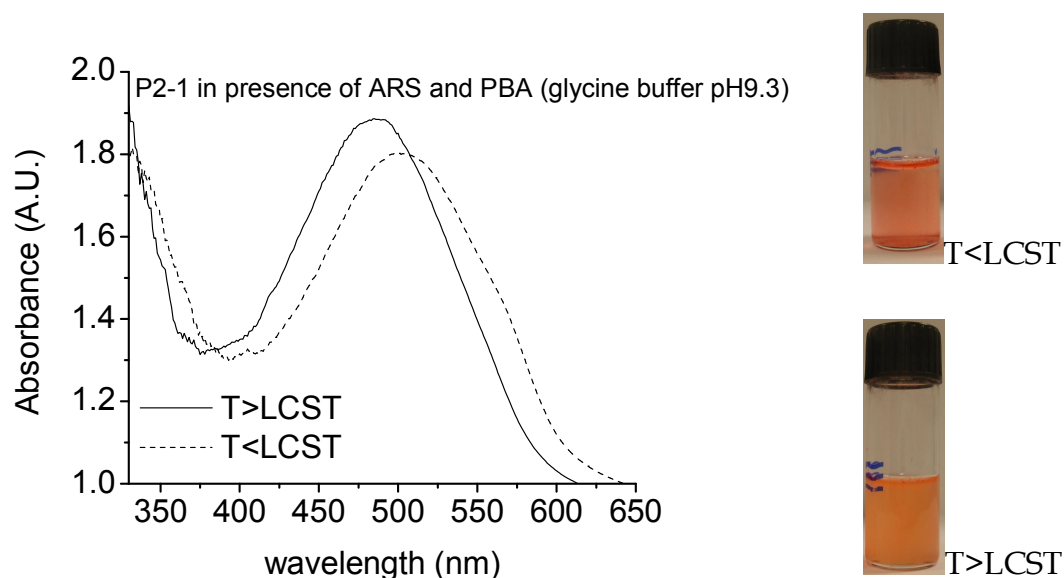


**Figure 2-15.** Left, Absorbance curve of **P2-1** below and above LCST and on the right, visual inspection of diol binding and release below and above LCST.

The assay used in this work was inspired by a recent paper of Ge et al. where they studied the release of diols from a copolymer microgel system that consisted of NIPAM as the thermoresponsive unit and acrylamidophenylboronic acid as the diol-binding moiety [33]. In this work, glucose or AR could be loaded and released from the microgel in a temperature dependent manner. The colorimetric change of a microgel suspension containing AR, as the latter was released from the microgel particles, was used to monitor the release mechanism of this system. We employed the same concept by developing the reversible binding assay with the polymers, AR and polymer-bound glucose as described previously.

Actually, the assay is mainly based on the fact that the boronic acid-diol complexes form classic equilibria despite the covalent nature of the binding. In fact, the equilibrium established between a boronic acid and a cis-diol containing compound is much more complex (figure 2-16).

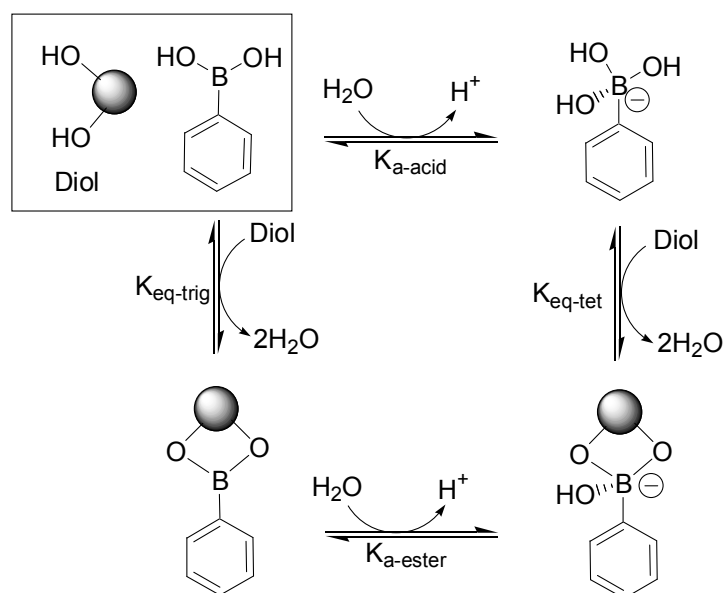


**Figure 2-16.** The dynamic equilibria of PBA with a diol molecule (adapted from reference [29]).

The boronic acid exists in two states that form an equilibrium, these are the trigonal and the negatively charged tetrahedral forms. In presence of a diol, the trigonal and tetrahedral forms will form boronate esters which are slightly more acidic when in tetrahedral form. It is apparent that three acids exist in equilibrium, the boronic acid, the diol which has pK around 12 in the case of glucose, and the boronate ester formed. The optimum pH for effective boronic acid- diol complexation is considered to be above the pK<sub>a</sub> of the boronic acid (that is 8.8 for PBA). The role of pH and buffer concentration are also known to play significant role in the binding events that happen in these systems but have not yet been fully elucidated [28, 29]. Nevertheless it has been found that the optimum pH for effective PBA-AR complexation is proposed to be around 7 [29].

We therefore repeated the AR assay as mentioned before by replacing the buffer with phosphate buffered saline (pH 7.4) in order to mimic microenvironmental conditions of biological relevance.

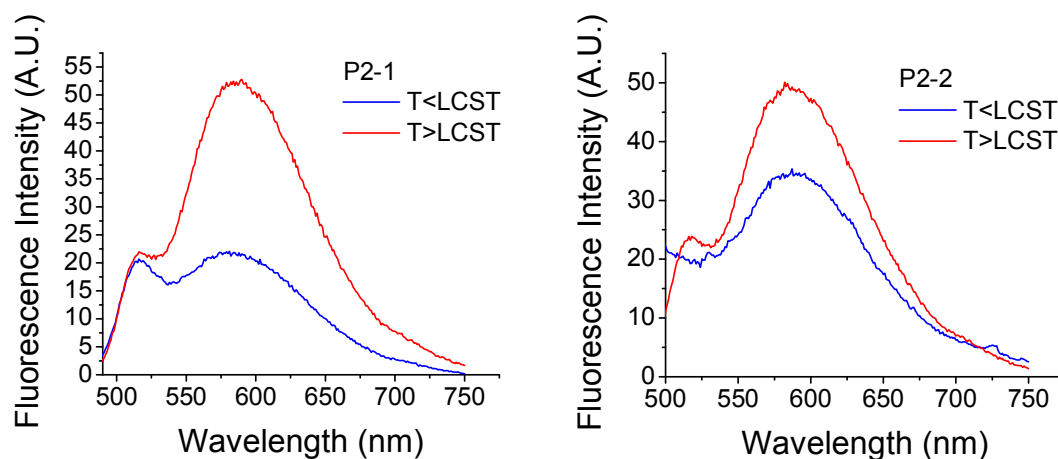


**Figure 2-17.** Reversible binding assay of **P2-1** and **P2-2** with AR and PBA in PBS pH 7.4.

As shown in figure 2-17, it was possible to demonstrate the reversible PBA-diol binding in respect to temperature for **P2-1** but a lesser extent for **P2-2**. In both cases the phenomenon could not be probed as efficiently as when the experiment was performed at pH 9.3, that is above the pK of PBA. Particularly for **P2-2** a modest increase in fluorescence above LCST could be attributed to steric factors affecting the GlcN-PBA complexation affinity due to the linking position of the sugar moiety to the polymer backbone. Therefore reversible binding events may not have been probed efficiently at lower pH.

The experiment could be repeated for several temperature cycles with consistent oscillation in fluorescence intensity for both polymers in respect to temperature, thus demonstrating the reversible binding character in a “switchable” manner.

Finally, a series of control experiments were conducted to ensure the specificity of the interaction in response to temperature. AR with PBA but polymer-free did not show any fluorescence increase due to temperature increase.

Spectra of polymer samples with AR but no PBA were also recorded as controls. As expected, no fluorescence was detected as no fluorophore existed in solution in this control. Finally, **P2-1** and **P2-2** in presence of PBA but no dye did not show any fluorescence.

Careful attention was paid to the control experiment using poly(NIPAM) homopolymer in presence of alizarin and PBA. Studies on the behaviour of small fluorophores in presence of thermoresponsive polymers have shown that the fluorescence properties of such compounds are dramatically affected by the phase transition of the polymers. In particular, sparingly soluble fluorescent probes, such as pyrene, are known to exhibit significant increase of their emission in hydrophobic environments, which might occur when the polymers collapse into globules from solution. Polar media (i.e. water) cause significant quenching of the emission of the fluorophore molecules which is suppressed as the polymer collapses above LCST; the latter will collapse by forming hydrophobic globules as water is being expelled during coil-to-globule transition. The sparingly soluble dye can thus be trapped in these regions due to their hydrophobic nature and therefore suppress the quenching of the solvent [34]. Therefore in a polymer-rich microenvironment the emission capacity of alizarin could be significantly affected by these events that are not related to the specific binding of PBA to the dye. Fortunately, in dilute polymer solution only minor fluorescence intensity increase was detected (~ 16%) which was thought not to be significant to influence the reading of the fluorescence intensity in the alizarin assay.

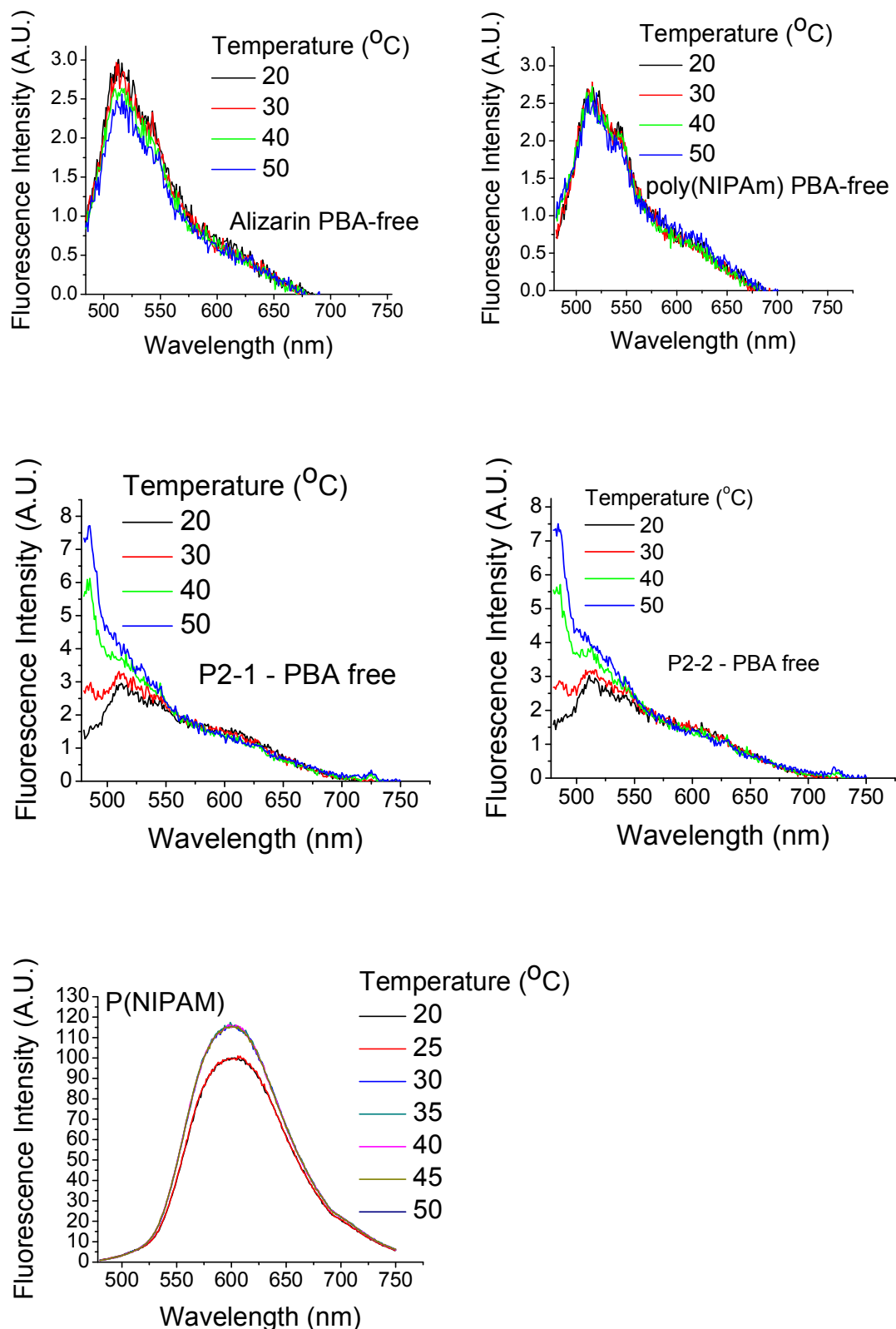


**Figure 2-18.** Control fluorescence experiments showing negligible increase in fluorescence maxima of alizarin red (AR) at 578 nm with and without thermoresponsive polymers over assays of varying temperature (AR excitation energy, 460 nm – PBA = phenylboronic acid).

### 2.2.6. Glycopolymer biorecognition using lectins

Glycopolymers have been used in the past to study the multivalent interactions of sugars with lectins. Lectins are carbohydrate binding proteins found in most living organisms [35]. We sought to use Con A for this study as it has high specificity for glucose [36] and mannose [37] and therefore would serve as a relevant biological model-host to study the biorecognition properties of the polymers. In alkaline environments, con A exists as a tetramer and therefore four binding sites are prone to bind with sugars [38].

Mixing two aqueous solutions of polymer and lectin will result in formation of large complexes that consist of glycopolymers bound to the multiple carbohydrate binding sites (figure 2-19) [39].

In other words, the lectin acts as a pseudo-crosslinker and gradually, the large aggregates formed drop out of solution. This is indicated by gradual increase in the turbidity of the solution that can be monitored towards time via UV/Vis spectroscopy (figure 2-20) [39].

It can be seen that large polymer-lectin complexes are formed with time progression. These complexes are considered to be partially solvated and no complete precipitation is observed unless high molecular weight polymers are used that can promote quantitative lectin precipitation [39]. For example, Ladmiral et al., tested a library of mannose containing polymers for their potency with Con A and found that only heavily mannose-derivatized polymers could rapidly agglutinate the lectin quantitatively [40].

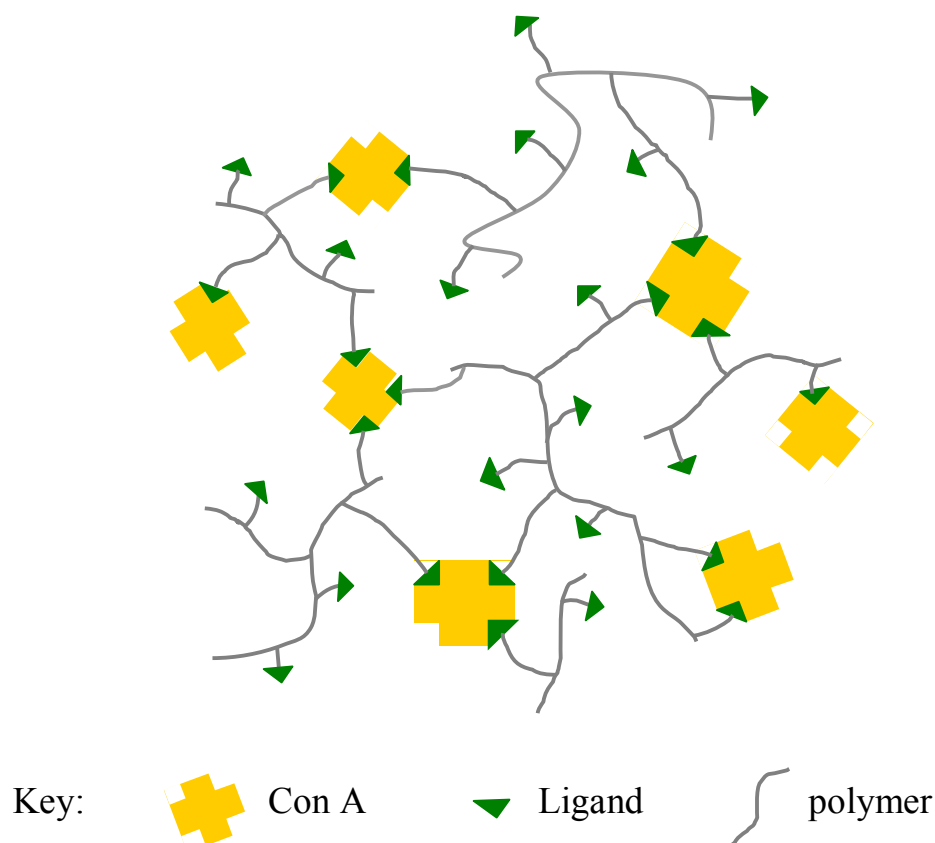


**Figure 2-19.** Schematic showing the complex formation between the tetrameric lectin with the polymer bound ligand, that is glucose.

Both polymers seem to have the same trend of aggregation capacity. We therefore examined the amount of lectin that the polymers can agglutinate by isolating the large aggregates formed via centrifugation. The polymer-lectin solid aggregates were collected and dissociated by addition of free glucose. The soluble lectin could then be detected by UV/Vis by measuring the absorbance at 240 nm. As expected, **P2-1** and **P2-2** could agglutinate similar amounts of lectin (figure 2-21, ~7-8.5  $\mu\text{g}$  per 5 mg of polymer). Similar quantitative precipitation studies have also been performed by the groups of Haddleton and Kiessling [9, 39-41] but are not directly comparative to data here since they used mannose-decorated polymers of varying molecular weights and architectures.

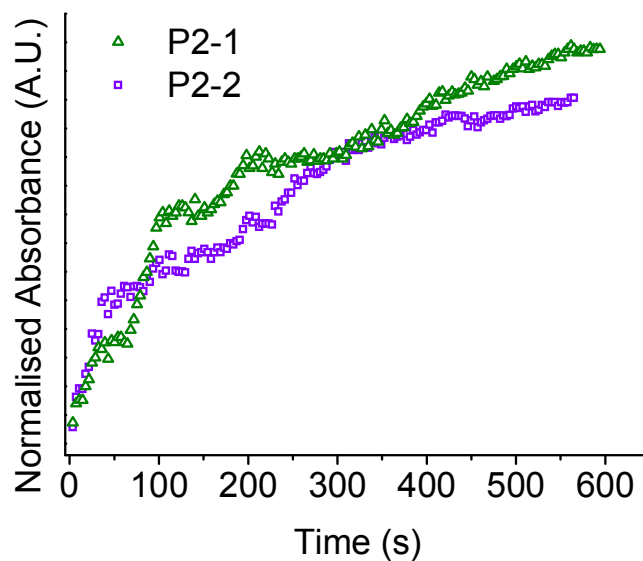


**Figure 2-20.** Polymer interaction with Con A. Gradual increase in turbidity due to polymer-Con A complexation, as measured by UV/Vis spectrometry at 550 nm.

However, these studies do confirm the specific character of the polymer-protein interactions via the sugar groups and establish the multivalent nature of the polymers biorecognition properties.

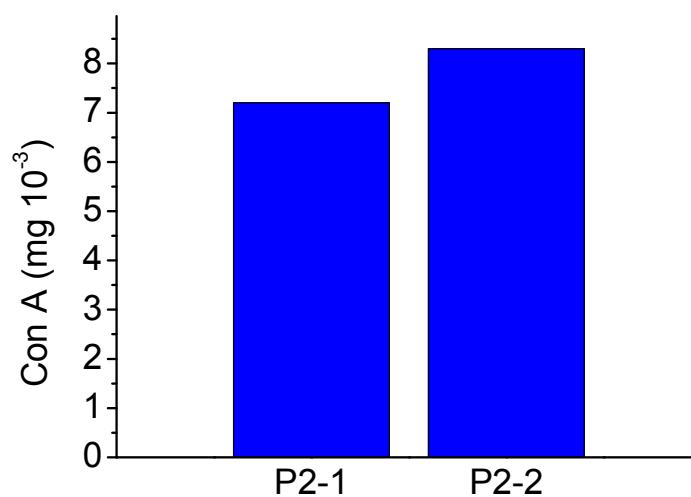


**Figure 2-21.** Quantitative estimation of protein "scavenging" by polymers P2-1 and P2-2.

It should be mentioned that there are several factors that can strongly influence the binding of the polymers to the lectins saccharide binding sites such as the site of sugar derivatization, the length of the linker to the polymer backbone, and the hydrophilicity of the linker. A hydrophobic linker such as the alkyl chain used in this study would be preferable as it has been reported that such chains stabilise the sugar in the binding sites of Con A, which has a hydrophobic pocket-like region near the sugar binding site. Also, a longer spacer sterically favours the binding events as it provides increased degrees of freedom and keeps the sugar moiety away from the polymer backbone. Finally, the site of sugar derivatization is pivotal to the overall binding. The overall binding is facilitated by cooperative hydrogen bonding between the O3, O4 and O6 sugar atoms and the Tyr100, Asp2-208, Arg228, Asn14 and Leu99 residues of the lectin which ensures high binding selectivity [36-38, 42].

The hydroxyls at C1 and C2 are known to be exposed to the solvent when the sugar is bound to the lectin and therefore are prone to derivatization since they do not actively participate in the binding events. Therefore, derivatization of glucose at C1 position in the case of **P2-1** and glucosamine at position C2 for **P2-2** were judged as the most desirable sites for the glycopolymers synthesis.

### 2.2.7. Polymer-bacteria interactions

Having established that the synthetic glycode could be hidden and revealed by a temperature switch (alizarin assay) in a highly specific manner (con A assays), we carried out bacterial binding assays with polymers **P2-1** and **P2-2** and a green fluorescent protein-tagged *Escherichia coli* strain (MG1655pGFP). This strain produces Type 1 fimbriae containing the *fimH* protein that possesses carbohydrate recognition sites (CRS) with high affinity for mannose ( $K_d$  2.3  $\mu$ M) and glucose ( $K_d$  9.24 mM) [43]. Similarly to Con A, the *fimH* domain accommodates mannose molecules through hydrogen

bonding and hydrophobic interactions. Only the anomeric -OH is known to not participate in the binding events. This justifies our synthesis route which involved sugar derivatization of the polymers through the anomeric reactive sites. Also, the -OH at position C2 does form a hydrogen bond with an N-terminal amine of the protein but is not detrimental to the overall binding as the other hydroxyls seem to be mostly responsible for the strong binding of mannose (or glucose) with the *fimH* domain [5, 44, 45]. The interaction between cell-surface receptors and the multiple copies of sugar moieties on the polymers resulted in bacteria-polymer complex formation (figure 2-22).

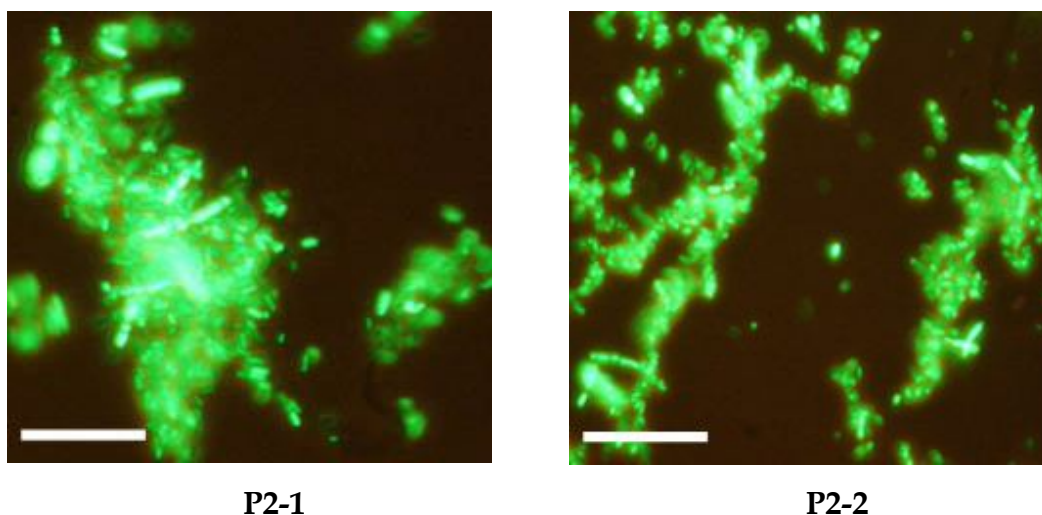


**Figure 2-22.** Polymer-bacteria aggregates using polymers **P2-1** and **P2-2** as tested with *E. coli* MG1655pGFP (scale is 10  $\mu\text{m}$ , O.D. 0.7-0.8).

The mode of interaction was probed by competition assays with *fimH* ligands. Increasing amounts of added glucose showed a gradual decline in the size of the aggregates formed with respect to glucose concentration increase (figure 2-24). Total inhibition of bacterial cluster formation occurred when the concentration of added glucose in the polymer-bacterial suspension (300  $\mu\text{L}$ ) reached 0.01 mM, which correlated well with the numbers of glucose residues on the polymers (effective glucose concentration  $\sim$ 0.04 mM).

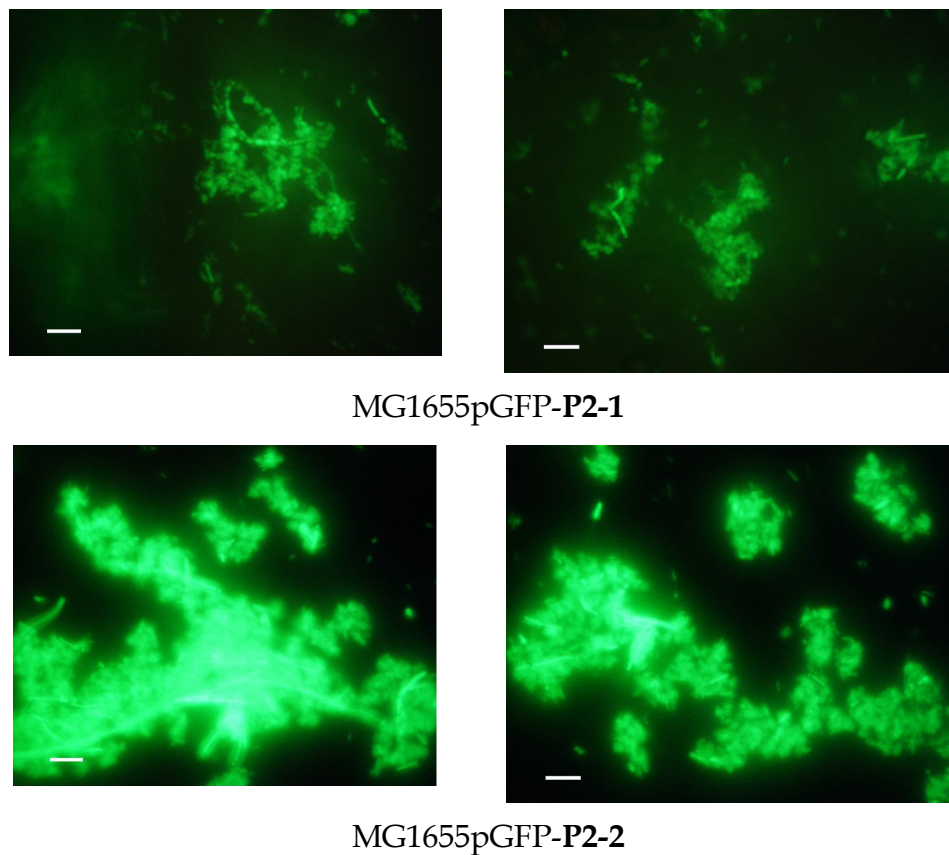


**Figure 2-23.** Typical images of bacterial aggregates in presence of P2-1 or P2-2 at room temperature. Extensive bacterial aggregation of *fimH* expressing *E. coli* upon addition of thermoresponsive glycopolymers at temperatures below polymer LCST (white bar: 25  $\mu\text{m}$ , O.D. 0.7-0.8).

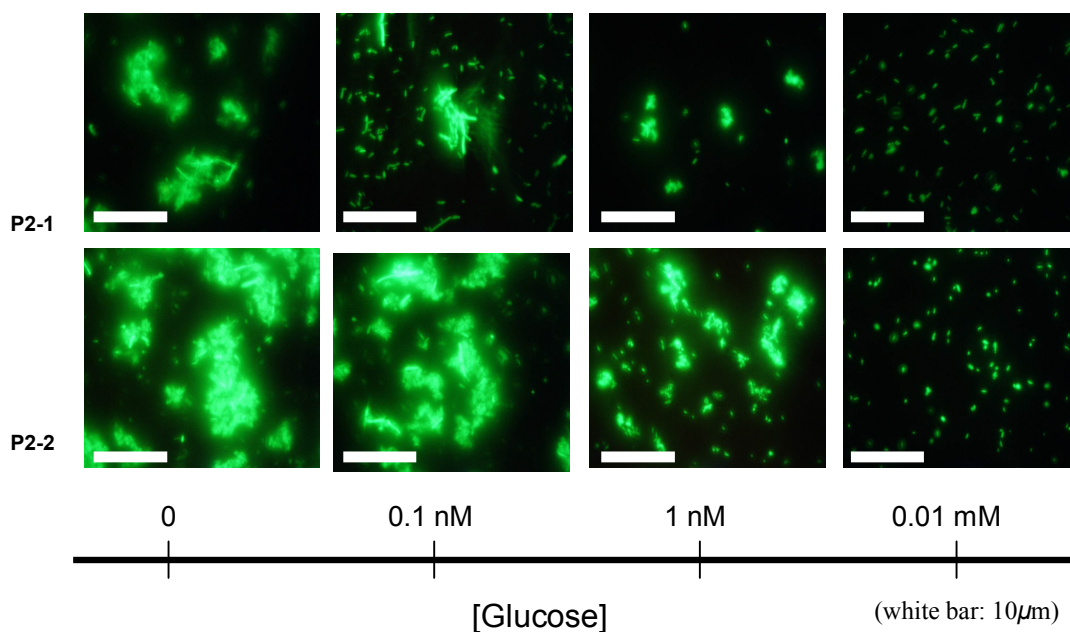


**Figure 2-24.** Polymer (10 mg/mL)-glucose competition assay; gradual reduction of cluster size due to glucose increase (white bar is 10  $\mu\text{m}$ , O.D. 0.8)

The competition assay was quantified by performing image analysis of photomicrographs which confirmed the findings of visual inspection.

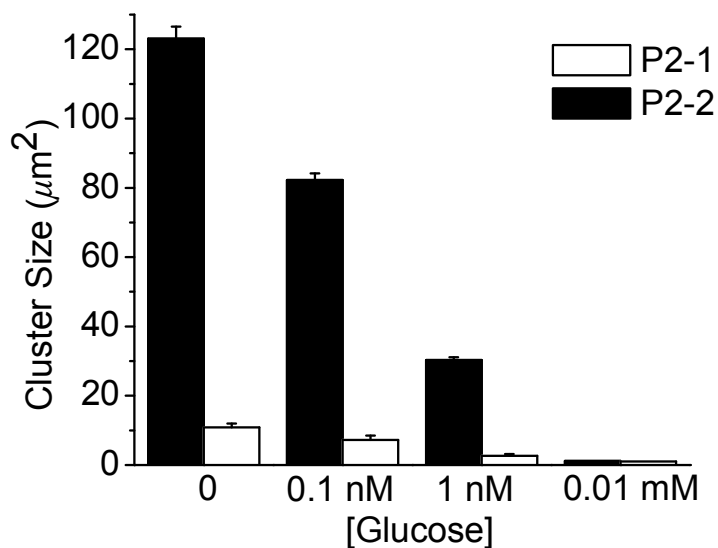
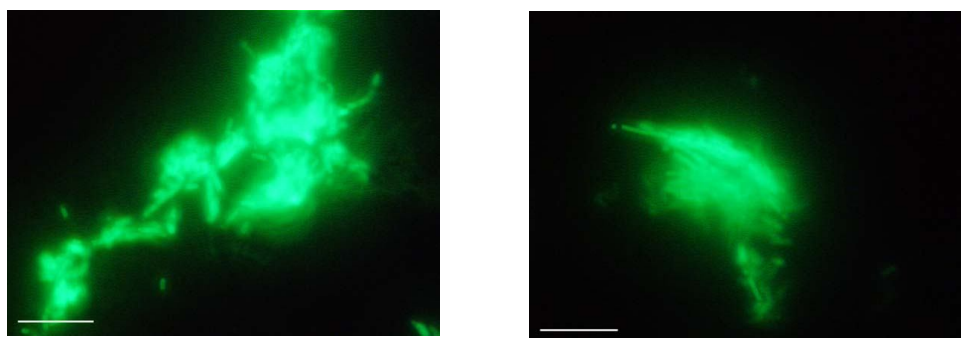


**Figure 2-25.** Reduction in size of polymer-bacteria aggregates with increasing amounts of glucose.

By contrast, addition of sucrose, which exhibits lower affinity for *fimH* than glucose, did not inhibit formation of bacteria polymer clusters [43].



MG1655pGFP-P2-1+sucrose (0.01 mM)

MG1655pGFP-P2-2+sucrose (0.01M)

**Figure 2-26.** Retention of polymer-bacteria aggregates in presence of sucrose (non-competing ligand for FimH).

Analogous competition assays have been performed by Disney et al. [11] where they challenged the potency of mannosylated fluorescent polymers with free mannose upon the formation of bacteria clustering. The values of mannose concentration they obtain for complete bacterial clustering inhibition are in the range of tens of mM which are significantly higher than those in the present study. This difference is attributed primarily to the higher potency of mannose than glucose for binding to *FimH* [43, 46] and to some extent to the higher molecular weight of the materials used by Disney et al.

Additional negative control experiments were also conducted using either *E. coli* that does not express the *FimH* protein or precursor polymers that do not have functional sugars attached. This data supported the high specificity of the polymers interaction with the CRSs found on bacteria pili (figure 2-27); Mixture of *E. coli* Top10, which does not produce Type 1 fimbriae with P2-1 or P2-2 showed no aggregates formation, and the same experiments with precursor polymers lacking sugar residues and the MG1655pGFP strain also showed negligible bacterial aggregation under both temperature conditions.

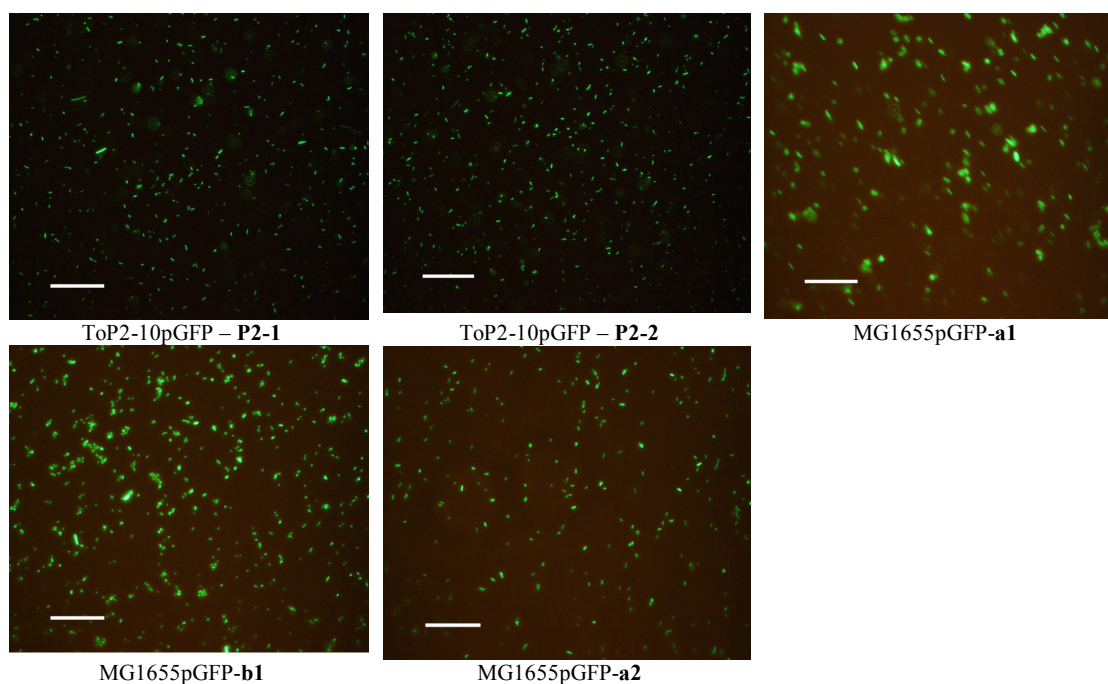


**Figure 2-27.** Control experiments using a mutant *E. coli* strain without *fimH* and polymers **P2-1** and **P2-2**. Additional control assays with precursor polymers lacking sugar segment and MG1655pGFP strain also showed negligible bacterial aggregation at room conditions (white bar: 10  $\mu\text{m}$ ).

The key experiment was to establish the reversibility of polymer-cell interactions via temperature-mediated ligand display. The strength of glucose binding to *fimH* [43] is lower than that to PBA [23] ( $K_{\text{eq}}$  for the diol-boronate ester: 4.6  $\text{M}^{-1}$ , pH 7.4), but crucially, the affinity constant for glucose-*fimH* is lower than that of mannose-*fimH*, the principal biological target sugar for *E. coli* MG1655. We therefore hypothesized that the polyvalent interactions of the glucose-polymers would be strong enough to promote bacterial aggregation below LCST but sufficiently weak to facilitate reversibility upon application of a thermal stimulus, since the polymers showed reversible binding with PBA. Indeed, thermal cycling of bacteria-polymers suspensions revealed reversible bacterial aggregation (figure 2-28).

In cell suspensions at temperatures above LCST (45  $^{\circ}\text{C}$ ) where the polymers were in a globular phase, bacteria were uniformly dispersed, but when left at room conditions below LCST, large aggregates were formed (ranging from

15 to 120  $\mu\text{m}^2$ ). Reincubation of the suspensions at higher temperatures for 5 min (at 45 °C), followed by mild vortexing to break preformed clusters, and subsequent maintenance at 45 °C showed no aggregation. To close the thermal loop, cooling to room temperature promoted bacterial aggregation once more (figures 2-28 and 2-29).

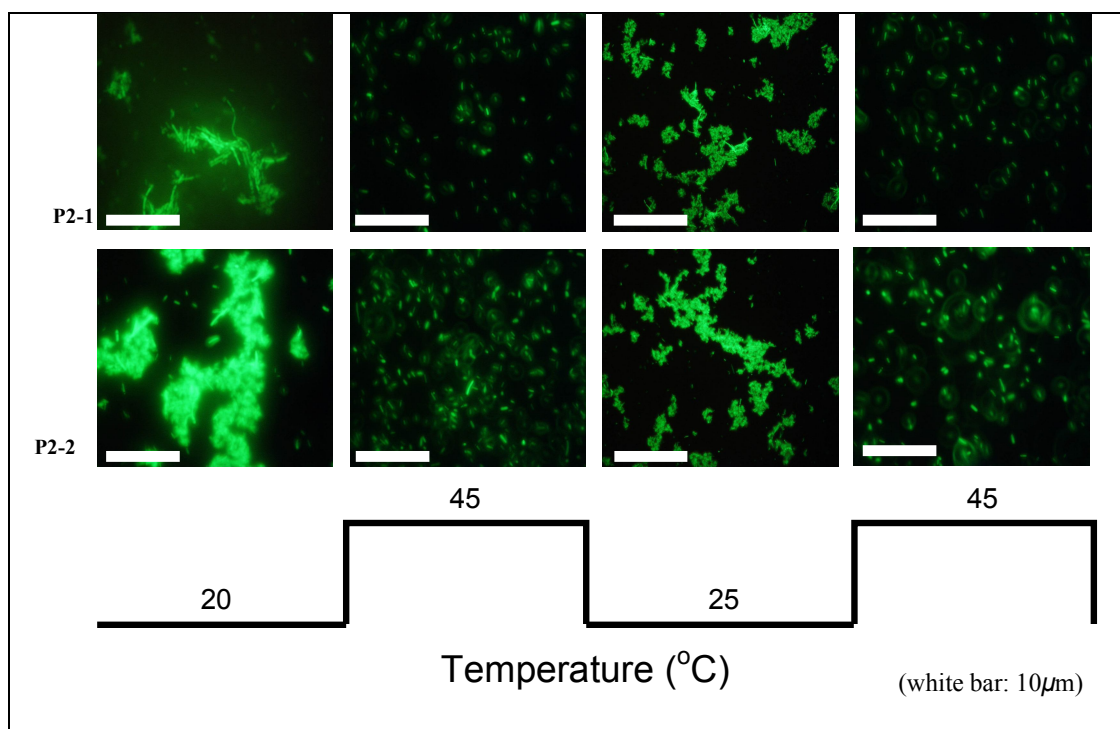


**Figure 2-28.** Control of bacterial aggregation formation by thermal oscillation across LCST in presence of **P2-1** and **P2-2**.

This behaviour was repeatable over three cycles. Larger bacterial aggregates were formed between **P2-2** and *E. coli* MG1655pGFP compared to those formed by **P2-1** and *E. coli*. This was most likely due to the higher molar mass of **P2-2** ( $M_w \sim 20$  kDa) compared to **P2-1** ( $M_w \sim 16$  kDa) and sugar content ( $\sim 12$  glucose units per chain for **P2-2** compared to 6 for **P2-1**). However, it is also probable that the different-length spacers and attachment positions of the glucose residues in copolymers **P2-1** and **P2-2** affected ligand-receptor accessibility and hence extent of cell interactions. Image analysis confirmed that **P2-2** indeed induced larger bacterial formation but also revealed that during temperature cycling progression the polymer-bacteria clusters formed tended to decrease in size. This is attributed to the

experimental setup as some polymer might adhere to the relative hydrophobic glass cover slip and eventually not participating in the aggregation phenomena.

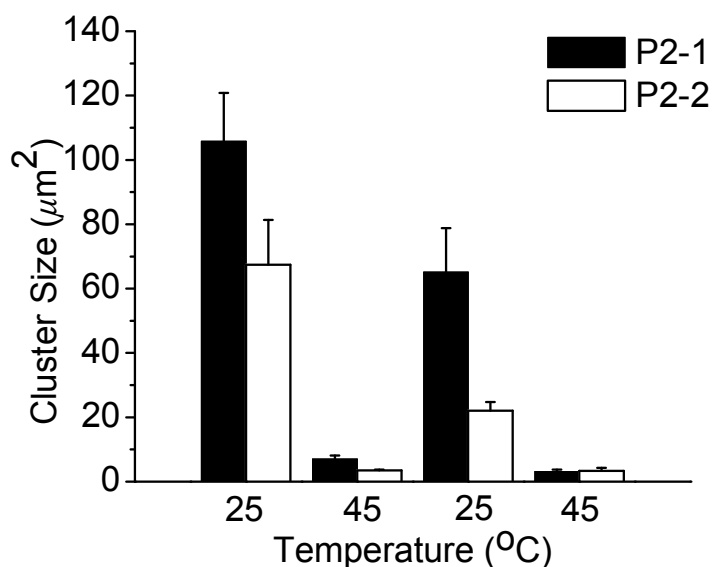


**Figure 2-29.** Reversible bacterial cluster assembly/disassembly in presence of P2-1 and P2-2 by temperature oscillation.

### 2.3. Conclusions

In conclusion we have shown that it is possible to place bacterial aggregation under external control through a combination of thermoresponsive polymer chains, accessible functionality, and choice of sugar moiety. The advantages of using synthetic polymeric materials for bacterial interactions are numerous; the intrinsic “soft” nature of polymers confers compatibility with biological organelles, while the variety and flexibility of polymer architectures and structures through design suggests polymers can be highly effective materials for bacteria-matter interactions. Polymer functionalization is readily accessible as shown by the facile syntheses while recognition properties of the sugar components can be probed by exploiting the boronic acid-diol interactions coupled to a fluorescent-based assay. Biorecognition properties were also demonstrated by studying the interactions with a model lectin.

These materials demonstrate that an increased functionality can be achieved without compromising the intrinsic thermoresponsive character by rational design. Additionally, the study shows that “on/off” behaviour of these polymers does not only exhibit the reversible ligand display attached on the polymer but rather controls multivalent events with biological hosts in a highly specific and reversible manner. Therefore, the present study probably shows that tailor-made “smart” polymers aiming at specific interactions might be a means of mimicking the subtle biological phenomena that occur in the biological microenvironment in order to achieve highly specific cell-sensing materials for pathogen detection and elimination.

Potential extension of this concept of specific cell/protein binding of these materials “at will” could be used for the development of smart materials not only for cell sensing and biomolecular applications but also as “smart scaffolds” for tissue engineering and regenerative medicine exploiting the abundance of polysaccharides and glycoresidues in cell growth, proliferation and differentiation processes.

#### 2.4. References

1. Monack, D.M., A. Mueller, and S. Falkow, *Persistent bacterial infections: The interface of the pathogen and the host immune system*. *Nature Reviews Microbiology*, 2004. **2**(9): p. 747-765.
2. Dickert, F.L., P. Lieberzeit, and O. Hayden, *Sensor strategies for microorganism detection - from physical principles to imprinting procedures*. *Analytical and Bioanalytical Chemistry*, 2003. **377**(3): p. 540-549.
3. Bertozzi, C.R. and L.L. Kiessling, *Chemical glycobiology*. *Science*, 2001. **291**(5512): p. 2357-2364.
4. Mammen, M., S.K. Choi, and G.M. Whitesides, *Polyvalent interactions in biological systems: Implications for design and use of multivalent ligands*

- and inhibitors*. *Angewandte Chemie-International Edition*, 1998. **37**(20): p. 2755-2794.
5. Sharon, N., *Carbohydrates as future anti-adhesion drugs for infectious diseases*. *Biochimica Et Biophysica Acta-General Subjects*, 2006. **1760**(4): p. 527-537.
  6. Choi, S.K., M. Mammen, and G.M. Whitesides, *Generation and in situ evaluation of libraries of poly(acrylic acid) presenting sialosides as side chains as polyvalent inhibitors of influenza-mediated hemagglutination*. *Journal of the American Chemical Society*, 1997. **119**(18): p. 4103-4111.
  7. Nguyen, S.T., L.K. Johnson, R.H. Grubbs, and J.W. Ziller, *Ring-Opening Metathesis Polymerization (Romp) of Norbornene by a Group-Viii Carbene Complex in Protic Media*. *Journal of the American Chemical Society*, 1992. **114**(10): p. 3974-3975.
  8. Lamanna, A.C., G.W. Ordal, and L.L. Kiessling, *Large increases in attractant concentration disrupt the polar localization of bacterial chemoreceptors*. *Molecular Microbiology*, 2005. **57**(3): p. 774-785.
  9. Gestwicki, J.E., C.W. Cairo, L.E. Strong, K.A. Oetjen, and L.L. Kiessling, *Influencing receptor-ligand binding mechanisms with multivalent ligand architecture*. *Journal of the American Chemical Society*, 2002. **124**(50): p. 14922-14933.
  10. Mowery, P., Z.Q. Yang, E.J. Gordon, O. Dwir, A.G. Spencer, R. Alon, and L.L. Kiessling, *Synthetic glycoprotein mimics inhibit L-selectin-mediated rolling and promote L-selectin shedding*. *Chemistry & Biology*, 2004. **11**(5): p. 725-732.
  11. Disney, M.D., J. Zheng, T.M. Swager, and P.H. Seeberger, *Detection of bacteria with carbohydrate-functionalized fluorescent polymers*. *Journal of the American Chemical Society*, 2004. **126**(41): p. 13343-13346.
  12. Salmaso, S., S. Bersani, S.S. Pennadam, C. Alexander, and P. Caliceti, *Avidin bioconjugate with a thermoresponsive polymer for biological and pharmaceutical applications*. *International Journal of Pharmaceutics*, 2007. **340**(1-2): p. 20-28.

13. Kumar, A., A. Srivastava, I.Y. Galaev, and B. Mattiasson, *Smart polymers: Physical forms and bioengineering applications*. Progress in Polymer Science, 2007. **32**(10): p. 1205-1237.
14. Stayton, P.S., T. Shimoboji, C. Long, A. Chilkoti, G.H. Chen, J.M. Harris, and A.S. Hoffman, *Control of Protein-Ligand Recognition Using a Stimuli-Responsive Polymer*. Nature, 1995. **378**(6556): p. 472-474.
15. Lee, H. and T.G. Park, *Conjugation of trypsin by temperature-sensitive polymers containing a carbohydrate moiety: Thermal modulation of enzyme activity*. Biotechnology Progress, 1998. **14**(3): p. 508-516.
16. Dizman, B., M.O. Elasri, and L.J. Mathias, *Synthesis and characterization of antibacterial and temperature responsive methacrylamide polymers*. Macromolecules, 2006. **39**(17): p. 5738-5746.
17. Fujimoto, K., C. Iwasaki, C. Arai, M. Kuwako, and E. Yasugi, *Control of cell death by the smart polymeric vehicle*. Abstracts of Papers of the American Chemical Society, 2001. **221**: p. U348-U348.
18. Hopkins, S., S. Carter, S. MacNeil, and S. Rimmer, *Temperature-dependent phagocytosis of highly branched poly(N-isopropyl acrylamide-co-1,2 propandiol-3-methacrylate)s prepared by RAFT polymerization*. Journal of Materials Chemistry, 2007. **17**: p. 4022-4027.
19. Rimmer, S., *Personal communication*. 2007.
20. Chan, G.Y.N., M.G. Looney, D.H. Solomon, and S. Veluayitham, *The synthesis of novel hybrid monomers*. Australian Journal of Chemistry, 1998. **51**(1): p. 31-35.
21. Kuckling, D., H.J.P. Adler, K.F. Arndt, L. Ling, and W.D. Habicher, *Temperature and pH dependent solubility of novel poly(N-isopropylacrylamide) copolymers*. Macromolecular Chemistry and Physics, 2000. **201**(2): p. 273-280.
22. Fales, F.W., *The Assimilation and Degradation of Carbohydrates by Yeast Cells*. Journal of Biological Chemistry, 1951. **193**(1): p. 113-124.

23. Springsteen, G. and B.H. Wang, *Alizarin Red S. as a general optical reporter for studying the binding of boronic acids with carbohydrates*. Chemical Communications, 2001(17): p. 1608-1609.
24. Davis, B.G., Fairbanks, A.J., *Carbohydrate chemistry*. 2002: Oxford Science Publications.
25. Ambrosi, M., A.S. Batsanov, N.R. Cameron, B.G. Davis, J.A.K. Howard, and R. Hunter, *Influence of preparation procedure on polymer composition: synthesis and characterisation of polymethacrylates bearing beta-D-glucopyranoside and beta-D-galactopyranoside residues*. Journal of the Chemical Society-Perkin Transactions 1, 2002(1): p. 45-52.
26. Polizzotti, B.D. and K.L. Kiick, *Effects of polymer structure on the inhibition of cholera toxin by linear polypeptide-based glycopolymers*. Biomacromolecules, 2006. 7(2): p. 483-490.
27. Roe, J.H., *The Determination of Dextran in Blood and Urine with Anthrone Reagent*. Journal of Biological Chemistry, 1954. 208(2): p. 889-896.
28. Yan, J., H. Fang, and B.H. Wang, *Boronolectins and fluorescent boronolectins: An examination of the detailed chemistry issues important for the design*. Medicinal Research Reviews, 2005. 25(5): p. 490-520.
29. Yan, J., G. Springsteen, S. Deeter, and B. Wang, *The relationship among pKa, pH, and binding constants in the interactions between boronic acids and diols--it is not as simple as it appears*. Tetrahedron, 2004. 60(49): p. 11205-11209.
30. Alarcon, C.D.H., S. Pennadam, and C. Alexander, *Stimuli responsive polymers for biomedical applications*. Chemical Society Reviews, 2005. 34(3): p. 276-285.
31. Yin, X., A.S. Hoffman, and P.S. Stayton, *Poly(N-isopropylacrylamide-co-propylacrylic acid) copolymers that respond sharply to temperature and pH*. Biomacromolecules, 2006. 7(5): p. 1381-1385.
32. Zhang, Y.J., S. Furyk, D.E. Bergbreiter, and P.S. Cremer, *Specific ion effects on the water solubility of macromolecules: PNIPAM and the*

- Hofmeister series*. Journal of the American Chemical Society, 2005. **127**(41): p. 14505-14510.
33. Ge, H., Y.W. Ding, C.C. Ma, and G.Z. Zhang, *Temperature-controlled release of diols from N-isopropylacrylamide-co-acrylamidophenylboronic acid microgels*. Journal of Physical Chemistry B, 2006. **110**(41): p. 20635-20639.
34. Winnik, F.M., *Quenching of Fluorescence from Pyrene-Labeled Poly(N-Isopropylacrylamide) Solutions Heated above Their Lower Critical Solution Temperature*. Macromolecules, 1990. **23**(6): p. 1647-1649.
35. Ambrosi, M., N.R. Cameron, and B.G. Davis, *Lectins: tools for the molecular understanding of the glycode*. Organic & Biomolecular Chemistry, 2005. **3**(9): p. 1593-1608.
36. Bradbrook, G.M., T. Gleichmann, S.J. Harrop, J. Habash, J. Raftery, J. Kalb, J. Yariv, I.H. Hillier, and J.R. Helliwell, *X-ray and molecular dynamics studies of concanavalin-A glucoside and mannoside complexes - Relating structure to thermodynamics of binding*. Journal of the Chemical Society-Faraday Transactions, 1998. **94**(11): p. 1603-1611.
37. Derewenda, Z., J. Yariv, J.R. Helliwell, A.J. Kalb, E.J. Dodson, M.Z. Papiz, T. Wan, and J. Campbell, *The Structure of the Saccharide-Binding Site of Concanavalin-A*. Embo Journal, 1989. **8**(8): p. 2189-2193.
38. Becker, J.W., G.N. Reeke, J.L. Wang, B.A. Cunningham, and G.M. Edelman, *Covalent and 3-Dimensional Structure of Concanavalin-a .3. Structure of Monomer and Its Interactions with Metals and Saccharides*. Journal of Biological Chemistry, 1975. **250**(4): p. 1513-1524.
39. Kanai, M., K.H. Mortell, and L.L. Kiessling, *Varying the size of multivalent ligands: The dependence of concanavalin a binding on neoglycopolymer length*. Journal of the American Chemical Society, 1997. **119**(41): p. 9931-9932.
40. Ladmiral, V., G. Mantovani, G.J. Clarkson, S. Cauet, J.L. Irwin, and D.M. Haddleton, *Synthesis of neoglycopolymers by a combination of "click*

- chemistry" and living radical polymerization. Journal of the American Chemical Society, 2006. 128(14): p. 4823-4830.*
41. Cairo, C.W., J.E. Gestwicki, M. Kanai, and L.L. Kiessling, *Control of multivalent interactions by binding epitope density. Journal of the American Chemical Society, 2002. 124(8): p. 1615-1619.*
  42. Becker, J.W., G.N. Reeke, B.A. Cunningham, and G.M. Edelman, *New Evidence on Location of Saccharide-Binding Site of Concanavalin-A. Nature, 1976. 259(5542): p. 406-409.*
  43. Bouckaert, J., J. Berglund, M. Schembri, E. De Genst, L. Cools, M. Wuhrer, C.S. Hung, J. Pinkner, R. Slattegard, A. Zavialov, D. Choudhury, S. Langermann, S.J. Hultgren, L. Wyns, P. Klemm, S. Oscarson, S.D. Knight, and H. De Greve, *Receptor binding studies disclose a novel class of high-affinity inhibitors of the Escherichia coli FimH adhesin. Molecular Microbiology, 2005. 55(2): p. 441-455.*
  44. Sharon, N. and H. Lis, *The structural basis for carbohydrate recognition by lectins. Molecular Immunology of Complex Carbohydrates-2, 2001. 491: p. 1-16.*
  45. Hung, C.S., J. Bouckaert, D. Hung, J. Pinkner, C. Widberg, A. DeFusco, C.G. Auguste, R. Strouse, S. Langermann, G. Waksman, and S.J. Hultgren, *Structural basis of tropism of Escherichia coli to the bladder during urinary tract infection. Molecular Microbiology, 2002. 44(4): p. 903-915.*
  46. Krogfelt, K.A., H. Bergmans, and P. Klemm, *Direct Evidence That the Fimh Protein Is the Mannose-Specific Adhesin of Escherichia-Coli Type-1 Fimbriae. Infection and Immunity, 1990. 58(6): p. 1995-1998.*

## Chapter 3

### *Sweet-talking block copolymer vesicles*

#### **3. Introduction**

The language of cellular interactions in nature includes a wealth of code based on sugar molecules and macromolecular frameworks [1, 2]. The complexity in carbohydrate structure is matched by a subtlety in function that leads to a huge variety of roles for these polymeric sugars in biology [3, 4]. It is not surprising therefore that chemists seek to “talk” to biological entities through the language of the glycode, for this would enable intervention in events such as cell-surface recognition, detection, and signalling, leading in turn to prevention of infectivity [5], treatment of disease [6], and even to control of new tissue formation [7].

It is now possible to synthesize polymeric materials of multiple functionality and of complex architecture that are difficult if not impossible to synthesize with conventional polymerization methods and use them as tools to understand these complex natural phenomena. The advantages of using polymeric materials in biology [8] mainly derive from the fact that the macromolecular nature of these materials confers compatibility with biological organelles and can be precisely fine tuned to achieve specific tasks in the biological microenvironments.

In particular, block copolymers have received considerable attention due to their potential to self assemble in aqueous solutions into supramolecular structures such as micelles, vesicles or worm-like cylinders [9-11]. Block copolymer structures with at least one of the blocks being based on glycomonomers (i.e. polymerizable sugar derivatives)

have been synthesized in the past with the scope of targeting specific biological receptors by exploiting the unique specificity of carbohydrate molecules when interacting with their corresponding hosts [1, 12, 13]. Generally, there are two approaches when one endeavours to synthesize this class of materials: a) polymerization of a pre-synthesized glycomonomer with subsequent copolymerization of the second monomer and b) post-functionalization of a pre-synthesized block copolymer with sugar moieties [12, 14, 15]. Most researchers prefer the first route since a glycomonomer will, in theory, give a better defined material albeit the chemistries used to synthesize these monomers are still not suitable for large scale or industrial use.

Li et al. performed systematic studies on the self assembly properties of a novel block-glycopolymer that consisted of polystyrene as the hydrophobic block and glucosyloxyethyl acrylate as the hydrophilic sugar-rich polymeric chain [16]. The polymer was synthesized by means of ATRP that enabled the researchers to keep the polydispersity low ( $PDI < 1.5$ ). Interestingly, it was found that not only the polymer could assemble into molecular aggregates but the shape and the morphology of the assemblies could be significantly influenced by the presence of HCl,  $CaCl_2$  or Con A. The exact mechanisms of this behaviour is not clarified but is mainly attributed to the response of the sugar-rich coronae.

Another inspiring example from the second route of synthesis comes from You et al. where they derivatized a preformed well-defined block copolymer of polybutadiene-block-polystyrene with thioglucoopyranose via standard irradiation procedures [17]. The -diene groups were derivatized with the sugar moiety almost quantitatively. The resulting block-glycopolymer could form sub-micron sized vesicles in water. This approach is regarded as highly robust and practical as the decoration of polymers with carbohydrate molecules is notoriously difficult due to the

lack of scalable chemistries for sugar decoration in an industrial context. Despite the fact that the above examples use sugar monomers to construct the hydrophilic block, the researchers, surprisingly, did not exploit the great potential of the carbohydrate moieties to interact with biological hosts.

The group of Dr Chaikof have performed studies of self-assembling block-copolymers with sugar segments on the coronae with the scope of mimicking biological organelles of carbohydrate functionality [18, 19]. By employing ROP and ATRP they synthesized a triblock copolymer of [poly(L-alanine)-b-poly(2-acryloyloxyethyl lactoside)-b-poly(L-alanine)] that could self-assemble into spherical aggregates that could interact specifically with the lectin *ricinus communis* agglutinin (RCA<sub>120</sub>) due to the presence of the lactose molecules of the glycopolymer chain. Similar studies have also been conducted by the Kataoka group who systematically studied sugar-rich block-copolymer micelles with the aim of implementing molecular devices for targeted drug delivery [20, 21]. They constructed a small library of sugar-containing micelles of the structure X-PEG-PLA with X being the carbohydrate molecule (glucose, galactose, lactose or mannose). Specific interactions were studied using agglutinin or Con A as standard lectins to probe the multivalent nature of the micelle-lectin aggregates formed. The small size of the micelles synthesized (ca 20-30 nm) allows for use of these materials as “active targeting drug vehicles”.

By rationally designing materials at the molecular level via embedding information for their supramolecular self-assembly at the macromolecular scale in a protein-like folding fashion, Kim et al. [22] were able to obtain micellar, vesicular or tubular structures by subtly changing the composition of the starting materials. The rod-coil amphiphiles used in this study consisted of tetra(p-phenylene) or di[tetra(p-phenylene)] as the

hydrophobic moiety and oligo(ethylene oxide) decorated with mannose as the hydrophilic segments. The coexistence of incompatible hydrophobic/hydrophilic moieties drove the supramolecular self-assembly of these materials in aqueous environments such that carbohydrate molecules at the outer surface were exposed ready to bind with CRSs. These materials were found to interact with *E. coli* in a strong multivalent manner, and the supramolecular structure was also found to play a key role in the binding process. Spherical micellar structures could bind more strongly with Con A compared to cylindrical micelles. Although this observation has yet to be fully characterised, the work clearly signifies the importance of supramolecular architecture when designing biofunctional materials using bottom-up approaches (i.e. self-assembly).

In parallel to these findings, the introduction of block copolymers that self assemble into supramolecular objects upon external stimuli has also been successfully reported [23, 24]. This degree of response increases the complexity of these systems and brings them closer to natural materials and processes that can adapt according to the environmental changes. Although, we are still far from self-adapting materials that can intrinsically respond and change their properties, these stimuli responsive polymers are perhaps a first step towards achieving this goal. For example, by combining self-assembling polymer with the correct choice of ligands, one could consider building materials and interfaces that are biomimetic in both structure and function.

Herein we describe an approach towards controlling cell-surface interactions and molecular transport at biointerfaces, by using self-assembling polymer vesicles with multiple copies of a simple glycoligand, glucose, as a first step towards a “conversation” between artificial cell mimics and real cells [25]. The key to this approach is the preparation of

synthetic polymers capable of assembling into capsule-like structures with sugar functionality presented into solution. The aim is to produce a simple mimic of eukaryotic cell surfaces, which might in turn be recognized by biological species that normally bind to glycosylated residues on the cell [26]. To do this, we prepared block copolymers with highly hydrophilic poly(2-glucosyloxyethyl methacrylate) (pGEMA) as one block and more sparingly water-soluble poly(diethyleneglycol methacrylate) (pDEGMA) as the second block by using controlled free-radical techniques (figure 3-1 and Table 3-I). We chose glucose as the recognition element, as it exhibits generally weak individual interactions with receptors, but when multiple copies are present on a polymer backbone strong binding can occur through polyvalency [27, 28].

### 3.1. Materials and Methods

#### 3.1.1. Materials and Instrumentation

All solvents were of analytical grade and were purchased from Sigma or Fisher Scientific. Reagents were all of at least 97% purity and were from Sigma unless otherwise stated. Beta-D-glucose pentaacetate (AcGlc) was purchased from Alfa Aesar. Concanavalin A and FITC-concanavalin A were from MP Biomedicals. Diethylene glycol methacrylate (DEGMA) was passed through neutral alumina column to remove impurities and inhibitors. The acetylated glucosyloxyethyl methacrylate (AcGEMA) monomer was synthesized according to a previously published procedure (see Appendix for characterization details) [29]. The polymers were characterized by Gel Permeation Chromatography (GPC) which was carried out using a Polymer Laboratories GPC 50 instrument with RI detector and DMF as mobile phase at 30 °C. Molecular weights were calculated based on universal calibration method using polystyrene standards. Further characterisation was via <sup>1</sup>H NMR (Bruker 400 MHz), with peak assignments based on those of the pGEMA and related

polymers reported by Ambrosi et al. [29]. Cloud point measurements were measured by using a Beckman DU 640 UV/Vis spectrophotometer equipped with a thermostat unit. A Nikon optical microscope equipped with a camera connected to a personal computer was used for optical microscopy studies. Adobe Photoshop CS2 version 9.0 software was used for image analysis.

### 3.1.2. Polymer Synthesis

#### 3.1.2.1. Synthesis of polymer P3-1

Acetylated glucoxyloxyethyl methacrylate (AcGEMA) was synthesized according to a published procedure [29]. In an N<sub>2</sub>-purged round-bottom flask, AcGEMA (3 g, 6.5 mmol) was dissolved in degassed MeOH (8 mL). The flask was sealed with a rubber septum and a degassed solution of CuBr (123 mg, 0.8 mmol) and 2,2-bipyridyl (bipy, 269 mg, 1.7 mmol) in MeOH (4 mL) was added through a glass syringe. Then, the initiator ethyl-2-bromoisobutyrate (128 mL) was added through a microsyringe and the flask was placed in an oil bath at 30 °C. After 90 min, the polymerization was stopped by exposing the reaction mixture to air. The resulting poly(AcGEMA) was isolated by dialysis against acetone using a cellulose 1000 MWCO membrane (yield 85 %). Deprotection of poly(AcGEMA) involved dissolving the polymer in a mixture of CHCl<sub>3</sub>/MeOH (1:1) (0.5 g/mL). A catalytic amount of NaOMe in MeOH was added to the solution (1 mM). The reaction was left under an atmosphere of N<sub>2</sub> until the solution became turbid. Poly(GEMA) was isolated by centrifugation and lyophilization (yield 75 %). Poly(GEMA) was used as macroinitiator to grow the pDEGMA block as follows: Diethylene glycol methacrylate (890 mg, 4.7 mmol) was added in a previously N<sub>2</sub>-purged round-bottom flask. The flask was sealed with a rubber septum and a freshly prepared solution of CuBr (13.6 mg, 0.1 mmol), bipy (29.8 mg, 0.2 mmol), and poly(GEMA), 200 mg in MeOH

(4mL) was added through a glass syringe. The flask was placed in an oil bath at 60 °C for 3 h. The reaction was stopped by exposing the reaction solution to air. The final product was recovered by dialyzed against water for 3 days and then freeze drying (yield 82 %).

### 3.1.2.2. Synthesis of polymer P3-2

AcGEMA (5 g, 10.8 mmol) was dissolved in MeOH (5 mL) in a 50 mL round-bottom flask. Azobisisobutyronitrile (AIBN, 7.5 mg) and RAFT agent cyan-2-ylidithiobenzoate (CDBA, 47.5 mg) were added to the flask, which was then purged with N<sub>2</sub> for 20 min. The rubber-septum-sealed flask was placed in an oil bath at 70 °C overnight, and then the reaction was stopped by opening the flask to air. The precursor polymer was recovered by dialyzing the reaction mixture against excess MeOH using 1000 MWCO membrane for 2 days (yield 82 %). Deprotection was carried out as described for P3-1 (yield 72%). The pDEGMA block was grown as follows: pGEMA (1 g) and DEGMA (1 g) were dissolved in EtOH (3 mL). AIBN (2.8 mg) and CDBA (19 mg) were added. The flask was sealed and the reaction mixture was purged with N<sub>2</sub> for 20 min, and the reaction was allowed to proceed overnight at 65 °C. The polymer was recovered by dialysis against water for 2 days and subsequent freeze drying for 24h (yield 79%).

### 3.1.3. Bacteria-vesicles interactions

Bacteria were grown in lysogeny broth (LB medium) up to the stationary phase (optical density=0.8) by incubation overnight at 37 °C in the dark. Aliquots (300 mL) were collected in eppendorf tubes and centrifuged at 13 000 rpm for 3 min. The supernatant was then replaced with freshly prepared phosphate buffered saline (PBS; pH 7.4) containing the polymer (4 mg/mL). The samples were vortexed for 5 s and left to settle for 15 min at room temperature (ca. 25 °C). Aliquots (10 mL) of the sample were collected with a micropipette, mounted on a glass slide with a cover slip

on top, and examined with an optical microscope. Control experiments were also conducted using a precursor polymer (see Results and Discussion section).

#### 3.1.4. Critical micelle concentration

A series of polymer samples in water were prepared by serial dilutions from a starting stock solution in water (4 mg/mL). A stock solution of pyrene was prepared by suspending pyrene in water and leaving it stirring overnight. Solids were removed and the resulting solution was used by adding 100  $\mu$ L in each polymer sample. The samples were vortexed for 5 seconds and left to settle at 23 °C or 37 °C. The excitation of each solution was examined in a Varian Cary Eclipse fluorescence spectrophotometer equipped with a peltier apparatus for temperature control. The peak of interest at 337 nm [30] was plotted against polymer concentrations to determine the CMC.

#### 3.1.5. Dynamic light scattering

A polymer solution was prepared by dissolving appropriate amounts of polymer in ELGA water. The polymer solution was filtered with a 1  $\mu$ m pore-size filter to eliminate dust contamination. A 60  $\mu$ L aliquot was added in a quartz cuvette and the sample was examined on a Viscotek 802 dynamic light scattering instrument. Scattered light coming from a 50 mW laser source (830 nm) was recorded from an internal light detector aligned at 90° from source. From standard auto correlation functions, measured correlation coefficients were related to hydrodynamic radii at varying temperatures via the Stokes-Einstein equation,  $R_H = kT / 6\pi\eta D$ , where  $R_H$  is the hydrodynamic radius,  $k$  is the Boltzmann constant,  $T$  is the temperature and  $\eta$  is the viscosity of the solvent. The size distribution of the scattering particles was determined by the average mass number of the particles.

### 3.1.6. Microscopy

Scanning Electron Microscope samples were prepared by placing a droplet of an aqueous polymer solution (**P3-1**, 3 mg/mL) on a carbon grid and left to dry overnight at room conditions. Standard plasma coating with gold was performed for 2 minutes before sample examination. Large vesicles from **P3-2** were examined directly using the optical microscope by placing 10  $\mu$ L of polymer solution on a glass slide and a coverslip on top.

### 3.1.7. Con A assay

The assay was performed in Tris buffer, pH 7.5 containing 1 mM  $\text{Ca}^{2+}$  and 1 mM  $\text{Mn}^{2+}$ . 0.5 mL polymer solution (14 mg/mL) was mounted on a quartz cuvette. The latter was placed in a UV/Vis spectrophotometer and absorbance at 600 nm was recorded with time at 20 °C. During absorbance recording further samples of protein solution (0.5 mL, 0.1 mg/mL) were added to the cuvette and the absorbance was recorded for 600 seconds.

### 3.1.8. Bacteria-Vesicles interactions and competition experiments

Vesicle-bacteria clusters were tested for stability to exogenous glucose competition by preparing bacteria-vesicles aliquots as described previously, then titrating in increasing amounts of glucose to give final concentrations of 0.05, 0.5 and 5 mM).

### 3.1.9. Interactions of ethidium bromide loaded vesicles with bacteria

Caution: Ethidium bromide is a very strong mutagen and possible carcinogen and must be handled with extreme care. A 4 mg/mL **P3-2** solution in PBS (0.1 M, 10 mL) was freshly prepared and 30  $\mu$ L of a stock ethidium bromide solution in water (10 mg/mL) were added using a micropipette. The solution was magnetically stirred for 1 hour and subsequently excess ethidium bromide, not incorporated inside the vesicles, was removed by dialysis of the polymer solution against excess volume of water using a 1000 MWCO cellulose membrane for 8 hours. The

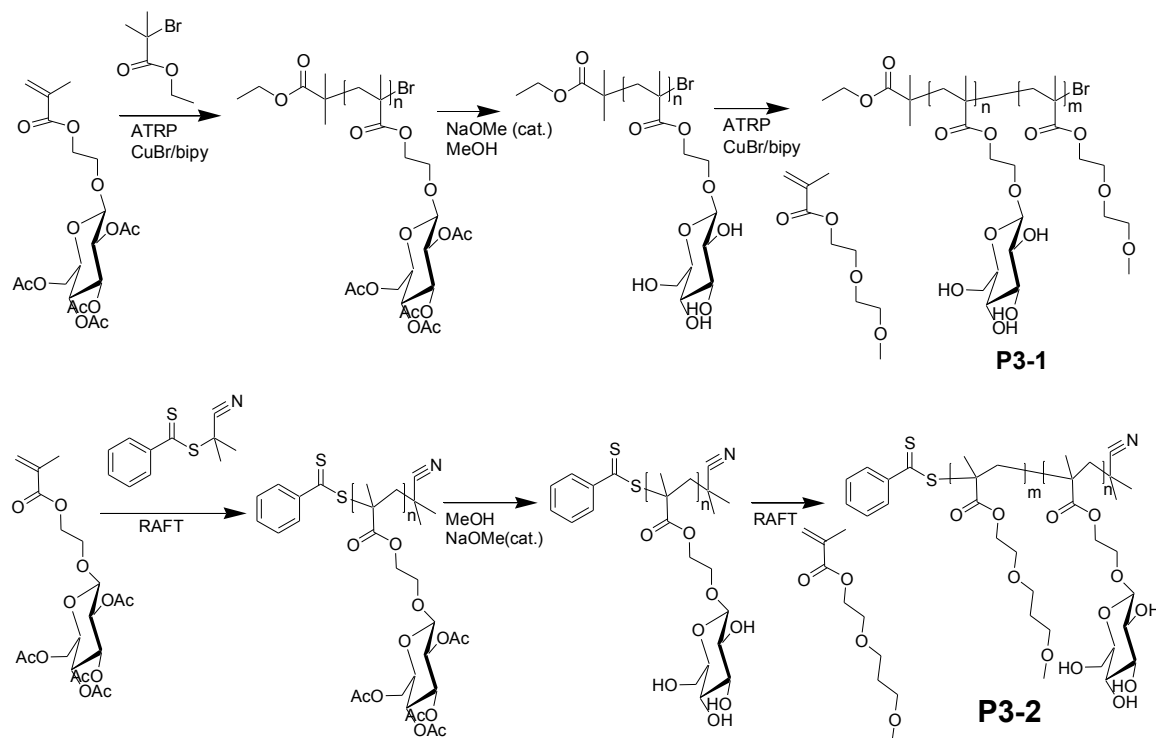
resulting solution was used as is for the polymer-bacteria samples preparation. Aliquots of previously grown bacteria (300  $\mu\text{L}$ ) were collected in Eppendorf tubes and centrifuged at 13000 rpm for 3 minutes. The supernatant was then replaced with the ethidium bromide -loaded vesicles solution. The samples were vortexed for 5 seconds and left to settle for 30 minutes at room conditions ( $\sim 25\text{ }^\circ\text{C}$ ). Aliquots (10  $\mu\text{L}$ ) of the samples were collected with a micropipette, mounted on a glass slide with a cover slip on top and examined with the optical microscope. Images were captured by using the microscope at optical or fluorescence modes, in order to detect and monitor vesicle-bacteria interactions and potential ethidium bromide diffusion inside the bacteria.

## 3.2. Results and Discussion

### 3.2.1. Polymers syntheses and characterization

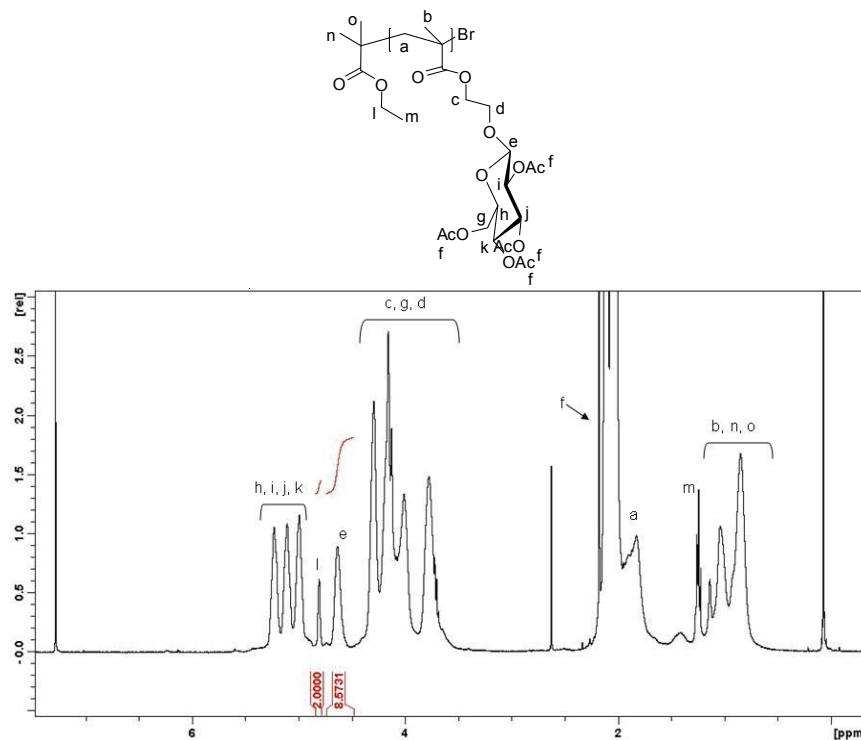
We prepared block copolymers with highly hydrophilic poly(2-glucosyloxyethyl methacrylate) (pGEMA) as one block and more sparingly water-soluble poly(diethyleneglycol methacrylate) (pDEGMA) as the second block by using controlled free-radical techniques (figure 3-1 and table 3-I).

We chose glucose as the recognition element, as it exhibits generally weak individual interactions with receptors, but when multiple copies are present on a polymer backbone strong binding can occur through polyvalency [27, 28]. Initial polymer synthesis involved growing a protected precursor polymer [29] by atom transfer radical polymerization (ATRP) or reversible addition-fragmentation chain transfer (RAFT) which was subsequently deprotected to render the block active and hydrophilic. This polymer was used as a macroinitiator to grow the pDEGMA block.



**Figure 3-1.** Syntheses of polymers (see Materials and Methods section).

For the ATRP route (**P3-1**) we employed the synthetic route by Vazquez-Dorbatt et al. [31] who synthesized biotinylated glycopolymers from the protected peracetylated glucoside monomer precursor.



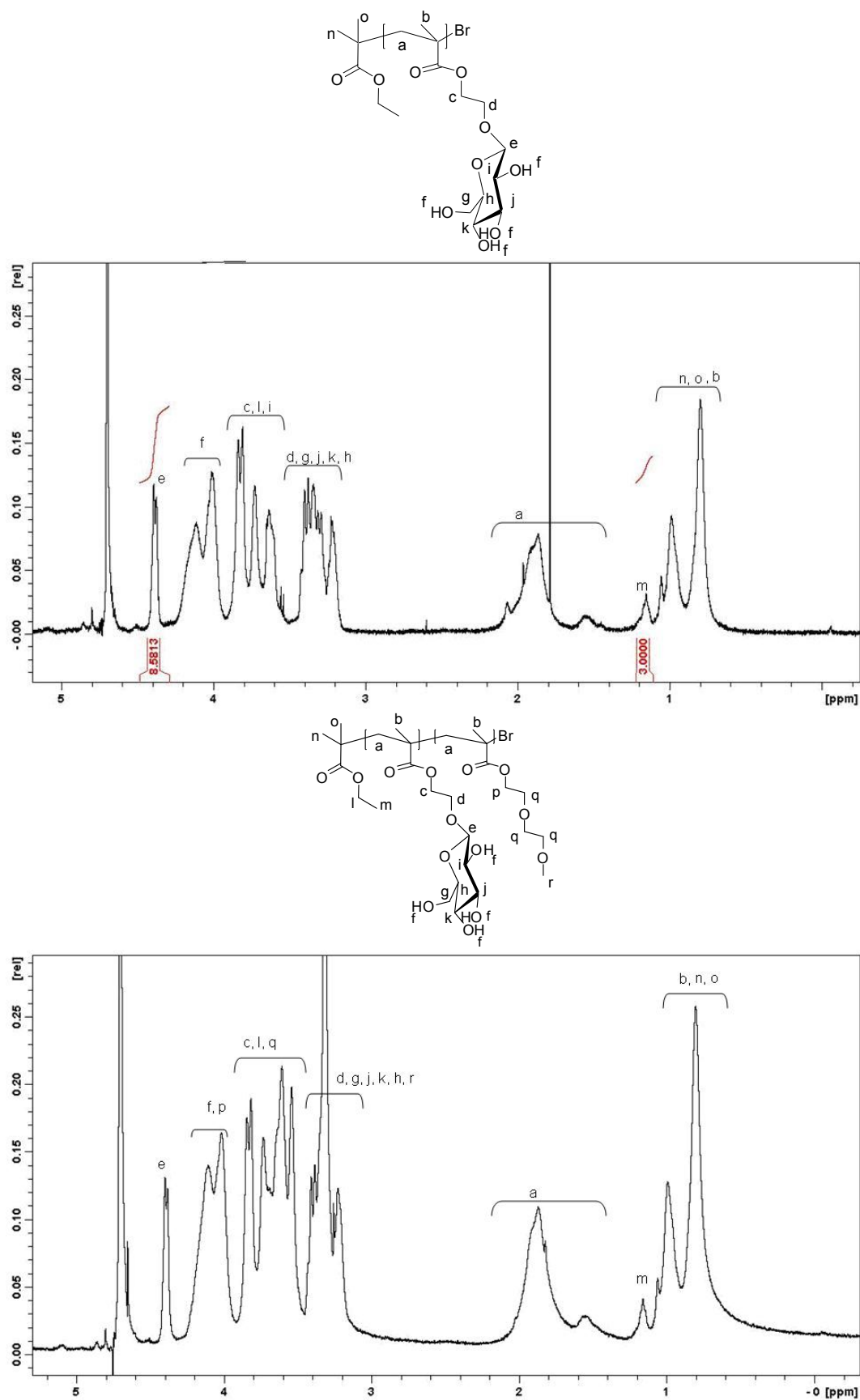


**Figure 3-2.** <sup>1</sup>H NMR allows determination of  $M_n$  values for P3-1 and its precursor polymers. Deacetylation of the sugar moieties and subsequent growth of the DEGMA block can both be monitored.

From the  $^1\text{H}$  NMR spectrum of the protected precursor it was possible to assign all the peaks of the sugar and the polymer backbone, but most importantly it was possible to accurately estimate the  $M_n$  of the polymer precursor by the relative integration of the anomeric proton (peak e, 4.7 ppm, figure 3-2) to the integral of the ethylene protons of the initiator (peak l, 4.8 ppm). The polydispersity of the protected polymer was low (PD, 1.19) which is indicative of the controlled nature of the polymerization.

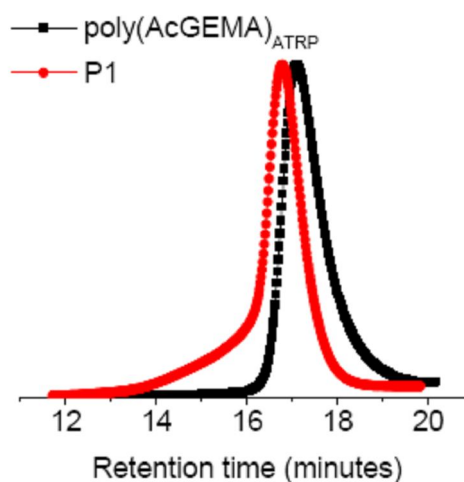


**Figure 3-3.** GPC trace of P3-1 and its precursor poly(AcGEMA)<sub>ATRP</sub>.

This result demonstrates the well-defined structure of the starting block, which proves the robustness of ATRP in the synthesis of block-copolymers. Subsequently, the deprotection reaction took place under Zemplen conditions (reaction mechanism is given in p. 54) and was monitored by  $^1\text{H}$  NMR. Initial experiments involved significant detachment of the sugar moiety from the polymer backbone due to hydrolysis of the methacrylate ester, but the use of 1:1 MeOH:CH<sub>3</sub>Cl in the deprotection mixture resulted in precipitation of the product as the latter was formed. This ensured quantitative deprotection of the polymer without detachment of the sugars from the polymer backbone as evidenced by the NMR spectrum of the deprotected block (figure 3-2).

Similarly with the RAFT method (**P3-2** precursor), we used the AIBN-RAFT initiator which is a commonly used RAFT agent for polymerization of methacrylate-based monomers and obtained a well-defined protected block. Also  $M_n$  could be determined by the relative integrals of the anomeric proton and the aromatic protons of the RAFT agent (4.7 and 7.7-7.9 ppm respectively, figure 3-4).

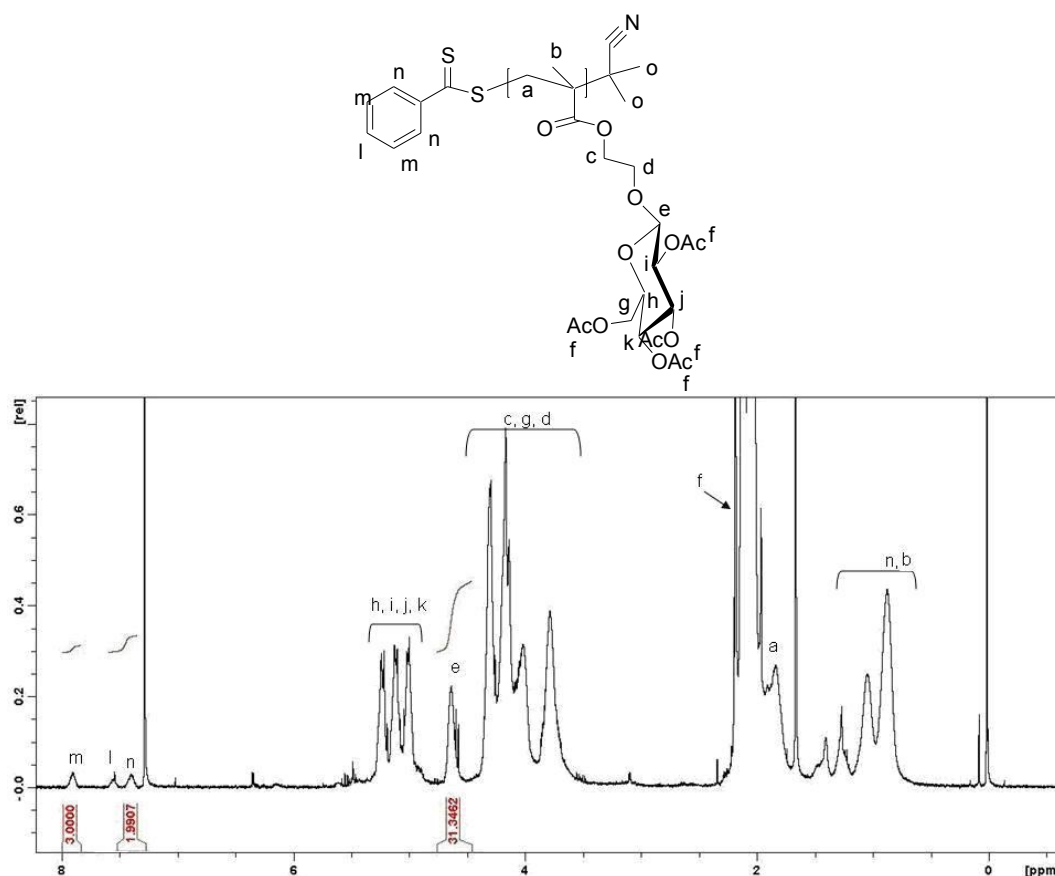
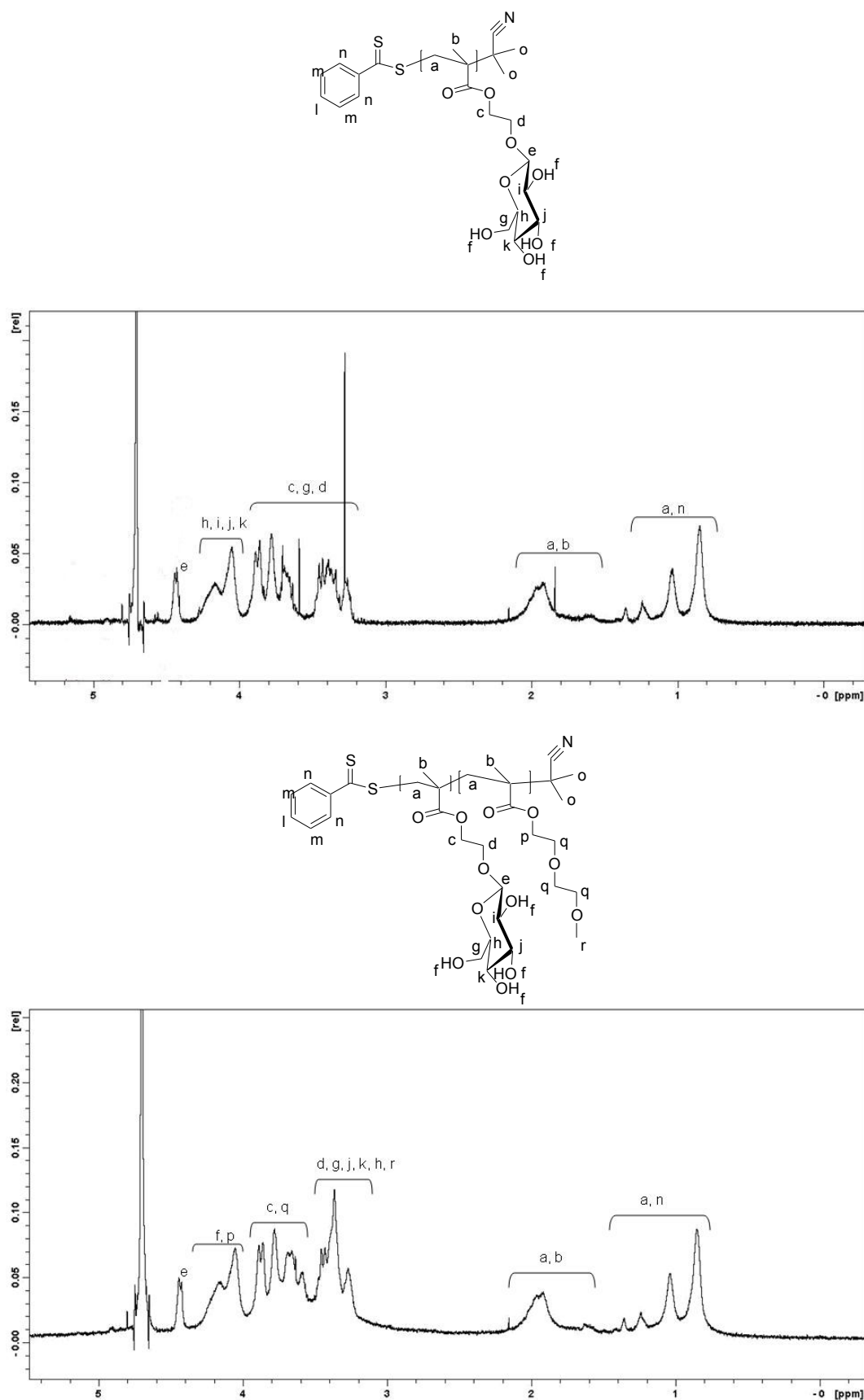
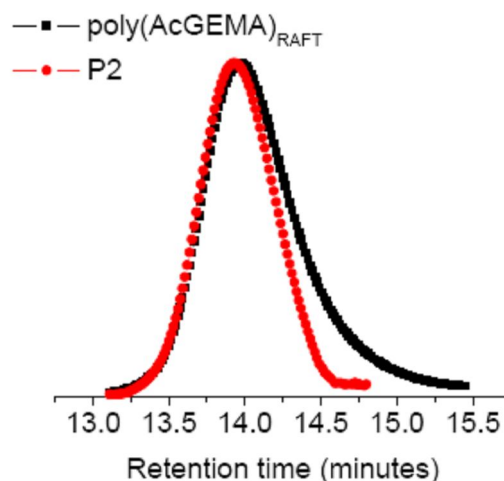


Figure 3-4. <sup>1</sup>H NMR of **P3-2** precursor polymers (continues in next page).



**Figure 3-4.**  $^1\text{H}$  NMR of P3-2 and its starting polymers. The PEGMA block is present in the spectra but it was not possible to quantify growth since the signals overlap with those of the sugars on the first GEMA block [29].

The  $M_n$  value correlated well with the GPC trace. Also the latter revealed again that the protected polymer had a very low polydispersity (P.D. 1.09) which implied that the polymer growth from the AIBN was kept to minimum. Deprotection was again quantitative and all the product could be isolated as a precipitate in the MeOH:CH<sub>3</sub>Cl solution.



**Figure 3-5.** GPC trace of **P3-2** and its precursor poly(AcGEMA)<sub>RAFT</sub>.

It should be noted that Vazquez-Dorbatt et al. report that they obtained partial gelation when targeting high DPs with the protected monomer, albeit conversions were confirmed to be high when targeting low DPs (90%) and this was the reason we employed RAFT for targeting higher DPs. The RAFT polymerization though gave slightly lower conversions (60%) at the DPs targeted although no gelation was observed. Nevertheless, we persisted on these polymerization conditions in order to prevent late termination of polymer chains by end-to-end coupling. This would ensure better control on the polymer architecture and uniformity when growing the second block of from the polymeric precursors.

Subsequent growth of the second DEGMA block was also successful by both methods. The growth of the polymers was evidenced qualitatively by <sup>1</sup>H NMR. In both spectra (for **P3-1** and **P3-2**), the diethylene glycol protons

coincide with sugar peaks and therefore it was not possible to quantify the relative growth of the polymer chains. A shifting of the GPC trace was apparent upon growth of the second block for both methods which confirms the growing of the polymer chain from the macroinitiators. In both cases, high conversions were achieved and the final polymers had low polydispersities below 1.5. Only in the case of **P3-1**, some tailing towards higher molecular weights was observed in the GPC trace, which might have resulted from polymer termination late in the process. Table 3-I summarizes the polymers properties related to their size and distribution of molecular weights.

**Table 3-I**  
Properties of polymers.

<i>Polymer (theoretical DP)</i>	$M_n$ [Da], DP ( $^1\text{H}$ NMR)	$M_n$ , DP, PD (GPC)	LCST [ $^{\circ}\text{C}$ ]
Poly(AcGEMA) <sub>ATRP</sub>	4100, 9	3800, 8, 1.19	-
<b>P3-1</b> (57 §)	-	11700, 50, 1.39	28
Poly(AcGEMA) <sub>RAFT</sub>	10400, 31	12900, 28, 1.09	-
<b>P3-2</b> (44 §)	-	15200, 36, 1.11	28

*Note: The deprotected intermediate poly(GEMA)<sub>RAFT</sub> was not characterized by  $^1\text{H}$  NMR due to low signal. GPC was also not conclusive.  $M_n$  of poly(GEMA)<sub>ATRP</sub> was 2600 as determined by  $^1\text{H}$  NMR (figure 3-2).*

*§DP refers to pDEGMA block only.*

### 3.2.2. LCST of polymers

We and others [32, 33] have systematically studied the thermal precipitation properties of PEG-based methacrylates in water. There are several reasons one would prefer OEGMA-based monomers to construct thermoresponsive polymers over the well-known NIPAM-based systems. First, DEGMA homopolymers exhibit a sharp LCST at around 28  $^{\circ}\text{C}$ , which is similar to the LCST of NIPAM homopolymers. Second, the LCST of OEGMA-based polymers can be fine tuned by combination of long-

PEG-chain methacrylates (hydrophilic) with short-PEG-chain methacrylates over a wide range of temperatures without losing the onset sharpness of the LCST curve (see [32, 34] for examples). Practically, this implies that polymerization conditions are suitable for both monomers and hence more predictable since both monomers (long and small chain) are of similar structure and reactivity [33]. Third and perhaps most importantly, OEGMA-based systems are considerably more biocompatible and less cytotoxic materials than their acrylamide counterparts [35]. This means that these materials could potentially be used for out-of-the-lab applications where contact with human tissue or blood is required.

In figure 3-6 are shown the LCST curves of **P3-1** and **P3-2** compared with that of a poly(DEGMA) homopolymer. It can be seen that the homopolymer exhibits a sharp coil-to-globule phase transition at 28 °C where the polymer drops out of solution and precipitates.

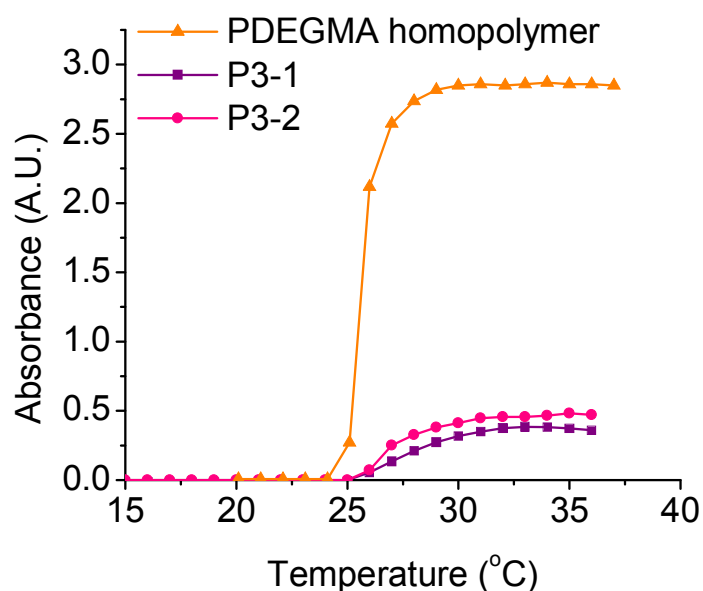


**Figure 3-6.** LCST of **P3-1** and **P3-2**. Comparison with a PDEGMA homopolymer.

As discussed in previous chapters, this behaviour is entropic and governed by the fine balance between the hydrophobic moieties, these are hydrocarbon backbone, and methoxy groups, and the well-solvated hydrophilic moieties that consist of oxyethylene containing groups on the polymer side chain and the methacrylate ester group of the polymer backbone. The latter can form hydrogen bonds with water and keep the polymer in solution. When heat is provided to the system, the hydrogen bonds will break and the hydrophobic interactions will dominate the system which will lead to the polymers collapsing above a critical temperature that is the LCST. The LCST onset of DEGMA seems to be around 28 °C. Above the LCST the polymer will flocculate and form irregular precipitates of no intrinsic order or structure.

In contrast, a double hydrophilic block copolymer such as **P3-1** or **P3-2**, will collapse in a totally different manner. The block copolymers collapsing follows a self-assembly process where the polymer chains form spherical aggregates of well-defined structure. These spherical aggregates consist of the hydrophobic, that is the collapsed DEGMA block, and the hydrophilic corona that consists of the soluble second block, that is GEMA (for **P3-1** and **P3-2**). This “partial” collapsing is evidenced in the LCST curves as a slight shifting and significant broadening of the LCST onset in both polymers. Similar LCST curves of double hydrophilic thermoresponsive polymers have also been reported by several groups either based on NIPAM or even PEGMAs as the responsive block [23, 24, 36]. This mechanism of polymer folding and self-assembly upon a thermal stimulus provides a significant advantage over a fixed pre-designed amphiphile with a readily attached hydrophobic segment: often an organic solvent must be used to dissolve the polymer initially and then evaporate it upon mixing with water to induce the self-assembly process which is not desirable when targeting specific biomedical application [11, 37]. Therefore in our system, no organic solvent is used in order to

formulate the final polymer superstructures. We therefore proceed to study the self-assembly properties of the polymers synthesised by using dynamic light scattering.

### 3.2.3. Self assembly properties

Dynamic light scattering (DLS) showed that below 15 °C, the polymers existed in solution as separate chains, but, at 20 °C, **P3-1** and **P3-2** assembled into vesicles with mean diameters of approximately 251 and 500 nm, respectively. At 37 °C (i.e., at temperatures above the lower critical solution temperature (LCST) of the pDEGMA blocks), the size of the vesicles decreased to around 182 and 300 nm for **P3-1** and **P3-2**, respectively, which we attribute to collapse of pDEGMA segments and an increase in the hydrophobicity of the vesicle “cores”. This was also confirmed by the CMC studies where we found that at temperatures above LCST the CMC was slightly lower implying more stable aggregates at these conditions [9] (figure 3-9).

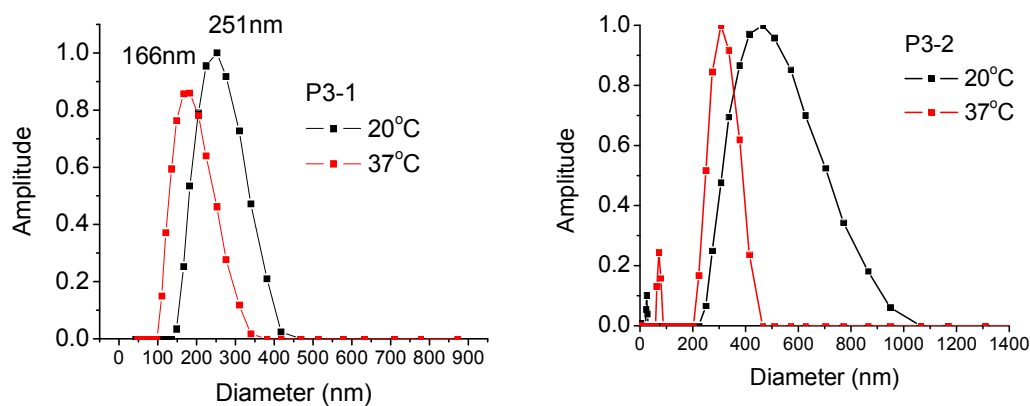


**Figure 3-7.** Dynamic light scattering data below and above the LCST of **P3-1** and **P3-2** [polymer=0.5mg/mL].

The appearance of assembled structures even below the LCST of the polymers seems to be intriguing as at low temperatures both blocks should be completely soluble and therefore no assembled superstructure

should be expected. The fact is that even a subtle difference of the hydrophilicity of the two blocks is enough to induce self-assembly phenomena and drive the polymer chains to form these closed packed aggregates (i.e. vesicles [11, 38]). This result implies that the surfactant packing parameter [38, 39] of the polymers synthesized is such that allows for self assembly even at temperatures just below the LCST.

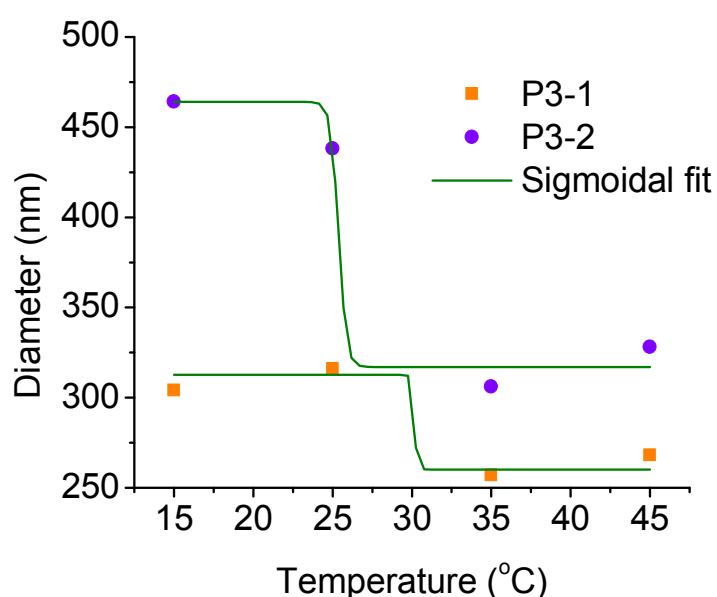


**Figure 3-8.** DLS data on size reduction of vesicles above the LCST of pDEGMA.

Above LCST the behaviour is more predictable as the PDEGMA block increases its hydrophobicity and therefore there is enough repulsive force (amongst the two blocks) and attractive force (hydrophobic interaction between polymer chains) to drive the assembly of the polymers [38, 40]. The assembled vesicles were further examined by optical and electron microscopy techniques.

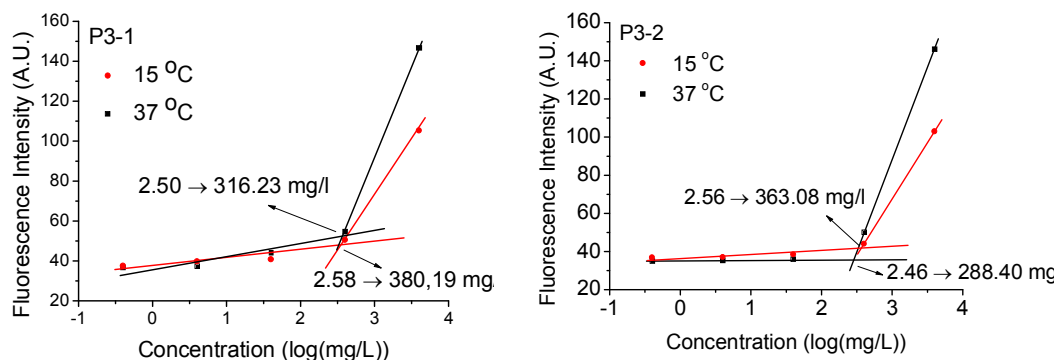


**Figure 3-9.** CMC graphs of P3-1 and P3-2 below and above LCST. Note the slight decrease in CMC values above LCST which is attributed to the complete collapsing of the PDEGMA block.

### 3.2.4. Microscopy

The relatively large size of some vesicles, particularly those for **P3-2** (ca. 10% of population has greater than 1  $\mu\text{m}$  diameter) conveniently allowed us to examine them by optical microscopy. In the optical microphotographs one can observe the formation of large vesicles that cannot be detected by DLS.

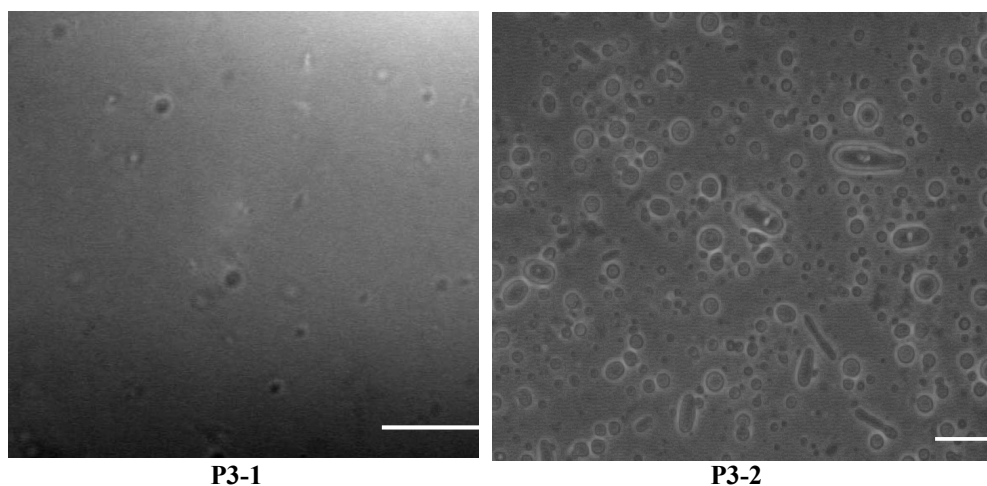


**Figure 3-10.** Optical microscopy images of **P3-1** and **P3-2** (scale is 10  $\mu\text{m}$ ).

Small objects that are detected in DLS are not visible under the optical microscope. This implies that there is a heterogeneous population of polymeric objects in each polymer solution. We also examined the

polymer vesicles using TEM. As shown in figure 3-11, spherical vesicles were detected with white core and a black corona. This is indicative of vesicles formation. The fact that the interior of the vesicles is white is attributed to the ethylene glycol chains that do not scatter electrons as the GEMA corona moieties [41].

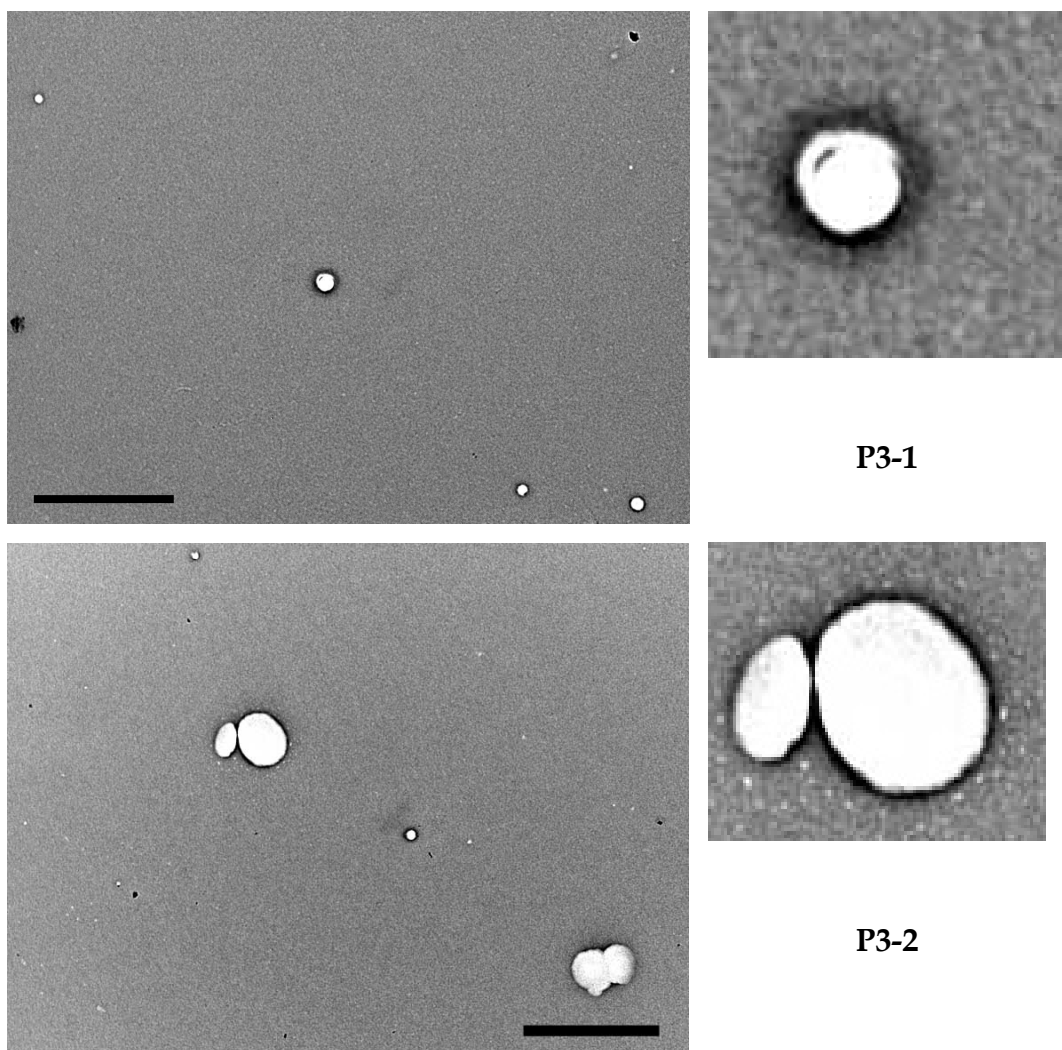


**Figure 3-11.** TEM micrographs of **P3-1** and **P3-2**. Images on the right side are digitally expanded for detail clarification (scale is 1  $\mu\text{m}$ ).

Closer examination and image analysis of the TEM images was used to determine the thickness of the vesicles bilayer which was found to be ca. 5-10 nm and correlates well with similar results from the literature [42].

### 3.2.5. Biorecognition properties (con A)

Polyvalent binding events at the surface of the vesicles were studied by assays with FITC-concanavalin A, (FITC-Con A; FITC=fluorescein isothiocyanate) a lectin with high affinity with glucose that has been extensively used to study carbohydrate-binding interactions [18]. As mentioned before Con A exists as a tetramer in alkaline solution and can host 4 sugar molecules. The exact mechanism of carbohydrate binding to the sugar binding pocket has been described in detail in chapters 1 and 2. Both **P3-1** and **P3-2** vesicles were able to accommodate the lectin at their surfaces as shown in figure 3-12, and turbidity assays showed that vesicles could agglutinate con A more efficiently than a model GEMA homopolymer.

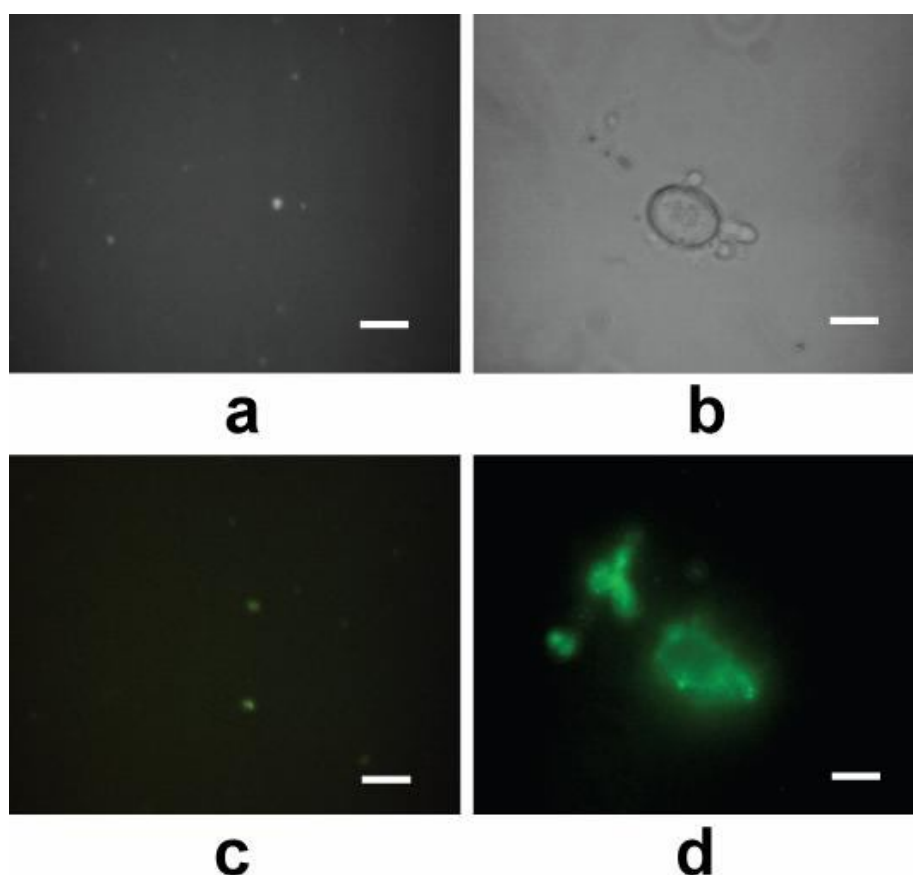


**Figure 3-12.** Interaction of glycopolymers with FITC-Concanavalin A. Images a, b depict **P3-1** and **P3-2** respectively, in phase contrast, showing the relative sizes of the vesicles, while c,d depict the same structures in confocal mode, with green fluorescence indicative of FITC-Con A (scale bars 1  $\mu\text{m}$ ).

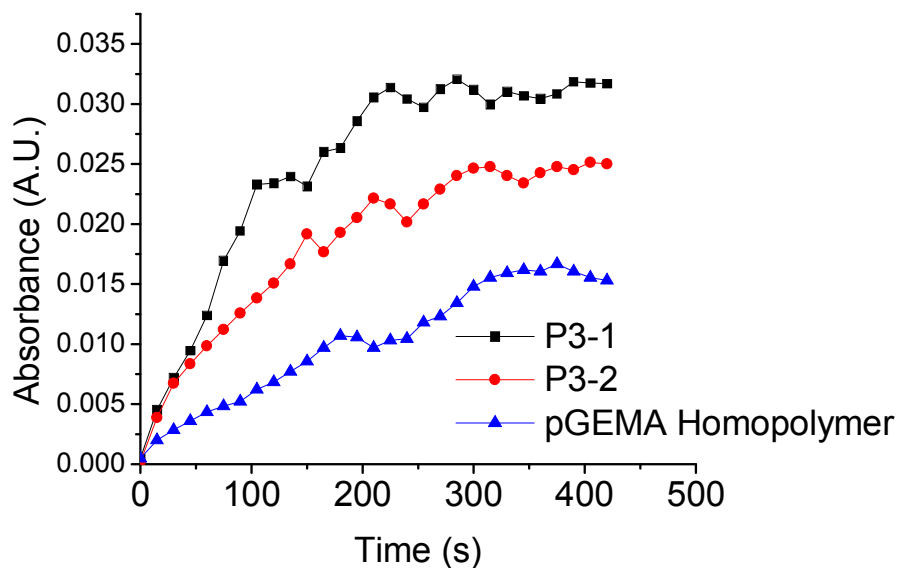


**Figure 3-13.** The turbidity assay of P3-1, P3-2 and pGEMA homopolymer with con A at the same concentrations (3 mg/mL).

Also the vesicle bound lectin was out-competed by addition of free glucose in the lectin-polymer solution. This resulted in displacement of the lectin from the vesicular corona which is indicative of the specificity of the lectin with the sugar moieties rather than other non-specific interactions (i.e. physical adsorption, hydrophobic interactions etc.).

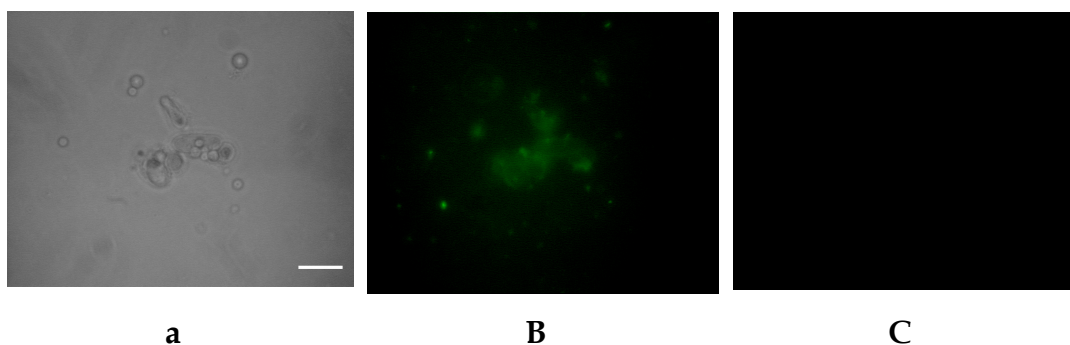


**Figure 3-14.** Competition assay of con A with glucose. A) vesicles in phase contrast, b) green vesicles in fluorescence mode indicative of FITC-Con A accommodation on the coronae and c) diminishing of green colour due to addition of glucose (0.01 mM) and dissociation of the polymer bound lectin (scale is 1  $\mu$ m).

Agglutination with con A was more pronounced in the case of smaller vesicles made by **P3-1** than **P3-2** (corresponding to around 30 and 60% increased con A absorbance for binding to **P3-2** and **P3-1**, respectively). Presumably, this is attributed to the relative surface to volume ratio which is higher for **P3-1** that forms small vesicles, therefore can accommodate more lectin at the corona. Similar results have also been reported by Kim et al. where they studied different supramolecular structures that were decorated with mannose [22]. They concluded that shape and size did indeed play a role in the binding effects with the lectin and that surface area is crucial for the polymer-lectin agglutination. When they compared supramolecular architectures of similar manno-amphiphiles they concluded that the higher the curvature of the molecular objects the higher the interaction with the lectin was. This is also confirmed by our studies using **P3-1** and **P3-2**.

It should also be mentioned that Sen Gupta et al. have performed systematic studies on virus particles decorated with glycopolymers and their interactions with concanavalin and reported on the very fast agglutination (within seconds) of the lectin with the virial chimeras [43]. This is perhaps the only example of a natural supramolecular object such as a virus that is modified with well defined glycopolymers to mediate polyvalent interactions in a biomimetic fashion as such exploited by **P3-1** and **P3-2**.

Therefore the vesicular structures derived from **P3-1** and **P3-2** seemed to provide two major advantages over linear homopolymer systems: 1) spatial accumulation of sugar moieties on the vesicular corona provided increased multivalent capacity and 2) variations of vesicular size resulted in changes in the overall association of biomolecule-vesicle complexes/aggregates.

### 3.2.6. Interactions with E coli

We next studied the binding activity of the vesicles with a mutant E. coli strain (MG1655pGFP) that is both fluorescent (GFP) and expresses the fimH protein, which has binding specificity for glucose and mannose. E. coli are rod-shaped bacteria of comparable size to the larger **P3-2** vesicles, and their binding characteristics with linear glycopolymers have been studied previously [44, 45]. The carbohydrate recognition sites (CRSs) found on the pili of E. coli are a few nanometers in diameter and can reach more than 3  $\mu\text{m}$  in length. Figure 3-15 shows the varying interactions of the different vesicles with E. coli. The small vesicles from **P3-1** formed large aggregates with bacteria (40–80  $\mu\text{m}^2$ , approximately 100–150 bacteria and 60–90 vesicles found in each cluster). In contrast, for **P3-2**, no large-area aggregates were formed, although we did observe persistent strong individual bacteria associations with large (ca. 1  $\mu\text{m}$  vesicles) in the mixture (figure 3-15). Negligible bacterial aggregation was induced when the vesicles interacted with an E. coli strain (Top 10) that did not express fimH, thus demonstrating the specific nature of the binding process owing to the sugar functionality. The induction of bacterial cluster formation followed the same trend as with Con A interactions, which we attributed to the differing size, mass, surface-volume ratios, and momentum in suspension of **P3-1** relative to **P3-2** vesicles.

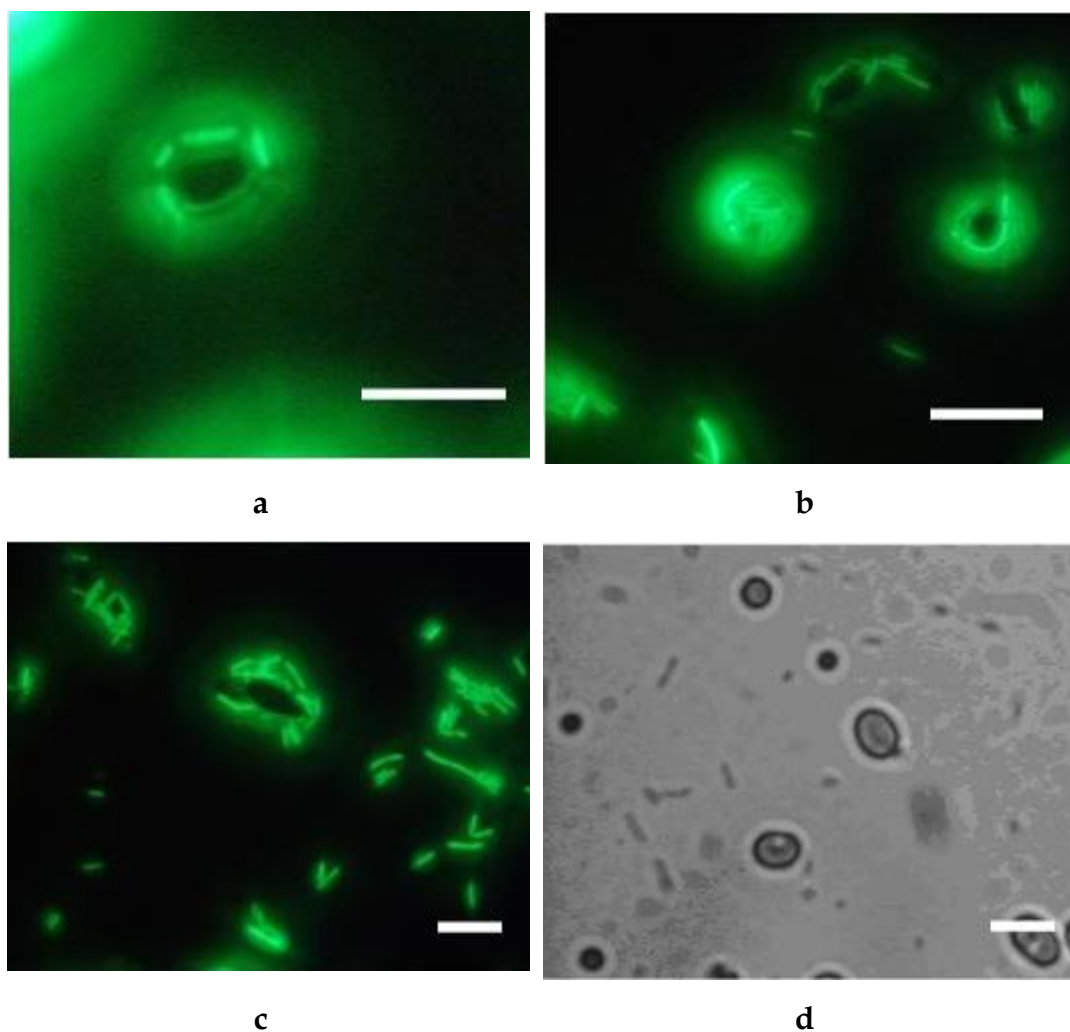


**Figure 3-15.** Association of vesicles with bacteria: Large (>1  $\mu\text{m}$ ) P3-2 vesicles bind but do not aggregate with *E. coli* MG1655pGFP as shown in images (a-c) in fluorescence mode; d) no binding of *E. coli* Top 10 to P3-2 vesicles is observed in phase-contrast mode.

Similar bacterial aggregates with supramolecular objects have also been reported by Lim et al. where glycoconjugate nanoribbons based on amphiphilic short peptides could induce the aggregation of *E. Coli* ORN178 which also expresses the *FimH* protein on its fimbriae [46]. The researchers conclude that only long nanoribbons could induce bacterial clustering and thus demonstrate the significance of size and morphology on these systems to probe these cooperative multivalent interactions with bacterial cells.

Perhaps this is the only study that describes distinct association of a natural organelle (i.e. bacterial pili) with a solely synthetic molecular object in a similar way that **P3-1** and **P3-2** interact with the bacterial cells.

Having established that polymer-vesicle binding involved surface-expressed glucose as the “language” of cell-vesicle interactions, we sought to “outtalk” the association through introduction of exogenous signals (i.e. free glucose). Addition of glucose into preformed bacterial-vesicle aggregates resulted in dose-dependent breakdown of the cell-polymer clusters (figure 3-16a-d). This effect was most noticeable for the smaller vesicles from **P3-1**, but was also apparent in the mixture of **P3-2** vesicles with *E. coli*.

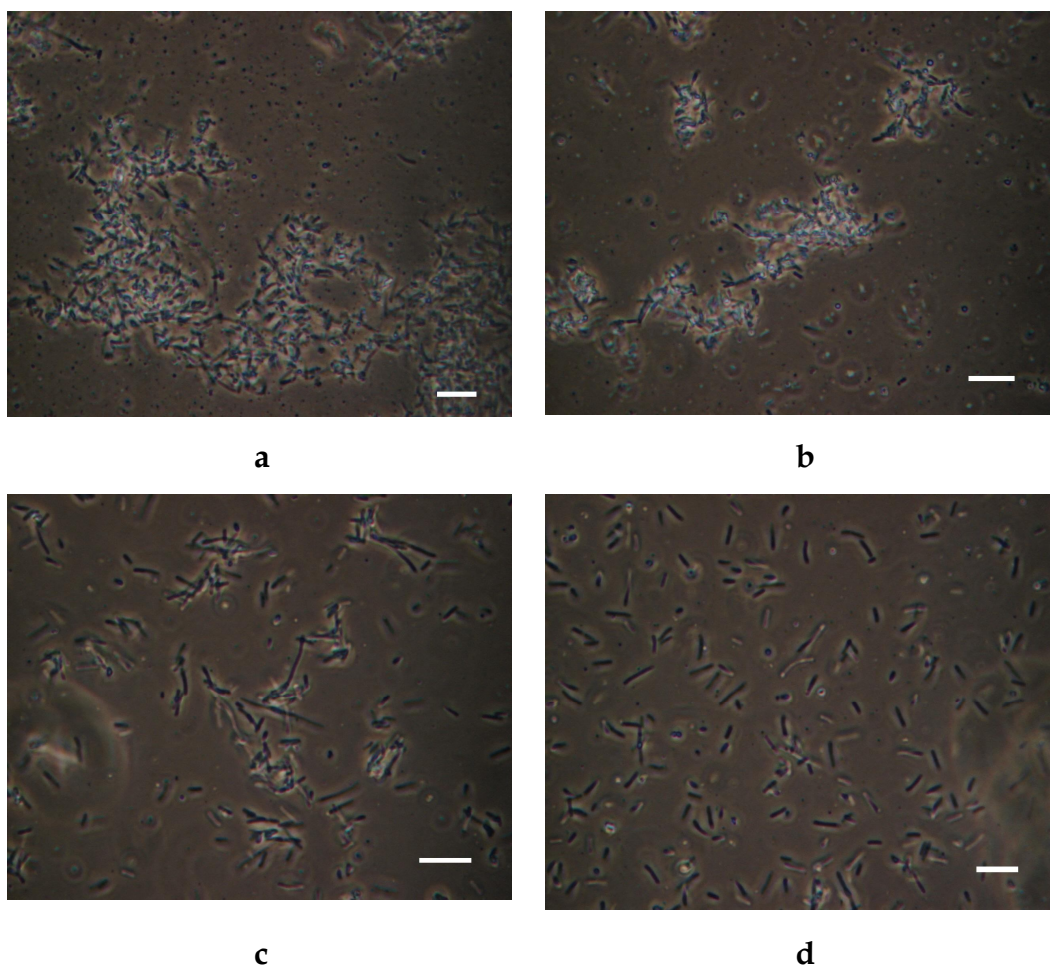


**Figure 3-16.** Polymer-glucose competition assay. **P3-1**-*E. coli* aggregates before (a) and after addition of 0.05 (b), 0.5 (c), and 5 mM glucose (d).

It was more difficult to quantify the binding interactions of **P3-2** and *E. coli* and the break-up of aggregates/clusters owing to the increased random motion in solution of the larger vesicles. However, for **P3-2**, polymers binding events of single vesicles with individual bacteria could be observed, which we reasoned might allow us to investigate a second mode of “communication” between vesicle and cell, namely, molecular transport.

### 3.2.7. Molecular transport

Our hypothesis was that the interfacial interaction of vesicles with bacteria might trigger disruption of the vesicular membrane and therefore vesicles containing molecular “information” could communicate this “information” when in contact with the bacteria. Large vesicles from **P3-2** were loaded with the dye ethidium bromide and cell-vesicle interaction studies were performed. As is apparent from figure 3-17e-g, bacteria associated with vesicle surfaces were initially green through GFP fluorescence, but over time (30 min) fluoresced orange-red through transfer of ethidium bromide from the vesicle interior to the bacterial cytoplasm.

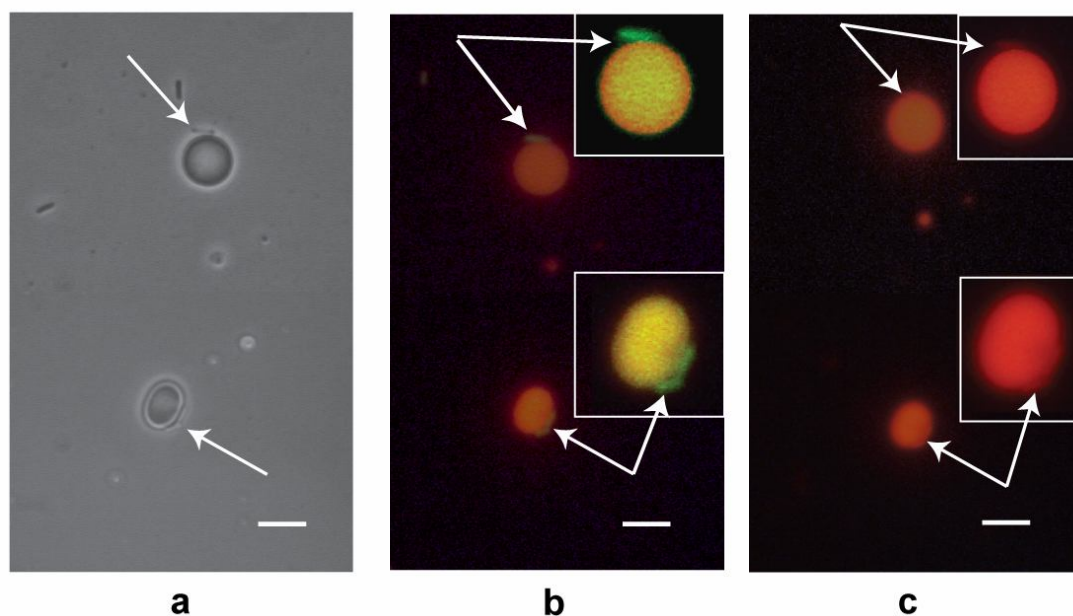


**Figure 3-17.** Molecular transport from P3-2 vesicles to *E. coli*. Image (a) shows vesicles and cells in phase-contrast mode, (b) shows the same cells in fluorescence mode; bacteria fluoresce green (GFP) and vesicles containing ethidium bromide fluoresce orange-red. Image (c) shows the same vesicle–cell partners after 30 min with bacteria now fluorescing orange-red owing to transfer of ethidium bromide. Insets in (b) and (c) show vesicles at higher image contrast and magnification for clarity. Scale bars in main figure are 1  $\mu\text{m}$ .

Only cells attached to vesicles exhibited ethidium bromide uptake over this time period, thus establishing the specificity of the information transfer.

These data demonstrate that not only can specific interactions between synthetic vesicles and cells occur, but also that a degree of control can be exerted in the information conveyed in these interactions. By changing the vesicular size it is possible to change an interaction from bulk aggregation to individual associations.

This in turn might lead to a sensitive method of cell detection or for control of signalling to individual cells. To the best of our knowledge this

is the first time that such molecular transport to a natural cell from an artificial biomimetic entity has been reported.

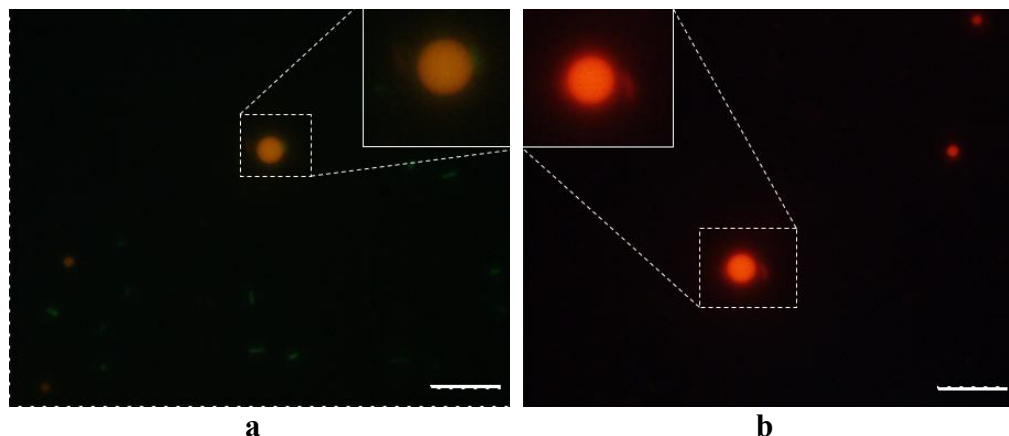


**Figure 3-18.** In (a) *E. coli* MG1655pGFP (green) and red **P3-2** vesicles loaded with ethidium bromide are seen to associate in discrete complexes. Image (b) shows the same vesicle captured after 30 minutes. Bacterium in close proximity with the vesicle turns red due to ethidium bromide transfer. Scale bars are 10  $\mu\text{m}$ .

Therefore, a more systematic study on the molecular mechanism that drives this transport is required. We hypothesize three possible mechanisms of transport: 1. disruption of the vesicular membrane upon interaction with the bacterial fibrils and active diffusion of the dye in the interior of the bacteria, 2. passive diffusion of dye -that is, leaking- and formation of a concentration gradient that is enough to stain a bacterium when in close proximity with the vesicles and 3. a combination of the previous two.

In general, other recent studies have correlated binding capabilities of molecular glycoobjects [47] to their supramolecular architecture, with specific goals of bacterial detection [22, 48, 49]. Our results imply that not only might the affinity of these materials be optimized by noncovalently linked supramolecular assemblies, but also that perhaps information transfer between cells and vesicles [50-52] might be achieved by rational design.

### 3.3. Conclusions

In conclusion, new block copolymers were designed that assemble into vesicles with surface display of glucose functionality. The polymerization methods used (RAFT and ATRP), proved to be highly robust and allowed for good control on the molecular architecture. The polymers synthesized could self-assemble in aqueous and the vesicles sized formed, can be controlled by comonomer content, block ratio, molar mass, and LCST. The vesicles were found to interact with bacterial cells and form large vesicle-bacteria aggregates due to the multivalent binding of the multiple sugar moieties of the vesicles corona with the FimH carbohydrate recognition sites on the bacterial fibrils. The close proximity of the molecular aggregates with the natural cells allowed information transfer of a common dye to the latter either through the glycosylated surface, or through the contents of the vesicles interior. The vesicles can thus be considered as a mimic, albeit primitive, of natural cells with their associated glycocalyx, with potential applications in cell sensing, therapeutics, and synthetic biology.

### 3.4. References

1. Bertozzi, C.R. and L.L. Kiessling, *Chemical glycobiology*. Science, 2001. **291**(5512): p. 2357-2364.
2. Pohl, N., *Cellular addresses: Step one in creating a glycode*. Chemistry & Biology, 2004. **11**(7): p. 891-892.
3. Pilobello, K.T. and L.K. Mahal, *Deciphering the glycode: the complexity and analytical challenge of glycomics*. Current Opinion in Chemical Biology, 2007. **11**(3): p. 300-305.
4. Kiessling, L.L. and C.W. Cairo, *Hitting the sweet spot*. Nature Biotechnology, 2002. **20**(3): p. 234-235.
5. Sharon, N., *Carbohydrates as future anti-adhesion drugs for infectious diseases*. Biochimica Et Biophysica Acta-General Subjects, 2006. **1760**(4): p. 527-537.

6. Doores, K.J., D.P. Gamblin, and B.G. Davis, *Exploring and exploiting the therapeutic potential of glycoconjugates*. Chemistry-a European Journal, 2006. **12**(3): p. 656-665.
7. Kim, S.H., J.H. Kim, and T. Akaike, *Regulation of cell adhesion signaling by synthetic glycopolymer matrix in primary cultured hepatocyte*. Febs Letters, 2003. **553**(3): p. 433-439.
8. Cunliffe, D., S. Pennadam, and C. Alexander, *Synthetic and biological polymers-merging the interface*. European Polymer Journal, 2004. **40**(1): p. 5-25.
9. Rodriguez-Hernandez, J., F. Checot, Y. Gnanou, and S. Lecommandoux, *Toward 'smart' nano-objects by self-assembly of block copolymers in solution*. Progress in Polymer Science, 2005. **30**: p. 691-724.
10. Antonietti, M. and S. Forster, *Vesicles and liposomes: A self-assembly principle beyond lipids*. Advanced Materials, 2003. **15**(16): p. 1323-1333.
11. Discher, D.E. and A. Eisenberg, *Polymer vesicles*. Science, 2002. **297**(5583): p. 967-973.
12. Ladmiral, V., E. Melia, and D.M. Haddleton, *Synthetic glycopolymers: an overview*. European Polymer Journal, 2004. **40**(3): p. 431-449.
13. Narumi, A. and T. Kakuchi, *Synthesis of Glycoconjugated Branched Macromolecular Architectures*. Polymer Journal, 2008. **40**(5): p. 383-397.
14. Yoshiko, M., *Synthesis and biological application of glycopolymers*. Journal of Polymer Science Part A: Polymer Chemistry, 2007. **45**(22): p. 5031-5036.
15. Spain, S.G., M.I. Gibson, and N.R. Cameron, *Recent advances in the synthesis of well-defined glycopolymers*. Journal of Polymer Science Part A: Polymer Chemistry, 2007. **45**(11): p. 2059-2072.
16. Li, Z.C., Y.Z. Liang, G.Q. Chen, and F.M. Li, *Synthesis of amphiphilic block copolymers with well-defined glycopolymer segment by atom transfer radical polymerization*. Macromolecular Rapid Communications, 2000. **21**(7): p. 375-380.
17. You, L.C. and H. Schlaad, *An easy way to sugar-containing polymer vesicles or glycosomes*. Journal of the American Chemical Society, 2006. **128**(41): p. 13336-3337.

18. Dong, C.M. and E.L. Chaikof, *Self-assembled nanostructures of a biomimetic glycopolymer-polypeptide triblock copolymer*. Colloid and Polymer Science, 2005. **283**(12): p. 1366-1370.
19. Faucher, K.M., X.L. Sun, and E.L. Chaikof, *Fabrication and characterization of glycocalyx-mimetic surfaces*. Langmuir, 2003. **19**(5): p. 1664-1670.
20. Nagasaki, Y., K. Yasugi, Y. Yamamoto, A. Harada, and K. Kataoka, *Sugar-Installed Block Copolymer Micelles: Their Preparation and Specific Interaction with Lectin Molecules*. Biomacromolecules, 2001. **2**(4): p. 1067-1070.
21. Yasugi, K., T. Nakamura, Y. Nagasaki, M. Kato, and K. Kataoka, *Sugar-Installed Polymer Micelles: Synthesis and Micellization of Poly(ethylene glycol)-Poly(D,L-lactide) Block Copolymers Having Sugar Groups at the PEG Chain End*. Macromolecules, 1999. **32**(24): p. 8024-8032.
22. Kim, B.S., D.J. Hong, J. Bae, and M. Lee, *Controlled self-assembly of carbohydrate conjugate rod-coil amphiphiles for supramolecular multivalent ligands*. Journal of the American Chemical Society, 2005. **127**(46): p. 16333-16337.
23. Qin, S.H., Y. Geng, D.E. Discher, and S. Yang, *Temperature-controlled assembly and release from polymer vesicles of poly(ethylene oxide)-block-poly(N-isopropylacrylamide)*. Advanced Materials, 2006. **18**(21): p. 2905-2909.
24. Li, Y., B.S. Lokitz, and C.L. McCormick, *Thermally responsive vesicles and their structural "locking" through polyelectrolyte complex formation*. Angewandte Chemie-International Edition, 2006. **45**(35): p. 5792-5795.
25. Cronin, L., N. Krasnogor, B.G. Davis, C. Alexander, N. Robertson, J.H.G. Steinke, S.L.M. Schroeder, A.N. Khlobystov, G. Cooper, P.M. Gardner, P. Siepmann, B.J. Whitaker, and D. Marsh, *The imitation game - a computational chemical approach to recognizing life*. Nature Biotechnology, 2006. **24**(10): p. 1203-1206.
26. Orner, B.P., R. Derda, R.L. Lewis, J.A. Thomson, and L.L. Kiessling, *Arrays for the combinatorial exploration of cell adhesion*. Journal of the American Chemical Society, 2004. **126**(35): p. 10808-10809.

27. Mammen, M., S.K. Choi, and G.M. Whitesides, *Polyvalent interactions in biological systems: Implications for design and use of multivalent ligands and inhibitors*. Angewandte Chemie-International Edition, 1998. **37**(20): p. 2755-2794.
28. Ishii, T., M.A. Mateos-Timoneda, P. Timmerman, M. Crego-Calama, D.N. Reinhoudt, and S. Shinkai, *Self-assembled receptors that stereoselectively recognize a saccharide*. Angewandte Chemie-International Edition, 2003. **42**(20): p. 2300-2305.
29. Ambrosi, M., A.S. Batsanov, N.R. Cameron, B.G. Davis, J.A.K. Howard, and R. Hunter, *Influence of preparation procedure on polymer composition: synthesis and characterisation of polymethacrylates bearing beta-D-glucopyranoside and beta-D-galactopyranoside residues*. Journal of the Chemical Society-Perkin Transactions 1, 2002(1): p. 45-52.
30. Li, Y.Y., X.Z. Zhang, J.L. Zhu, H. Cheng, S.X. Cheng, and R.X. Zhuo, *Self-assembled, thermoresponsive micelles based on triblock PMMA-b-PNIPAAm-b-PMMA copolymer for drug delivery*. Nanotechnology, 2007. **18**(21).
31. Vazquez-Dorbatt, V. and H.D. Maynard, *Biotinylated glycopolymers synthesized by atom transfer radical polymerization*. Biomacromolecules, 2006. **7**(8): p. 2297-2302.
32. Magnusson, J.P., A. Khan, G. Pasparakis, A.O. Saeed, W.X. Wang, and C. Alexander, *Ion-sensitive "isothermal" responsive polymers prepared in water*. Journal of the American Chemical Society, 2008. **130**(33): p. 10852-+.
33. Lutz, J.F., K. Weichenhan, O. Akdemir, and A. Hoth, *About the phase transitions in aqueous solutions of thermoresponsive copolymers and hydrogels based on 2-(2-methoxyethoxy)ethyl methacrylate and oligo(ethylene glycol) methacrylate*. Macromolecules, 2007. **40**(7): p. 2503-2508.
34. Lutz, J.F., O. Akdemir, and A. Hoth, *Point by point comparison of two thermosensitive polymers exhibiting a similar LCST: Is the age of poly(NIPAM) over?* Journal of the American Chemical Society, 2006. **128**(40): p. 13046-13047.

35. Vihola, H., A. Laukkanen, L. Valtola, H. Tenhu, and J. Hirvonen, *Cytotoxicity of thermosensitive polymers poly(N-isopropylacrylamide), poly(N-vinylcaprolactam) and amphiphilically modified poly(N-vinylcaprolactam)*. *Biomaterials*, 2005. **26**(16): p. 3055-3064.
36. Yanxiang Li, R.L., Wenyong Liu, Hongliang Kang, Min Wu, Yong Huang, *Synthesis, self-assembly, and thermosensitive properties of ethyl cellulose-g-P(PEGMA) amphiphilic copolymers*. *Journal of Polymer Science Part A: Polymer Chemistry*, 2008. **46**(20): p. 6907-6915.
37. Kita-Tokarczyk, K., J. Grumelard, T. Haefele, and W. Meier, *Block copolymer vesicles - using concepts from polymer chemistry to mimic biomembranes*. *Polymer*, 2005. **46**(11): p. 3540-3563.
38. Forster, S. and M. Konrad, *From self-organizing polymers to nano- and biomaterials*. *Journal of Materials Chemistry*, 2003. **13**(11): p. 2671-2688.
39. Hamley, I.W., *Nanoshells and nanotubes from block copolymers*. *Soft Matter*, 2005. **1**(1): p. 36-43.
40. Forster, S. and T. Plantenberg, *From self-organizing polymers to nanohybrid and biomaterials*. *Angewandte Chemie-International Edition*, 2002. **41**(5): p. 689-714.
41. Riley, T., T. Govender, S. Stolnik, C.D. Xiong, M.C. Garnett, L. Illum, and S.S. Davis, *Colloidal stability and drug incorporation aspects of micellar-like PLA-PEG nanoparticles*. *Colloids and Surfaces B: Biointerfaces*, 1999. **16**(1-4): p. 147-159.
42. Battaglia, G. and A.J. Ryan, *Bilayers and Interdigitation in Block Copolymer Vesicles*. *J. Am. Chem. Soc.*, 2005. **127**(24): p. 8757-8764.
43. Sen Gupta, S., K.S. Raja, E. Kaltgrad, E. Strable, and M.G. Finn, *Virus-glycopolymer conjugates by copper(I) catalysis of atom transfer radical polymerization and azide-alkyne cycloaddition*. *Chemical Communications*, 2005(34): p. 4315-4317.
44. Gestwicki, J.E., L.E. Strong, S.L. Borchardt, C.W. Cairo, A.M. Schnoes, and L.L. Kiessling, *Designed potent multivalent chemoattractants for Escherichia coli*. *Bioorganic & Medicinal Chemistry*, 2001. **9**(9): p. 2387-2393.

45. Pasparakis, G., A. Cockayne, and C. Alexander, *Control of bacterial aggregation by thermoresponsive glycopolymers*. Journal of the American Chemical Society, 2007. **129**(36): p. 11014-11015.
46. Lim, Y.B., S. Park, E. Lee, H. Jeong, J.H. Ryu, and M.S. Lee, *Glycoconjugate nanoribbons from the self-assembly of carbohydrate-peptide block molecules for controllable bacterial cell cluster formation*. Biomacromolecules, 2007. **8**(5): p. 1404-1408.
47. Sun, X.L., W.X. Cui, C. Haller, and E.L. Chaikof, *Site-specific multivalent carbohydrate labeling of quantum dots and magnetic beads*. ChemBiochem, 2004. **5**(11): p. 1593-1596.
48. Kim, B.S., W.Y. Yang, J.H. Ryu, Y.S. Yoo, and M. Lee, *Carbohydrate-coated nanocapsules from amphiphilic rod-coil molecule: binding to bacterial type 1 pili*. Chemical Communications, 2005(15): p. 2035-2037.
49. Joralemon, M.J., K.S. Murthy, E.E. Remsen, M.L. Becker, and K.L. Wooley, *Synthesis, characterization, and bioavailability of mannosylated shell cross-linked nanoparticles*. Biomacromolecules, 2004. **5**(3): p. 903-913.
50. Leson, A., S. Hauschild, A. Rank, A. Neub, R. Schubert, S. Forster, and C. Mayer, *Molecular exchange through membranes of poly(2-vinylpyridine-block-ethylene oxide) vesicles*. Small, 2007. **3**(6): p. 1074-1083.
51. Yaroslavov, A.A., N.S. Melik-Nubarov, and F.M. Menger, *Polymer-induced flip-flop in biomembranes*. Accounts of Chemical Research, 2006. **39**(10): p. 702-710.
52. Menger, F.M., K.H. Nelson, and Y.B. Guo, *Vesicle-enzyme communication*. Chemical Communications, 1998(18): p. 2001-2002.

## Chapter 4

### Quorum Quenching Polymers

#### 4.. Introduction

Having established a basic platform for understanding the principles of polymer-cell interaction/recognition (chapter 2) and extending the concept to vesicle-cell complex formation and “pseudo-communication” (chapter 3), we sought to further develop a more meaningful test of cell-polymer “cross-talk” that is bidirectional and dynamic to a level of achieving as much natural resemblance as possible. We therefore turned to already existing networks involved in cell-cell communication processes.

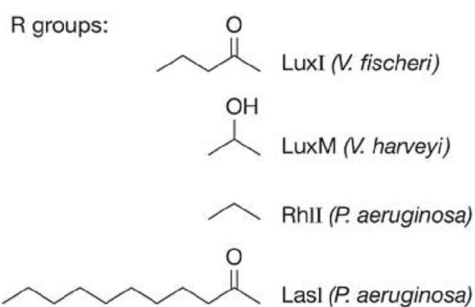
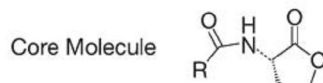
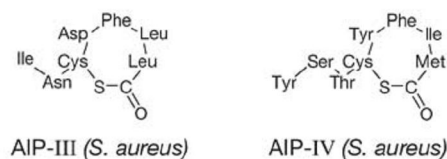
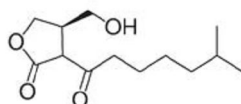
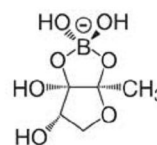
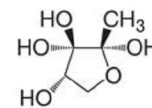
Quorum Sensing (QS) is a means of intercellular signalling by which bacteria control their population behaviour [1, 2], and QS systems have been characterised that influence cell-cell signalling, swarming, biofilm formation and pathogenicity [3-5]. In most biological systems, quorum sensing is facilitated by low molecular weight compounds that are produced and sensed by individual organisms. The latter can regulate their population density according to the presence of these small compounds which are named autoinducers [6, 7]. The term quorum sensing was first coined by Kenneth H. Wilson and John W. Hastings while studying the bacterium *photobacterium fischeri* (*Vibrio fischeri*) [8, 9]. It was observed that the bacteria did not express bioluminescence until they reached a certain population density. It was hence hypothesized that the molecular mechanism of the bioluminescence process must be controlled by small molecules that act as messengers that could travel between cells and regulate specific gene expression. These molecules were

termed “autoinducers” to point out that they could activate their own production and in turn activate a whole cascade of biomolecular processes related to the bioluminescence expression of these bacteria. Since then, many studies have suggested that quorum sensing is a universal concept in the world of microorganisms and the latter can extensively use this sort of molecular networks to facilitate cooperative behaviour to achieve cell-to-cell communication in between species but as well as for interspecies communication [7, 10, 11]. Ultimately, microorganisms can regulate their colonization behaviour, pathogenicity, toxins and virulence factors production etc. through quorum sensing in a perfectly orchestrated manner.

In gram negative bacteria, the majority of autoinducers are acyl homoserine lactones (AHLs). The acyl chain may vary in the carbon length, saturation level or presence or absence of oxo or hydroxyl substitutions (see table 4-I). The amphipathic character of these molecules resembles that of the lipids that make up the bacterial membrane and hence the AHLs can easily diffuse in and out the extracellular environment. On the other hand, in gram positive bacteria, generally the autoinducers are small cyclic peptides whose transport is facilitated via binding to membrane-bound histidine kinases [1, 6].

**Table 4-I**

Various autoinducers found in gram negative (left) and positive bacteria [1].

**a****Acyl-homoserine lactones (AHL)****b****Oligopeptide autoinducers****c****Streptomyces  $\gamma$ -butyrolactones**A-factor (*S. griseus*)**d****AI-2 family***V. harveyi**S. typhimurium*

Of particular interest for our analysis is the Auto-Inducer 2 (AI-2) molecule, which complexes with the LuxP protein via a furanosyl borate diester. AI-2 is an important signal that triggers a cascade of biomolecular reactions switching on the QS network in *Vibrios* and other bacterial species [1, 12].

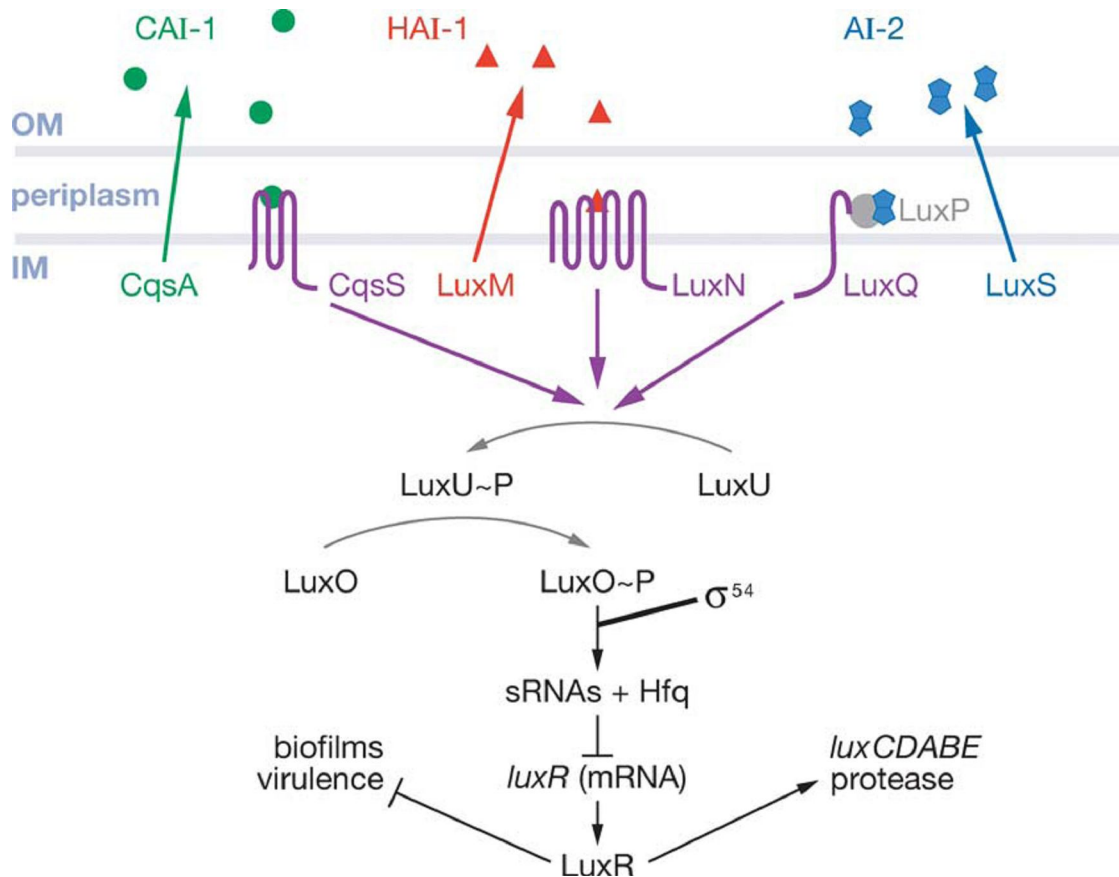


**Figure 4-1.** *Vibrio harveyi* quorum sensing network comprised by three autoinducers, CAI-1, HAI-1 and AI-2 [1].

The quorum sensing signalling pathway of *V. harveyi* consists of three autoinducers that are activated in parallel to activate the bioluminescence pathway of the bacteria. The LuxM synthase produces the autoinducer HAI-1 which binds to a membrane bound receptor histidine kinase (LuxN). The second autoinducer is the AI-2, which is a furanosyl borate diester, is partly produced by the LuxS enzyme [13]. The AI-2 is bound to the LuxP protein in the periplasm which can interact with another histidine kinase, LuxQ. The third postulated autoinducer (CAI-1), not yet fully characterised, is produced by the CqsA enzyme and can interact with the CqsS histidine kinase.

At low cell densities, all three sensor kinases LuxQ and LuxN and CqsS autophosphorylate, passing the phosphate signal via LuxU, to LuxO. In its phosphorylated state, LuxO with the transcription factor termed  $\sigma$ , activates small regulatory RNAs that interact with the Hfq RNA chaperone and

subsequently destabilize the LuxR transcriptional activator. The latter though is required for the activation of the luxCDABE luciferase operon responsible for the bioluminescence expression. Therefore, only at high population densities, where the sensors (LuxQ and LuxN and CqsS) interact with the LuxO (which is now dephosphorylated via LuxU) is the expression of the repression protein prevented and hence bioluminescence is expressed. It must be noted that all three sensors must co-operate in order to activate the bioluminescence network but at least one must be absent for the deactivation of the network.

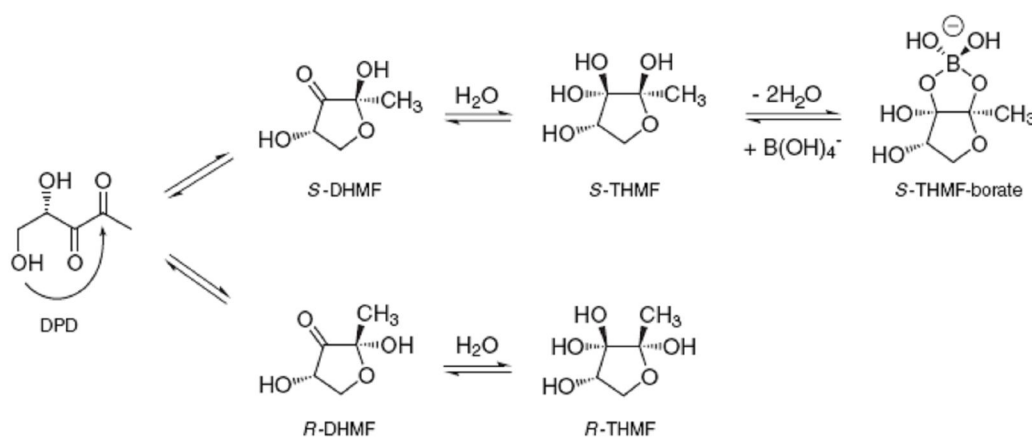


**Figure 4-2.** The AI-2 originates from the precursor molecule DPD that exists in equilibrium with other rearranged forms that are also active in the biological context. The upper pathway shows the biosynthesis route for *Vibrio harveyi* whereas in the lower pathway the R-THMF is produced in *Salmonella enterica* [6, 13, 14].

*V. harveyi* sense AI-2 levels in the microenvironment and adjust proportionally their population density; this in turn results in an increase in bioluminescence expression. Changes in light production can thus be used as sensitive probes of QS activity in *Vibrio* and other QS-communicating bacteria. Since the AI-2 molecule and other autoinducers are used for QS by certain important pathogens, capture/elimination of these molecules is a potential method of controlling infection, as well as sensitive mode of bacterial detection.

For example, researchers have exploited the fact that the lactone ring of the AHLs is hydrolyzable by certain lactonases and therefore the autoinducer can be rendered inactive [15]. Other approaches include the organic synthesis of QS antagonists in order to inhibit quorum sensing, a term often described as “quorum quenching” [16]. Estephane et al. synthesized AHL analogues that inhibited bioluminescence of *V. fischeri* by antagonizing the natural ligand for luminescence 3-oxo-hexanoylhomoserine lactone [17]. Kim et al. successfully synthesized quorum quenchers for *Pseudomonas Aeruginosa*, which is a common opportunistic pathogen. The compounds produced were furanone derivatives and showed significant QS suppression and inhibition of biofilm formation when tested under relevant bioassay conditions in vitro [18]. Another interesting approach was employed by Kato et al. [19] who tested *Serratia marcescens*, an opportunistic pathogen that produces a red tripyrrole pigment, 2-methyl-3-pentyl-6-methoxy prodigiosin, via an AHL-mediated QS mechanism at the stationary growth phase. When the bacteria were grown in the presence of an optimum concentration of cyclodextrins in the growth medium, it was observed that the production of prodigiosin was reduced by approximately 40% suggesting a reduction of the AHLs available to be detected by the bacteria. This is one of the very first studies in which a QS system has been targeted by a synthetic material and has been shown to interfere with the bacterial language with a rather biophysical manner than conventional (bio)chemical methods.

Despite the fact that the studies targeting autoinducers are increasing, limited studies have been conducted for the capture of AI-2, an important autoinducer found in both gram negative and gram positive bacteria. Ni et al. [20] examined a library of boronic acids, all commercially available, in an effort to identify potential candidates with inhibitory effects on the QS of *Vibrio harveyi*. Indeed, five of these compounds showed significant inhibitory action at the micromolar range when tested with the *Vibrio*

harveyi mutant MM32.

In the same context but from a different perspective, we report here the use of simple model-polymers as diol-scavengers in order to demonstrate the capturing of AI-2 analogues as the first steps towards potential QS control. Our initial aim was to modulate the QS network by introducing smart polymers in order to reversibly switch the gene expression “on” or “off” according to the polymers response to external stimuli. A stimulus responsive polymer would be active under certain conditions (i.e. specific temperature or pH) and inactive under non-relevant conditions in a fully reversible manner so that the QS network can be externally controlled at will (that is by applying externally stimuli changes in the microbiological environment). A successful proof of concept would be a very first step towards a novel means of interfering in QS networks by intervening only when needed and at the exact time point that QS modulation is critical (i.e. virulence production). Also, the mode of action proposed is not lethal for the bacteria but rather is a more preferable route of controlling the bacterial behaviour to prevent infections and ultimately disease thus avoiding potential mutations that often occur with conventional antibiotics. We present our very first results on the effect of polymers specifically designed to capture the AI-2 aiming at a polymeric modulator of QS systems as an alternative route to prevent infection and disease.

## **4.1. Materials and methods**

### **4.1.1. Materials and Instrumentation**

All solvents and reagents were of analytical or HPLC grade and purchased from Sigma or Fisher Scientific unless otherwise stated. Deuterated solvents were from Sigma or Cambridge Isotopes. N-isopropylacrylamide (NIPAm, Sigma) was recrystallised from hexane. Azobis(isobutylnitrile) (AIBN, Fisher) was recrystallised from ethanol.

Acrylamido phenylboronic acid (APBA) was synthesised according to previously published procedures (given below in detail). AI-2 was kindly provided by Benjamin G. Davis and Paul Gardner of Oxford University. GAL polymer was used as received. GEMA polymer was synthesized according to the protocol described at p. 97 ( the same batch was used). A galactosyloxyethyl methacrylate-bl-butylacrylate co-polymer (GAL) was used as received.

Gel Permeation Chromatography was carried out using Polymer Laboratories GPC 50 and 120 instruments with RI detector. Molecular weights were calculated based on universal calibration method using polystyrene standards. Tetrahydrofuran (THF) was used as the mobile phase with toluene trace as marker. <sup>1</sup>H NMR spectra were recorded on a Bruker 400 MHz. Cloud point measurements were measured by using a Beckman DU 640 UV/Vis spectrophotometer equipped with a thermostat unit. Fluorescence spectrometry was carried out with a Varian Cary Eclipse fluorescence spectrophotometer equipped with a peltier apparatus for temperature control. The KBr method was used for FT-IR samples preparation, which were examined on a Perkin Elmer Paragon 1000 FT-IR instrument.

#### **4.1.2.Synthesis of acrylamidophenylboronic acid (AAPBA)**

The method of synthesis was adapted from Shiomori et al. [21]. In detail, 3-Aminophenylboronic acid was dissolved in 2M NaOH (40 mL) and cooled in an ice bath. Acryloyl chloride was added dropwise to the solution with intensive magnetic stirring for 20 min. Hydrochloric acid (2M) was then added dropwise to the reaction mixture to adjust the pH to ca. 1. The precipitate of the product was removed by filtration and redissolved in distilled water on heating slowly to 60 °C. Then, the residual insoluble impurities were filtered off. The final product was obtained by crystallization of the solution overnight in a refrigerator (4

°C). The yield of the reaction was 35%.

<sup>1</sup>H NMR (DMSO): chemical shifts: 5.7 (dd, 1H, vinyl CH), 6.2, 6.4 (dd, 1H each, vinyl(CH<sub>2</sub>), 7.3, 7.5, 7.8, 7.8 (dd, d, d, s, 1H each, ArH), 8.0 (s, 2H, B(OH)<sub>2</sub>), 10.1 (s, 1H, NH). Data obtained is comparable to the literature [21].

FTIR: 3070 cm<sup>-1</sup> (weak), 750-800 cm<sup>-1</sup> (strong) and 860-900 cm<sup>-1</sup> (strong), amide: 1650 cm<sup>-1</sup>, for vinyl bond: 1645 cm<sup>-1</sup>.

MS: Mass 190.99, found 190.0638.

#### 4.1.3. Synthesis of Poly(NIPAM-co-APBA)

Typical example of free radical polymerization for poly(NIPAM-co-APBA) is given below. In a thick walled Schlenk flask, NIPAm and APBA at molar ratios 95:5 were dissolved in THF (1 g/mL). 0.01 equivalent AIBN was added in the flask followed by three freeze thaw cycles using a vacuum line. The flask was placed in an oil bath at 65 °C for 18 hours. After cooling down to room temperature, the polymer was isolated by double precipitation in large excess of diethyl ether and dried under vacuum at 40 °C overnight. The final product was characterised by <sup>1</sup>H NMR. Diagnostic peaks correlated well with literature data [21].

GPC,  $M_n$ : 17000,  $M_w/M_n$ = 2.39.

#### 4.1.4. Cloud point measurements

LCST turbidity assays were performed by measuring the absorbance of polymer samples (in glycine buffer, 0.1 mM) in respect to temperature (1 deg/min). The LCST was considered as the initial onset of a sharp increase in absorbance at 500 nm.

#### 4.1.5. AR assay for reversible binding to Poly(NIPAM-co-APBA)

To a freshly prepared glycine buffer (pH 9.3) AR (0.01 mM), and polymer Poly(NIPAM-co-APBA) (3 mg/mL) were dissolved. Sample (1 mL) was added in a quartz cuvette (1 cm path length) and the full fluorescence spectrum was recorded at temperatures above and below LCST (AR excitation energy at 460 nm).

#### 4.1.6. AR assay for reversible PBA binding to diol containing polymers (PVA, GEMA and GAL)

To a freshly prepared glycine buffer (pH 9.3) AR (0.01 mM), phenylboronic acid (PBA, 0.05 mM) and polymer (5 mg/mL for PVA, GEMA and 2 mg/mL for GAL) were dissolved. Immediate change in colour from burgundy to orange and subsequent slight colour fading was observed upon addition of PBA and polymer respectively. Sample (1 mL) was added in the quartz cuvette and the full fluorescence spectrum was recorded before and after the addition of each polymer at constant temperatures (25 °C).

#### 4.1.7. AB Medium

NaCl (17.5 g) and MgSO<sub>4</sub>·7H<sub>2</sub>O (7.5 g) were dissolved in 950 mL distilled water and the pH was adjusted to 7.5 with aqueous KOH. Vitamin-free casamino acids (2.0 mL) were added, and the total volume was brought to 1 L with distilled water. The mixture was sterilised by autoclaving at 120 °C for 20 min.

Immediately before use, glycerol (400 µL 50% aqueous solution), potassium phosphate (200 µL 1.0 M aqueous solution) and L-arginine (200 µL 0.1 M aqueous solution) were added to 19 mL sterile solution, and vortexed thoroughly.

#### 4.1.8. *Vibrio harveyi* BB170 and MM32 culture

*Vibrio harveyi* BB170 (30 µg/mL) was inoculated in 2 mL LB from a fresh

plate. The bacteria were then grown with aeration at 30°C for 16 h. We then inoculated with this preculture AB medium (1:5000) and vortexed carefully. The inoculated medium was combined with the sample of interest (i.e. polymer solution) at 9:1 ratio (i.e. 20  $\mu$ L sample and 180  $\mu$ L AB mix). Bioluminescence and optical density (490 nm) were recorded at 30 °C every 30 minutes for at least 6 hours in a 96-well plate. For *V. harveyi* MM32, AI-2 was added to a final concentration of 10  $\mu$ M. Final polymer concentrations tested were set at 0.3 mg/mL in order to achieve excess diol presence relative to AI-2. The experiments were conducted in duplicate and all curves are derived from the mean values. The unpaired Student's *t*-test with  $p < 0.05$  was used as a limit to indicate statistical significance.

## 4.2. Results and discussion

### 4.2.1. Synthesis and scavenging properties of poly(NIPAM-coAPBA)

For our initial attempts to bind QS signal molecules we decided to use copolymers based on NIPAM due to its predictable LCST behaviour at temperatures around the growth conditions of the *Vibrio* species. We prepared an acrylamidophenylboronic acid monomer in order to scavenge the AI-2 through boronate ester formation via the diols present on the molecule.

The polymer was produced by free radical polymerization according to a published method [21]. We could trace all chemical groups of interest of the polymer by  $^1\text{H}$  NMR (figure 4-3). The ratio of the monomers could be determined (NIPAM:APBA, ~97:3) by integrating the aryl protons of APBA (6.5-8 ppm) relative to the isopropyl proton of NIPAM (3.8 ppm).

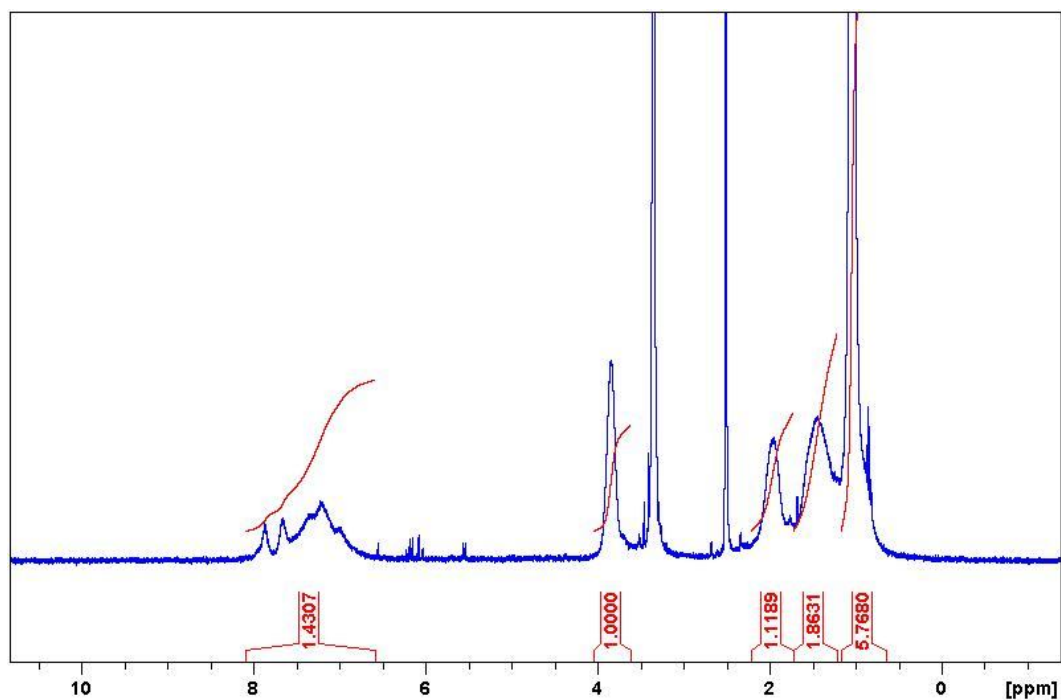


**Figure 4-3.** <sup>1</sup>H NMR of poly(NIPAM-co-APBA).

Boronic acid containing thermoresponsive polymers have been extensively studied for the sensing and capture of glucose for application in diabetes therapy [21-23]. Glucose binding to the thermoresponsive polymer poly(N-isopropylacrylamide-co-acrylamidophenylboronic acid) results in a change in the overall hydrophilicity of the polymer which can be monitored as an increase of the LCST of the polymer [21-23]. Therefore, the LCST of the polymer can be used as a read-out mechanism of glucose binding. We sought to exploit this mechanism to trace the binding of AI-2 to a boronic acid thermoresponsive polymer.

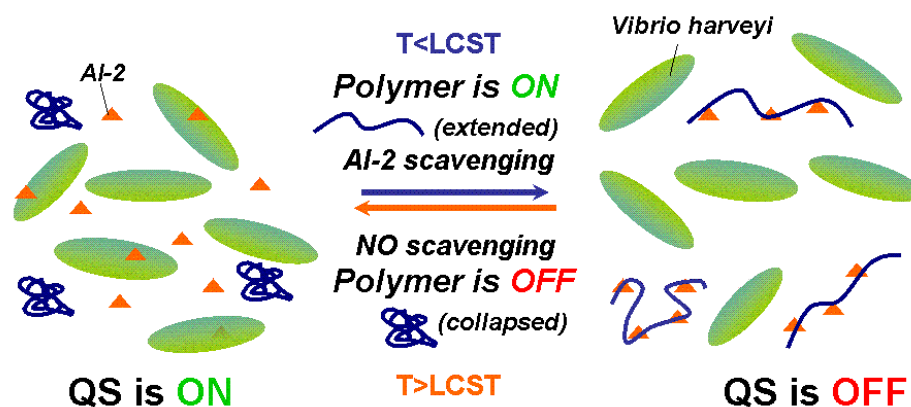


**Figure 4-4.** QS control concept by smart polymers. The QS response of the bacteria is governed by the activation of polymers through a temperature stimulus.

Hence, our first experiments were based on AI-2 analogues that consisted of glucose-boric acid complexes that resemble the structure of the autoinducer.

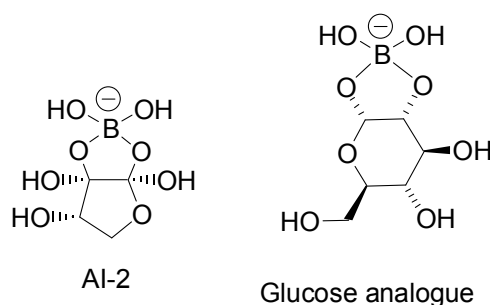


**Figure 4-5.** The structure of AI-2 and its glucose analogue.

Addition of the AI-2 analogues in a polymer solution showed a marked change in the LCST of the polymer thus confirming our initial hypothesis of the binding mechanism (figure 4-6). We performed these experiments at different pH values as the boronic acid binding to diols is pH dependent. The optimum pH was 9.2, i.e. at the  $pK_a$  of phenylboronic acid but we observed that the binding phenomenon was also apparent at pH 7.4 which is more relevant to the bacterial growth conditions [24, 25]. Also control experiments without sugar but with varying pH were conducted to see the effect of pH on the polymer as the boronic acid moieties are ionizable and expected to be more hydrophilic in a charged state, that is in alkaline

conditions (ca. pH 9). In the control experiment, pH affected the LCST onset to some extent (ca. 1 deg celsius) (figure 4-7a). At pH 5.6, where boronate ester formation is not favored, the LCST onset is the same even in the presence of 5 mM glucose-borate which indeed confirms the absence of any scavenging phenomena (figure 4-7b). Dose-dependent increase of the LCST was observed at pH 9.2 (figure 4-7d) where approximately 5 degrees celsius increase of the LCST onset was observed with 5 mM glucose. At pH 7.4, we also observed an increase in the LCST onset at high concentrations of glucose (figure 4-7c). This is attributed to the fact that only a fraction of the boronic acid moieties are ionized and hence able to sequester the diol. Nevertheless, we anticipated that at bacterial growth conditions, a sufficient fraction of boronic acid groups should be in a charged and “active” form to capture the AI-2 which is found in micromolar quantities in the bacterial microenvironment.

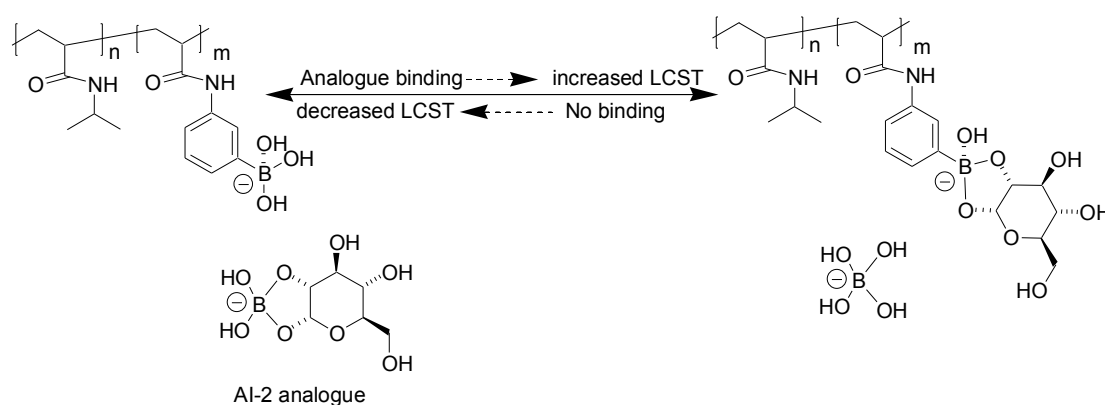


**Figure 4-6.** LCST control experiment without addition of sugar. Effect of pH on the LCST of the polymer.

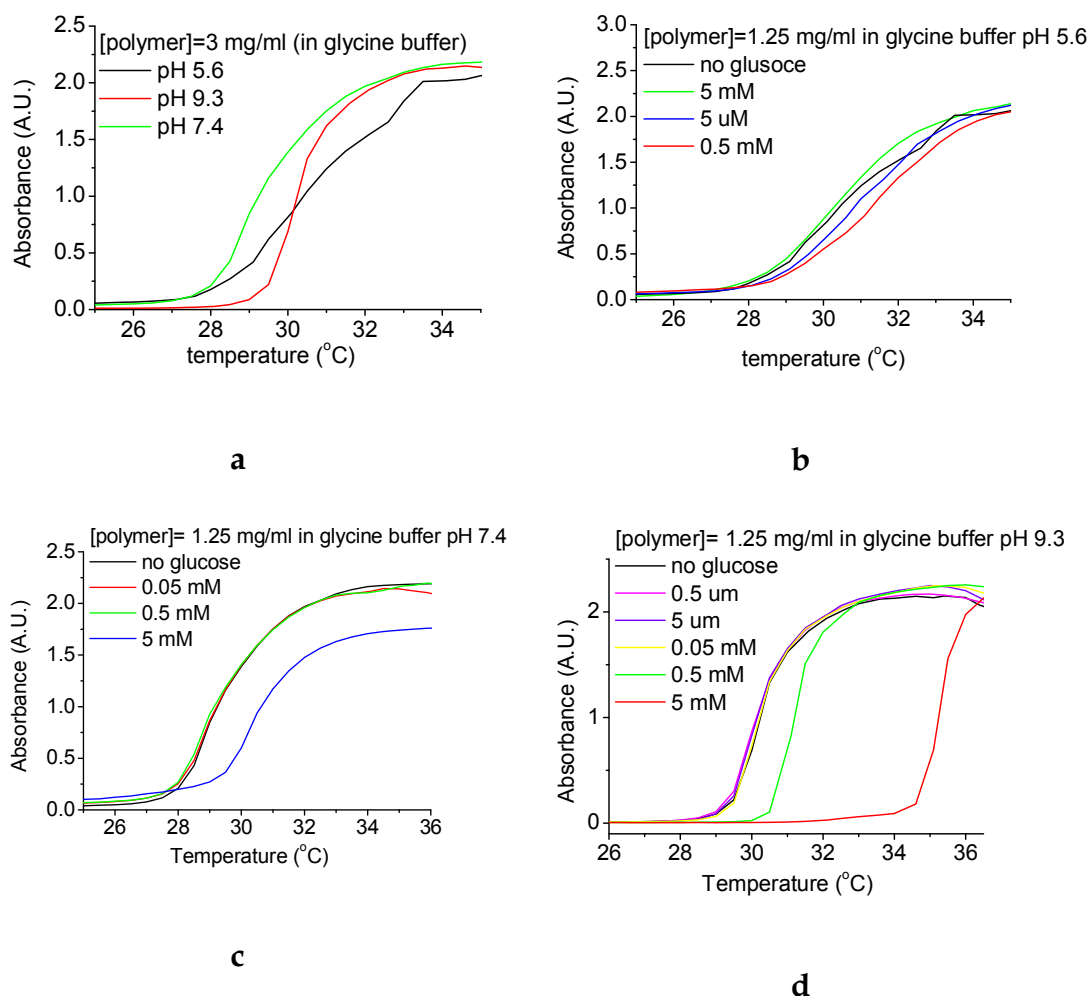


**Figure 4-7.** Cloud point curves of Poly(NIPAM-co-APBA) at varying pH (a), and in presence of glucose analogues at different pH at a, b, and c.

In order to demonstrate the reversible mode of action of the polymers according to temperature stimulus we employed a fluorescence assay based on the diol-containing dye alizarin red S (AR) [26].

It is well-known that AR is able to interact with boronic acid through reversible boronate formation [26, 27]. The colour of AR depends on the conditions and appears as burgundy in alkaline pH ( $\sim 10$ ) [26, 28]. Mixing of the polymer with the dye resulted in a colour change from light burgundy to orange indicating the formation of copolymer-AR complex (figure 4-8). When the mixture was placed in a water bath ( $\sim 40$  °C, above

the LCST), the colour change returned as in a polymer-free state suggesting the release of AR molecules from the copolymer in a temperature dependent manner.

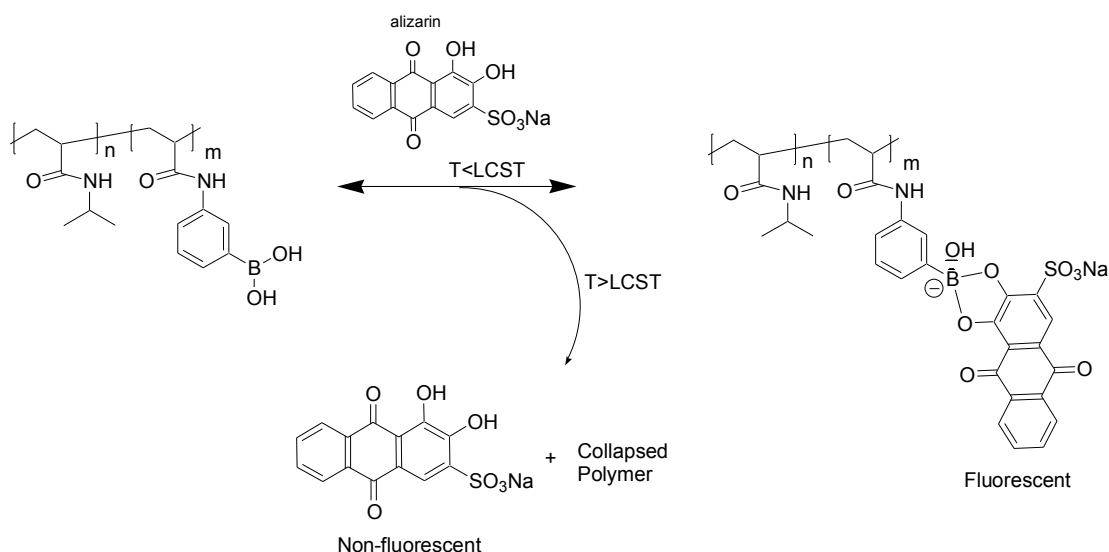


**Figure 4-8.** Schematic of the alizarin assay developed to probe the diol capturing/release at different temperatures around LCST.

Emission spectra collected at different temperatures demonstrated that the fluorescence decreased gradually as the temperature increased (figure 4-9), however, there was a dramatic decrease in the fluorescence emission maxima above 30 °C, which coincided with the LCST onset of the polymer. This suggested that as the copolymer collapsed from solution, the AR was released from the copolymer chains. The mechanism underlying the fluorescence changes is as follows: when the AR was in the unbound state, the protons of hydroxylanthraquinones quenches the fluorescence. Binding of a boronic acid (figure 4-8) to the diols of ARS removed the active proton and prevented fluorescence quenching, therefore the decrease in fluorescence was associated with the release from the copolymer [27]. An alternative explanation could be that possibly AR was not released from the copolymer and fluorescence was quenched through AR being buried within the collapsing polymer. However, it was demonstrated by a previous study investigating AR/diol release from boronate containing microgels of similar nature, that AR molecules were

not trapped but rather released from copolymer chains [27]. It should also be reminded that the boronate-diol complex exists as an equilibrium and therefore a temperature switch of the polymer is likely to induce release of the diols as discussed previously.

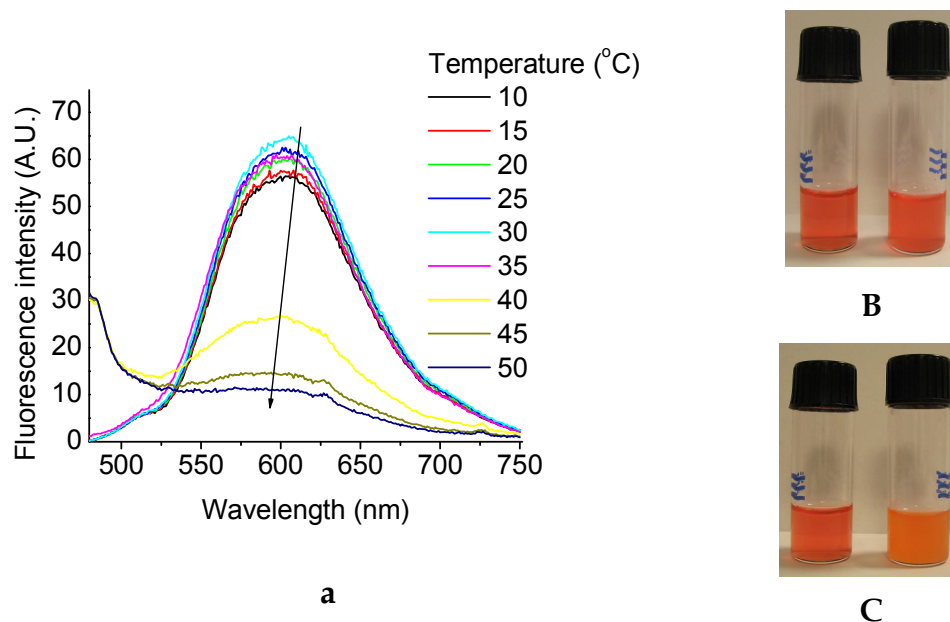


**Figure 4-9.** Alizarin fluorescence spectra at varying temperatures in presence of the polymer (a) and visual inspection of the colorimetric change above (b) and below (c) LCST.

Unfortunately, when the polymers were tested using the bacteria growth media, the LCSTs were significantly decreased due to the salt-rich environments hence preventing us from using them under cell culture conditions. Also, the fact that the boronic acid groups were only 5% of the monomer content demanded high polymer concentrations in the growth media to reach the level of the AI-2 in order to achieve sufficient scavenging. We therefore attempted to synthesize copolymers of higher boronic acid content by combining a third hydrophilic monomer (acrylamide) but observed either significant gelation of the final polymer in the end of the polymerization or complete loss of the sharp LCST. Hence, we decided to continue the studies with simple linear, water soluble polymeric materials of high diol content that would act as effective

boronate scavengers at relevant concentrations.

#### 4.2.2. Polyhydroxyl quorum quenchers

The polymers were designed to span a range of diol contents and solution structures; specifically these were: polyvinyl alcohol (PVA Sigma, M.W. 30-60.000 Da), poly(glucosyloxyethyl methacrylate) (GEMA), and a block copolymer poly(*n*-butyl acrylate)-co-poly(galactosyloxyethyl methacrylate) (GAL) that was used as received (figure 4-10).

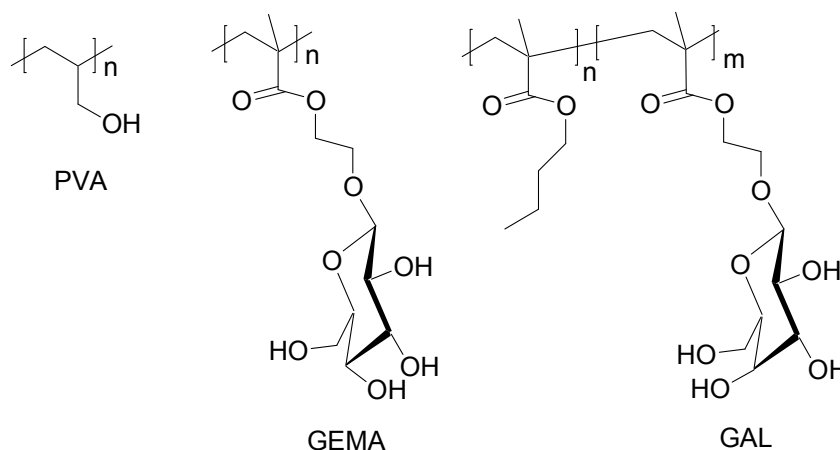


**Figure 4-10.** Structures of QS-capture polymers.

We selected PVA as a commercially available biocompatible polymer known to interact with boronic/boric acids [29, 30]. GEMA was synthesised in order to use glucoside repeat units which also bind strongly with boronic acids. We designed GAL as a model block copolymer that forms micelles in solution, offering the possibility that the galactose-rich shell could bind AI-2 while the micellar architecture could be used to provide a “scaffold” to present the galactose ligands in an optimum exposed form to sequester AI-2.

In order to trace the activity of the polymers under bio-relevant concentrations we refined the alizarin red assay. We considered this assay

as a simple analogy of a QS network where the dye plays the role of the bacterial cell that responds to the presence of the autoinducer – represented by the boronic acid- and the polymer as the scavenger. Simple as it is, it allowed us to detect whether the polymers can scavenge boronic acids as might occur in a “switched on” bacterial quorum sense network (figure 4-11).

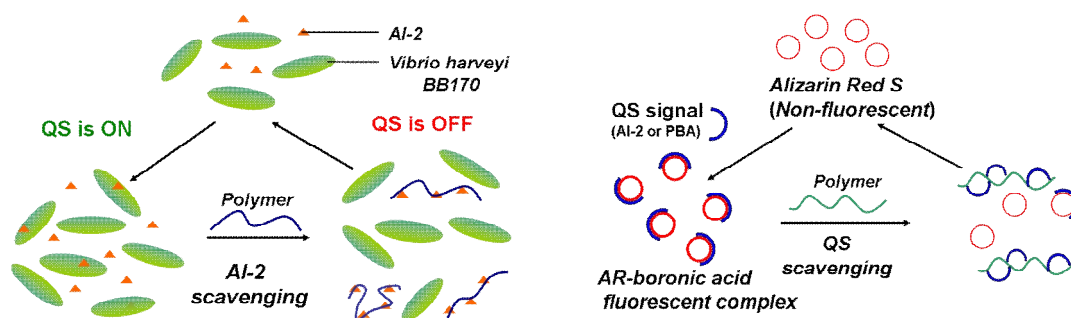


**Figure 4-11.** QS scavenging network (a) in comparison with AR and QS-analogue phenylboronic acid (PBA).

Preliminary experiments with PBA indicated significant suppression of fluorescence intensity by all the polymers. Also, the polymers scavenged the borate as the alizarin assay showed via significant decrease of the fluorescence intensity due to competitive binding of the autoinducer whether to the polymer or the dye. Note that borate is part of the active form of the AI-2 and hence capturing of borate molecules could potentially lead to QS suppression.

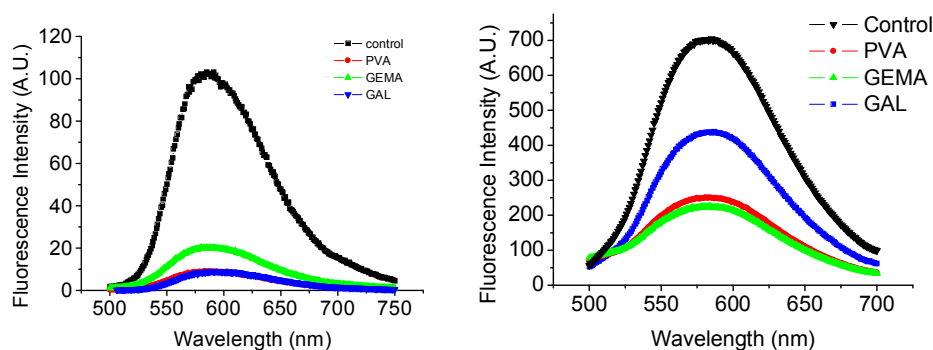


**Figure 4-12.** Left, fluorescence intensity of AR (0.01 mM) in presence of PBA (control, 1 μM) and after addition of the polymers (2 mg/mL). Right, the same experiment but with borate instead of PBA.

Bioluminescence assays were carried out using wild strain *Vibrio harveyi* BB170 that produces its own AI-2 QS signal, in the presence and absence of polymers. Light production-time curves shifted to the right in all cases, indicative of a delay in bioluminescence onset in presence of the polymers (figure 4-13). In addition, there were at least 4 distinct phases in the bioluminescence-time curves for assays in the presence of polymers, in contrast to the lag/recovery/steady-state phases observed for *Vibrio harveyi* BB170.

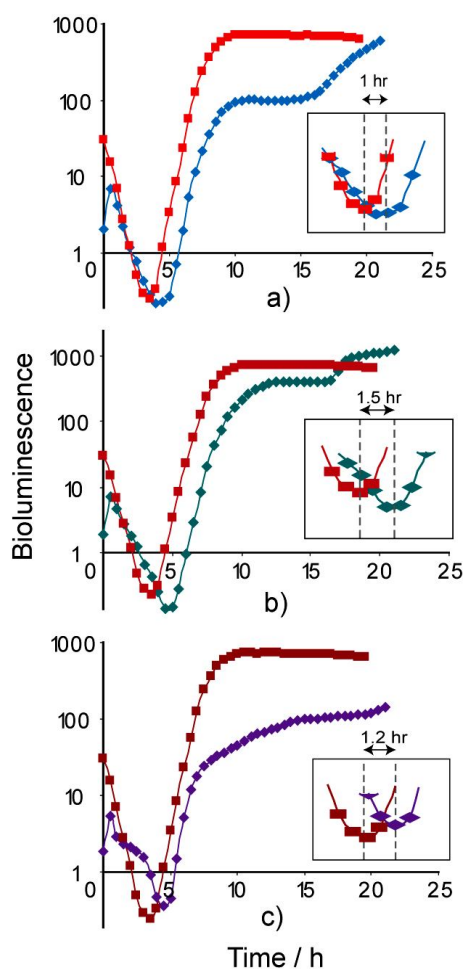


**Figure 4-13.** Light production with time for *Vibrio harveyi* in the absence and presence of PVA (a), GAL (b) and GEMA (c). Bioluminescence curves in the absence of polymer are shown in red - insets show expansions of the delay time of luminescence onset.

GEMA and PVA polymers, and to lesser extent GAL, induced significant decreases in the light production after 4 hours of incubation where the bioluminescence maxima is observed (ca. in 10 hours). Similar assays were carried out using the MM32 strain, which lacks the LuxN enzyme, responsible for DPD biosynthesis but which responds to AI-2 if added externally. Again, a significant decrease was observed in the light production maxima for all three polymers tested (figure 4-14).

Specifically for BB170 the fold induction was ~83, 24 and 84% for PVA, GAL and GEMA whereas for the case of MM32 it was ~56, 38 and 40 % for PVA, GAL and GEMA respectively.

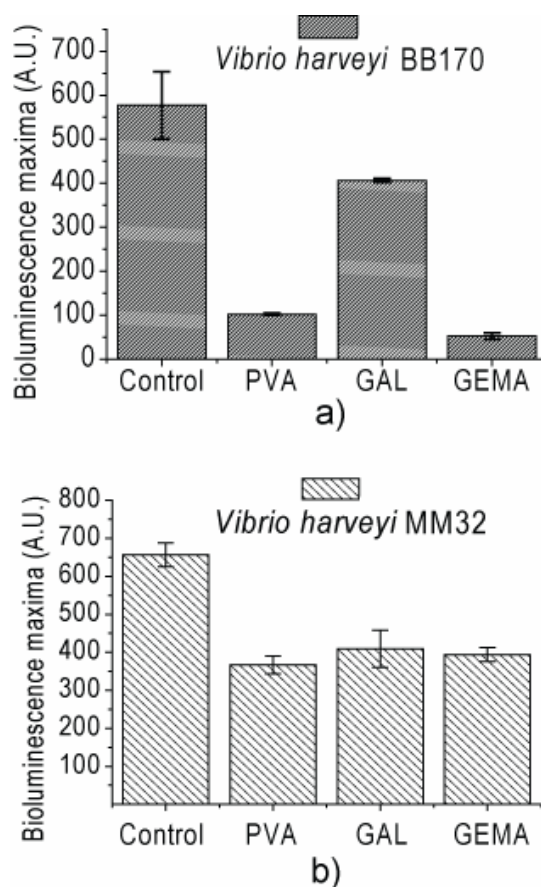


**Figure 4-14.** Comparison of light production maxima in presence of PVA, GAL and GEMA polymers for *Vibrio harveyi* strains BB170 (a) and MM32 (b). Controls refer to light production in absence of polymers without (a) and with (b) added AI-2.

Growth curves of bacteria indicated no toxicity for any of the polymers and in all cases the total bioluminescence tended to 'normal' after 20-24h. Bacteria appeared to grow normally and in all cases reached an optical density around 0.3 after 10-12 hours (figures 4-15 and 4-16), however there was some differentiation in the growth rate when polymers were present in the BB170 (figure 4-15) culture compared to the control sample.

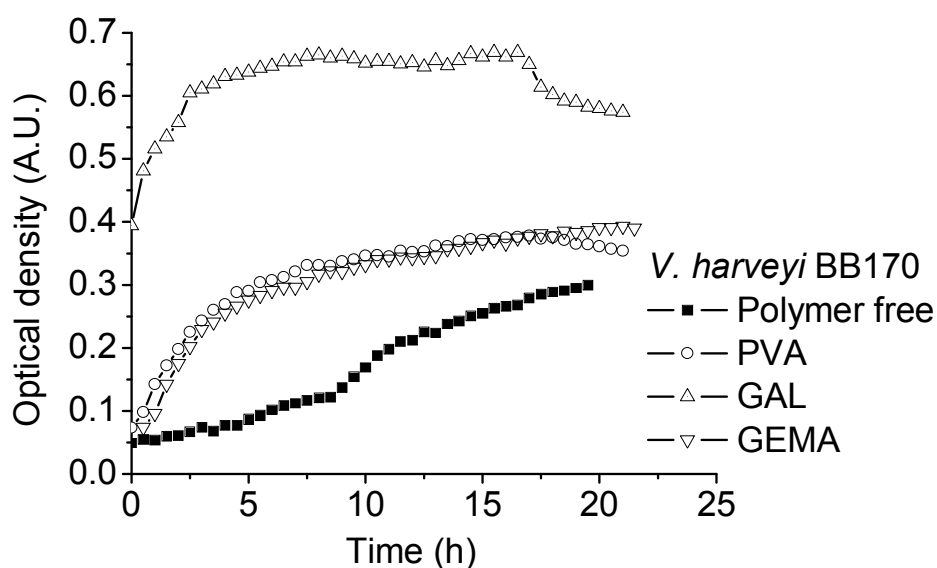


**Figure 4-15.** Growth curves for *V. harveyi* BB170. Increased O.D. is observed in the case of GAL as the latter exists as micellar dispersion.

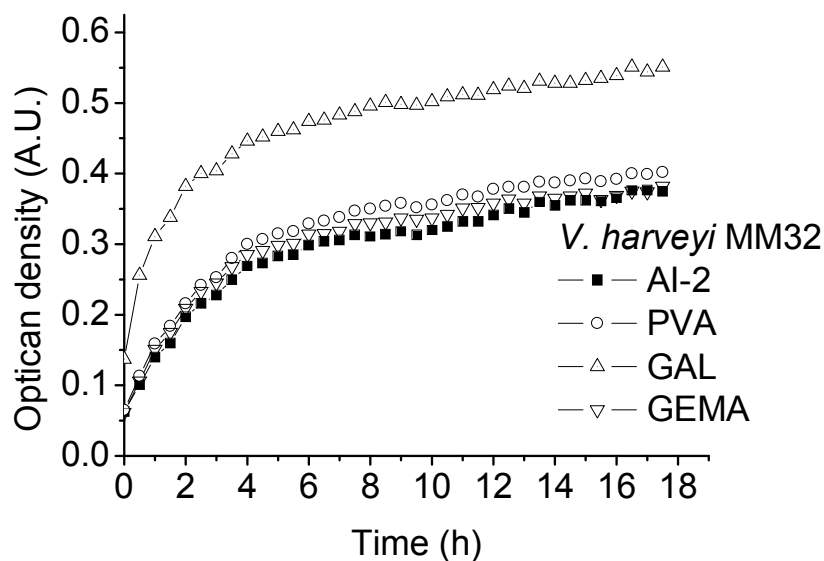


**Figure 4-16.** Growth curves for *V. harveyi* MM32. Increased O.D. is observed in the case of GAL as the latter exists as micellar dispersion.

Taken together the results suggest that, at least from a phenomenological perspective, there is indeed an effect of the polymers on the quorum sensing network and ultimately on their gene expression, though it is not unambiguous yet whether the effect can be solely attributed to the scavenging of AI-2 by the polymers. We do not know exactly whether there is indeed an effect of the polymers to the cells directly or whether there is an artefact on the instruments reading due to the polymers presence in the growth media.

Several alternative scenarios can be envisaged: i) active scavenging of the AI-2 occurs but the boronate-diol complex equilibrium ( $K_a=9.2$ ) prevents complete suppression of the QS signal as there will always be some non-polymer-bound AI-2 in solution under assay conditions (pH 7.4); ii). local accumulation of polymer occurs to bacteria in a heterogeneous fashion, but does not affect the whole population and hence residual luminescence arises; iii) association of bacterial cell-surface proteins takes place with the polymers preventing free diffusion of AI-2 across the bacterial membrane.

It should be noted that PVA is widely used as a surfactant and prior work has established cell binding by glycopolymers [31-33]. All the three factors are likely to be contributors to the overall effect to varying extents, but the fact that AI-2 binds to all the polymers under physiologically-relevant conditions is strongly supportive of a 'quorum-quench' mechanism.

### 4.3. Conclusions

In summary, we report for the first time the effects of poly(hydroxyl) materials and glycopolymers on QS signalling, and the delay and suppression of bioluminescence in *Vibrio harveyi*. The polymers showed activity to some extent as modulators that can scavenge an important autoinducer found in many bacterial species. These results are promising as the materials used were simple in structure (one polymer was commercially available). Therefore we envisage that based on our findings we will be able to apply the appropriate principles in the materials design to improve the activity of our polymeric scavengers based on the current findings.

On the other hand, we failed to demonstrate the proof of principle with thermoresponsive polymers as it was not possible to target the AI-2 under bioassay conditions. However, we strongly believe that better designed polymers that are capable to respond at the exact conditions needed is certainly possible, and in combination with our findings based on the polyhydroxyl compounds, our vision of smart quorum quenchers will become reality. For example, wise selection of monomers in order to achieve higher LCST response by retaining the sharpness of the onset and incorporation of a diol or boronate containing monomer would be a potential effective AI-2 scavenger (figure 4-17) .

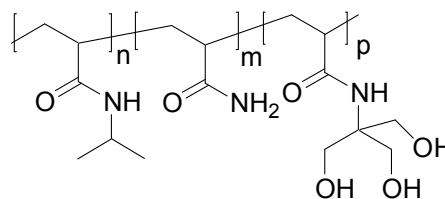


**Figure 4-17.** A model triblock copolymer that could act as a smart AI-2 scavenger. The NIPAM moiety acts as the thermoresponsive unit whereas the acrylamide shifts the LCST at suitable levels. The tris-hydroxy moiety acts as the scavenger.

Finally, despite the apparent effect of the polymers on the bioluminescence expression there need to be more studies to fully understand the mechanism by these polymers operate on the QS networks and whether polymers can be devised that actively respond to the bacterial communication pathways. Do the polymers affect gene expression or is their effect limited to secondary interactions perhaps not directly related to the gene factory itself? Whatever the answer is, we strongly believe that our approach could potentially lead to a novel means of intervening in bacterial infection processes in a mild and more 'natural' way than conventional antibiotics.

#### 4.4. References

1. Waters, C.M. and B.L. Bassler, *Quorum sensing: Cell-to-cell communication in bacteria*. Annual Review of Cell and Developmental Biology, 2005. **21**: p. 319-346.
2. Gonzalez, J.E. and N.D. Keshavan, *Messing with bacterial quorum sensing*. Microbiology and Molecular Biology Reviews, 2006. **70**(4): p. 859-875.
3. Hammer, B.K. and B.L. Bassler, *Quorum sensing controls biofilm formation in Vibrio cholerae*. Molecular Microbiology, 2003. **50**(1): p. 101-114.
4. Irie, Y. and M.R. Parsek, *Quorum sensing and microbial biofilms*. Bacterial Biofilms, 2008. **322**: p. 67-84.
5. Defoirdt, T., N. Boon, P. Sorgeloos, W. Verstraete, and P. Bossier,

- Quorum sensing and quorum quenching in Vibrio harveyi: lessons learned from in vivo work.* ISME J, 2007. **2**(1): p. 19-26.
6. Camilli, A. and B.L. Bassler, *Bacterial small-molecule signaling pathways.* Science, 2006. **311**(5764): p. 1113-1116.
  7. Hughes, D.T. and V. Sperandio, *Inter-kingdom signalling: communication between bacteria and their hosts.* Nature Reviews Microbiology, 2008. **6**: p. 111-120.
  8. Nealson, K.H. and J.W. Hastings, *Bacterial Bioluminescence - Its Control and Ecological Significance.* Microbiological Reviews, 1979. **43**(4): p. 496-518.
  9. Nealson, K.H., T. Platt, and J.W. Hastings, *Cellular Control of Synthesis and Activity of Bacterial Luminescent System.* Journal of Bacteriology, 1970. **104**(1): p. 313-&.
  10. Jayaraman, A. and T.K. Wood, *Bacterial quorum sensing: Signals, circuits, and implications for biofilms and disease.* Annual Review of Biomedical Engineering, 2008. **10**: p. 145-167.
  11. Whitehead, N.A., A.M.L. Barnard, H. Slater, N.J.L. Simpson, and G.P.C. Salmond, *Quorum-sensing in gram-negative bacteria.* Fems Microbiology Reviews, 2001. **25**(4): p. 365-404.
  12. Xavier, K.B. and B.L. Bassler, *Interference with AI-2-mediated bacterial cell-cell communication.* Nature, 2005. **437**(7059): p. 750-753.
  13. Miller, S.T., K.B. Xavier, S.R. Campagna, M.E. Taga, M.F. Semmelhack, B.L. Bassler, and F.M. Hughson, *Salmonella typhimurium Recognizes a Chemically Distinct Form of the Bacterial Quorum-Sensing Signal AI-2.* Molecular Cell, 2004. **15**(5): p. 677-687.
  14. Chen, X., S. Schauder, N. Potier, A. Van Dorsselaer, I. Pelczer, B.L. Bassler, and F.M. Hughson, *Structural identification of a bacterial quorum-sensing signal containing boron.* Nature, 2002. **415**(6871): p. 545-549.
  15. Liu, D., J. Momb, P.W. Thomas, A. Moulin, G.A. Petsko, W. Fast, and D. Ringe, *Mechanism of the quorum-quenching lactonase (AiiA)*

- from *Bacillus thuringiensis*. 1. Product-bound structures. *Biochemistry*, 2008. **47**(29): p. 7706-7714.
16. Geske, G.D., J.C. O'Neill, and H.E. Blackwell, *Expanding dialogues: from natural autoinducers to non-natural analogues that modulate quorum sensing in Gram-negative bacteria*. *Chemical Society Reviews*, 2008. **37**(7): p. 1432-1447.
  17. Estephane, J., J. Dauvergne, L. Soulere, S. Reverchon, Y. Queneau, and A. Doutheau, *N-acyl-3-amino-5H-furanone derivatives as new inhibitors of LuxR-dependent quorum sensing: Synthesis, biological evaluation and binding mode study*. *Bioorganic & Medicinal Chemistry Letters*, 2008. **18**(15): p. 4321-4324.
  18. Kim, C., J. Kim, H.Y. Park, H.J. Park, J.H. Lee, C.K. Kim, and J. Yoon, *Furanone derivatives as quorum-sensing antagonists of Pseudomonas aeruginosa*. *Applied Microbiology and Biotechnology*, 2008. **80**(1): p. 37-47.
  19. Kato, N., T. Morohoshi, T. Nozawa, H. Matsumoto, and T. Ikeda, *Control of gram-negative bacterial quorum sensing with cyclodextrin immobilized cellulose ether gel*. *Journal of Inclusion Phenomena and Macrocyclic Chemistry*, 2006. **56**(1-2): p. 55-59.
  20. Ni, N.T., H.T. Chou, J.F. Wang, M.Y. Li, C.D. Lu, P.C. Tai, and B.H. Wang, *Identification of boronic acids as antagonists of bacterial quorum sensing in Vibrio harveyi*. *Biochemical and Biophysical Research Communications*, 2008. **369**(2): p. 590-594.
  21. Shiomori, K., A.E. Ivanov, I.Y. Galaev, Y. Kawano, and B. Mattiasson, *Thermoresponsive properties of sugar sensitive copolymer of N-isopropylacrylamide and 3-(acrylamido)phenylboronic acid*. *Macromolecular Chemistry and Physics*, 2004. **205**(1): p. 27-34.
  22. Shiino, D., Y. Murata, A. Kubo, Y.J. Kim, K. Kataoka, Y. Koyama, A. Kikuchi, M. Yokoyama, Y. Sakurai, and T. Okano, *Amine containing phenylboronic acid gel for glucose-responsive insulin release under physiological pH*. *Journal of Controlled Release*, 1995. **37**(3): p. 269-

- 276.
23. Kataoka, K., H. Miyazaki, T. Okano, and Y. Sakurai, *Sensitive Glucose-Induced Change of the Lower Critical Solution Temperature of Poly[N,N-Dimethylacrylamide-Co-3-(Acrylamido)Phenyl-Boronic Acid] in Physiological Saline*. *Macromolecules*, 1994. **27**(4): p. 1061-1062.
  24. Yan, J., G. Springsteen, S. Deeter, and B.H. Wang, *The relationship among  $pK(a)$ ,  $pH$ , and binding constants in the interactions between boronic acids and diols - it is not as simple as it appears*. *Tetrahedron*, 2004. **60**(49): p. 11205-11209.
  25. Springsteen, G. and B.H. Wang, *A detailed examination of boronic acid-diol complexation*. *Tetrahedron*, 2002. **58**(26): p. 5291-5300.
  26. Springsteen, G. and B.H. Wang, *Alizarin Red S. as a general optical reporter for studying the binding of boronic acids with carbohydrates*. *Chemical Communications*, 2001(17): p. 1608-1609.
  27. Ge, H., Y.W. Ding, C.C. Ma, and G.Z. Zhang, *Temperature-controlled release of diols from N-isopropylacrylamide-co-acrylamidophenylboronic acid microgels*. *Journal of Physical Chemistry B*, 2006. **110**(41): p. 20635-20639.
  28. Arimori, S., C.J. Ward, and T.D. James, *The first fluorescent sensor for boronic and boric acids with sensitivity at sub-micromolar concentrations - a cautionary tale*. *Chemical Communications*, 2001(19): p. 2018-2019.
  29. Hashimoto, S. and K. Furukawa, *Immobilization of Activated-Sludge by Pva Boric-Acid Method*. *Biotechnology and Bioengineering*, 1987. **30**(1): p. 52-59.
  30. Peppas, N.A. and N.K. Mongia, *Ultrapure poly(vinyl alcohol) hydrogels with mucoadhesive drug delivery characteristics*. *European Journal of Pharmaceutics and Biopharmaceutics*, 1997. **43**(1): p. 51-58.
  31. Pasparakis, G., A. Cockayne, and C. Alexander, *Control of bacterial aggregation by thermoresponsive glycopolymers*. *Journal of the*

- American Chemical Society, 2007. **129**(36): p. 11014-11015.
32. Pasparakis, G. and C. Alexander, *Synthetic polymers for capture and detection of microorganisms*. *Analyst*, 2007. **132**: p. 1075-1082.
33. Damas, C., T. Leprince, T.H.V. Ngo, and R. Coudert, *Behavior study of polyvinyl alcohol aqueous solution in presence of short chain micelle-forming polyols*. *Colloid and Polymer Science*, 2008. **286**(8-9): p. 999-1007.

## Chapter 5

### Concluding Remarks – Future Prospects

#### 5.1.

In 2006, we and others reported on a modern version of the well-known Turing Test with the aim to clarify the principles needed to approach the concept of artificial cellularity [1]. In the 50s Alan Turing proposed an intellectual test in order to answer the question “can machines think?” [2]. His test involved a human interrogator that could ask questions to another human (intelligent) being and to the computer to be tested (figure 5-1). The two subjects -human and machine- are in individual rooms separate from the interrogator. The aim of the latter is by asking questions to any of the subject aiming to draw a conclusion on which room is each subject. If the interrogator fails, the test for the machine is successful as the former is practically “fooled” by a non-intelligent object. Thus we can claim that the machine is intelligent *de facto*. This very test circumvents the dilemmas regarding the definitions of terms such as “intelligence” and “consciousness” as it directly compares the subject with a standard model that we already regard as intelligent, that is a human being.

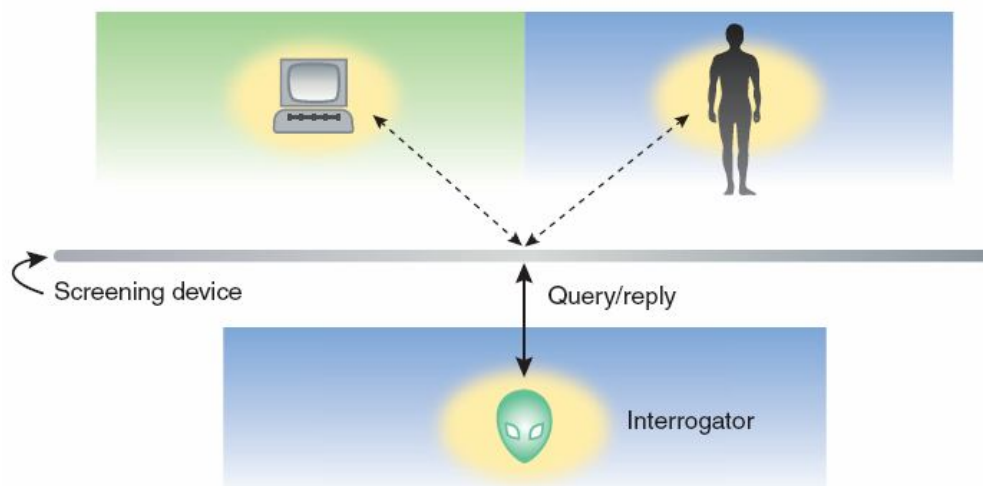


**Figure 5-1.** The Turing test concept. The interrogator attempts to distinguish the man from the machine by querying the subjects [1, 2].

The analogous test reported, is a biological version of the Turing test that seeks to answer the question “how alive an artificial entity can be” (figure 5-2). Our perception of what is alive and what is not, and of the list of properties that a system must have in order to be called “alive” are controversial as there is still no scientific consensus on the definition of life itself in the biological context and the criteria indeed to claim that we could implement a living system one day.

The latter is partly the subject of synthetic biology, a relatively modern and highly multidisciplinary field of research that seeks answers to how living systems work [3]. There are considerable efforts towards understanding the principles that render a biological cell self-sustainable and self-reproducible [4]. For example, self-reproducible synthetic vesicles have been demonstrated by several groups [5, 6]. Also, the construction of “protocells” that mimic very basic functions of natural cells have been reported with the ultimate aim of understanding the conditions that living systems emerge and develop [7, 8].

Our approach slightly differs in the sense that we mostly seek for a generic platform to test “living” candidates that emerge from synthetic protocols and therefore development of such a modified chemical Turing test would circumvent the lack of definitions in the area of artificial cellularity simply by placing nature as the ultimate judge.

In parallel to the original Turing test, we propose the use of a reporter cell species with the role of the interrogator (figure 5-2, table 5-I). The natural cells are able to communicate and sense each other by the exchange of biomolecular messages that are mediated by small molecules or through adhesion phenomena by ligand-receptor interactions. For example, as discussed in chapter four, in the bacterial kingdom, autoinducers and

quorum sensing seems to be a common means of communication even between different species.

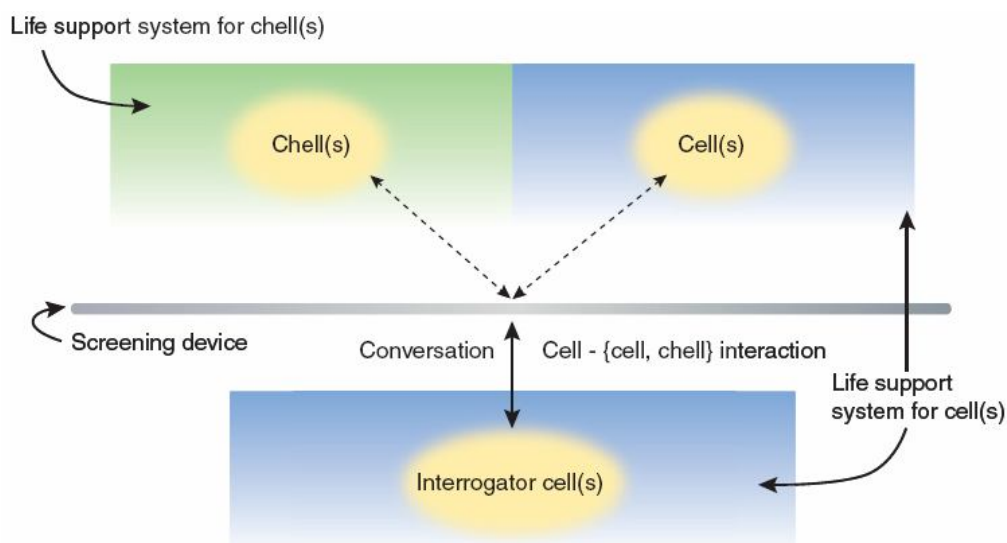


**Figure 5-2.** The proposed modification of the Turing Test with chemical cells or “CHELLS”. The interrogator cells attempt to distinguish other cells of their own kind and artificial chemical cells through chemical exchange of small molecules that comprise the cellular language [1].

Therefore, if one is able to understand this very language and manage to train our artificial systems to talk with the natural cells using their language in a way that the latter cannot distinguish whether their company is someone of their own, then one can consider the “CHELL” test a success.

It is anticipated that, by increasing the complexity of these systems to a level that they can “talk” to their natural counterparts as the latter evolve (that is,

**Table 5-I**  
Comparison of the Turing test with its biological counterpart.

	Turing test for intelligence	Turing test for life
Imitated emergent property	Thought	Cellular functions (e.g., metabolism, evolution and containment)
Embodiment of property	Computational digital machine	Chemical system (e.g., artificial cell or ‘chell’)
Probing mechanism	Questions/answers mediated by natural language	Questions/answers mediated by (natural) physico-chemical language (e.g., interconversion of chemical potentials, mechanical transduction, signaling)

long periods/cycles of “communication”) then they must exhibit some properties of natural cells that only living systems seem to possess and these are self-sustainability, evolution capacity, and information transport (i.e. metabolism).

This Thesis was aimed at taking the first practical steps towards a conceptually simple, if difficult to realize, question: can non-biological materials and natural cells ‘talk’ to each other? Communication is fundamental to how living systems adapt to environments, while materials that can respond and adapt to their environments have applications in areas as diverse as medicine, engineering, art and design. One would envisage that responsive and adaptive material ‘populations’ will form a new class of artificial/biological hybrids that are fundamentally different from existing synthetic systems.

In order to test the central hypothesis that cross-talk is possible between non-biological materials and natural cells, the thesis aimed at three main areas:

1. *Generation of artificial materials that interact with natural systems;*
2. *Intervention in, and regulation of, natural communication pathways;*
3. *Development and evolution of synthetic-natural feedback loops.*

These were to be addressed by developing novel response materials sensitive to biological stimuli, and applying these materials in ‘proto-cells’ to control microbiological population (‘Quorum’) sensing, gene regulation and feedback. One can envisage as a longer-term goal that completion of all these objectives, albeit an ambitious idea, might lead not only to new forms of materials with practical application as sensors, diagnostics and therapeutic devices, but which may, as a longer-term objective, exhibit properties that extend beyond mimicry of biological interactions into the realms of artificial cellularity. In the following paragraphs we will evaluate the progress that

has been made so far and consider future perspectives that could potentially contribute to the final implementation of this concept.

We therefore constructed a wish-list as a challenge-benchmark of the properties that an ideal artificial entity should have in order to successfully pass our imitation game:

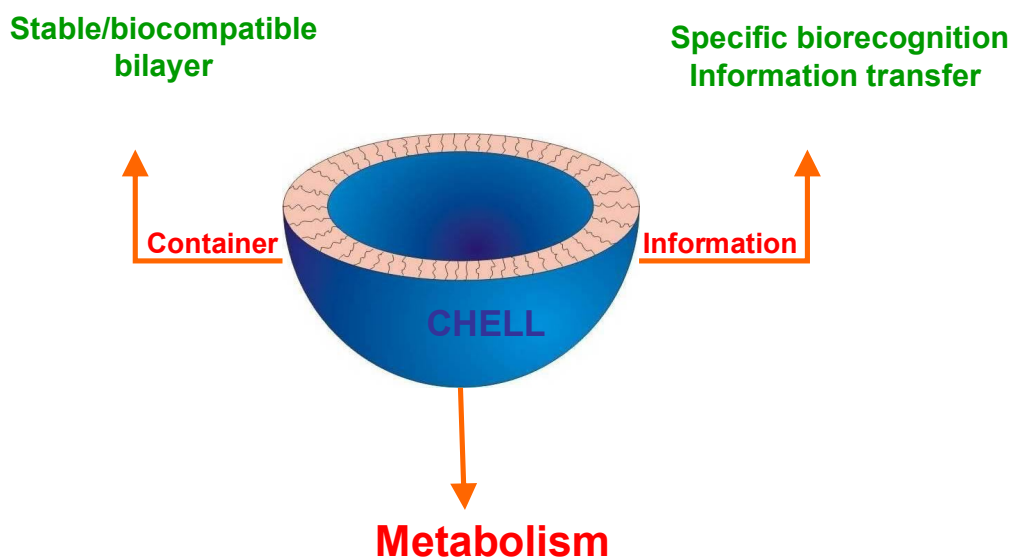


**Figure 5-3.** The basic requirements that a primitive CHELL must fulfill to pass successfully the imitation game.

As can be seen from figure 5-3 the central component of this artificial entity is its container (presented here as a bilayer similar to natural cell membranes). We call this ideal system, a CHELL from the term chemical cell first because it resembles the natural cells (they are indeed closed containers) and second they can regulate chemical components not necessarily of biological origins. The membrane of the CHELL must be stable enough, ideally biocompatible so that there is no cytotoxicity to allow in vivo regulation and possess a variety of ligands that can mediate interaction with natural cells (i.e. membrane proteins, carbohydrates etc.). Also, the membrane should be permeable with high selectivity and dynamic in its transport properties according to both external and internal signaling events. Finally, a metabolic

system is required so that the CHELLS are capable to generate information and manage energy input. Ideally, CHELLS must be self-reproducible with the ability of transporting information along different generations so that a pseudo-evolvable nature is developed. The wish-list is rather ambitious and in practice describes the functions of a natural cell, but we think that compartmentalization of the conceptualization of the CHELLs processes is required to achieve the ambitious goal set.

In figure 5-4 an ideal imitation game is schematically described. The bilayer membrane of the CHELLs consists of polymeric materials that respond to external stimuli such as pH or temperature. This in turn can alter the diffusion properties of the membrane and hence regulate the transport of molecular messages across the bilayer. At each stimulus trigger a cell-CHELL interaction is probed by formation of discrete vesicle-cell complexes similar to those presented in chapter 3. Upon formation of the complexes, the CHELLS are in close proximity with the natural cells to mediate molecular transport and initiate a “conversation”. The molecular signals from the CHELLS to the cells have a measurable impact on the latter that can be monitored by conventional biomolecular assays (i.e. gene expression profiles, protein/DNA production etc.). Conversely, the cells respond and express their own signals that are captured by the CHELLS. These signals should also have an impact to the pseudo-metabolism of the CHELLS and alter their cell-signaling production. Removal of the external stimulus completes the conversation loop by shutting off the molecular transport and reversing of the clustering formation. In the schematic shown this communication cycle is carried out by exploiting a model quorum sensing network of *E. Coli* as the molecular language. The convenience of QS in the language establishment derives from the fact that it is mediated by small molecules, the autoinducers, which can be coupled with the pseudo-metabolic system will be discussed later.

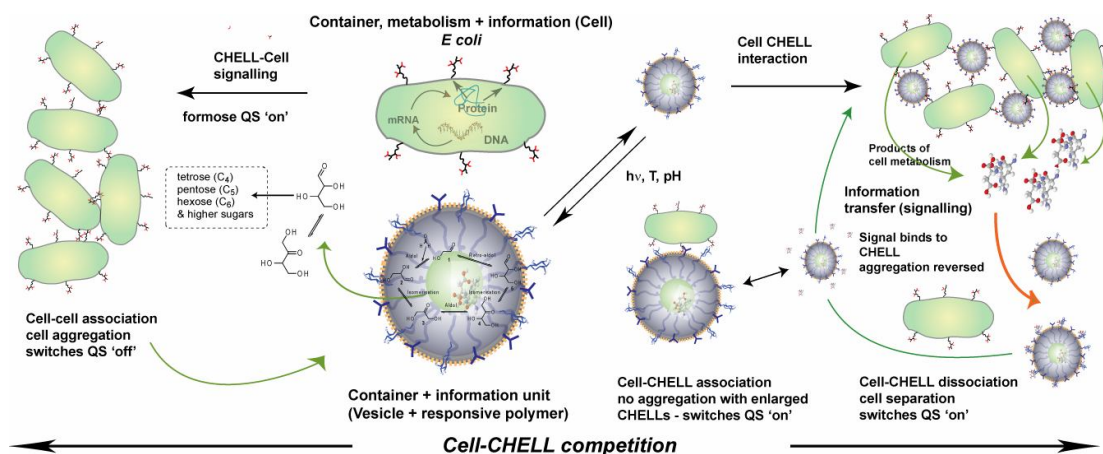


**Figure 5-4.** Cell-CHELL interactions. Schematic representation of an ideal conversation loop between bacterial cells with their artificial counterparts.

So far we have been able to access the adhesion phenomena through simple carbohydrate molecules that are recognized by sugar recognition sites expressed on bacterial surfaces (i.e. fimH motif). We have also been able to demonstrate the triggering and control of these events by introducing well-studied thermoresponsive polymers as described in chapter two. These smart glycopolymers are a primitive step to achieve this dynamic adhesion with high specificity via multivalency. The thermoresponsive property of the polymers is retained upon sugar incorporation as pendant units and we also achieve high specificity of recognition events when the polymers were tested with lectins (proteins known for their high specificity to carbohydrates).

We also extended this approach by introducing block-copolymers that assemble into vesicles and can also trigger bacteria-vesicles cluster formation via ligand-receptor interactions. The sugar-rich coronae of the vesicles ensure the high specificity of interaction similar to the glycocalyx found in mammalian cells. Also molecular transport was facilitated from the vesicles to the interior of bacterial cells as evidenced by the ethidium bromide transfer assay. It was demonstrated that only when specific ligand-receptor (recognition of the sugar moieties by the fimH motifs) events took place then molecular transport was facilitated.

Also, the vesicles were found to alter their size according to temperature stimuli as the core segments are made of PDEGMA units. This implies that the diffusion coefficient of the vesicular bilayer should also change upon thermal perturbation not only due to the size change but also due to the physicochemical change of PDEGMA. This effect has not yet been exploited in the current study but clearly poses implication for a stimulus triggering/enhancement of the transport events studied in this model. For example, different diffusion rates across the vesicular bilayer are expected at varying temperatures as the amphiphilic character of the polymeric shell is dramatically altered via the LCST. This could be a rather crude approach of selective transport across the membrane of the vesicles, which is accomplished in cellular membranes mainly through membrane bound proteins.

In chapter four we explored for the first time the possibility of quorum sensing suppression by introducing simple polymeric scavengers that could capture autoinducers. We studied the quorum sensing network of *Vibrio harveyi* as a model which is well characterized and can be easily monitored by bioluminescence assays. We have demonstrated that modulation of the QS network of *V. harveyi* can be achieved by simple poly-hydroxyl compounds that can capture the AI-2. Several boronic acid/boronate sequestering polymers were tested as polymeric scavengers for capture of these small molecules that mediate intercellular communication. Indeed, there seemed to be significant suppression of the quorum sensing in these bacteria and we believe that this control of quorum sensing by our primitive polymeric quorum quenchers will be applicable in the vesicle-bacteria interactions. Unfortunately the use of thermoresponsive polymers for externally triggered QS modulation as described in the aims of the PhD (chapter 1) was not conducted due to time constraints.

Ideally, we sought to couple the bacterial language, partly integrated by the AI-2 transport-diffusion among bacterial cells, with a pseudo-metabolism, the formose reaction. The formose reaction is a prebiotic reaction that produces carbohydrates from formaldehyde catalyzed by a divalent metal such as calcium hydroxide (figure 5-5). The beauty of the reaction stems from the fact that the reactants are intriguingly simple, but the products are of organic nature not possible to be found in an abiotic world and hence considered as pre-biotic reaction. Interestingly, addition of boric acid (another compound of great abundance especially in the oceans) in the reaction mixture will result in formation of the AI-2 among the reaction products (figure 5-5).

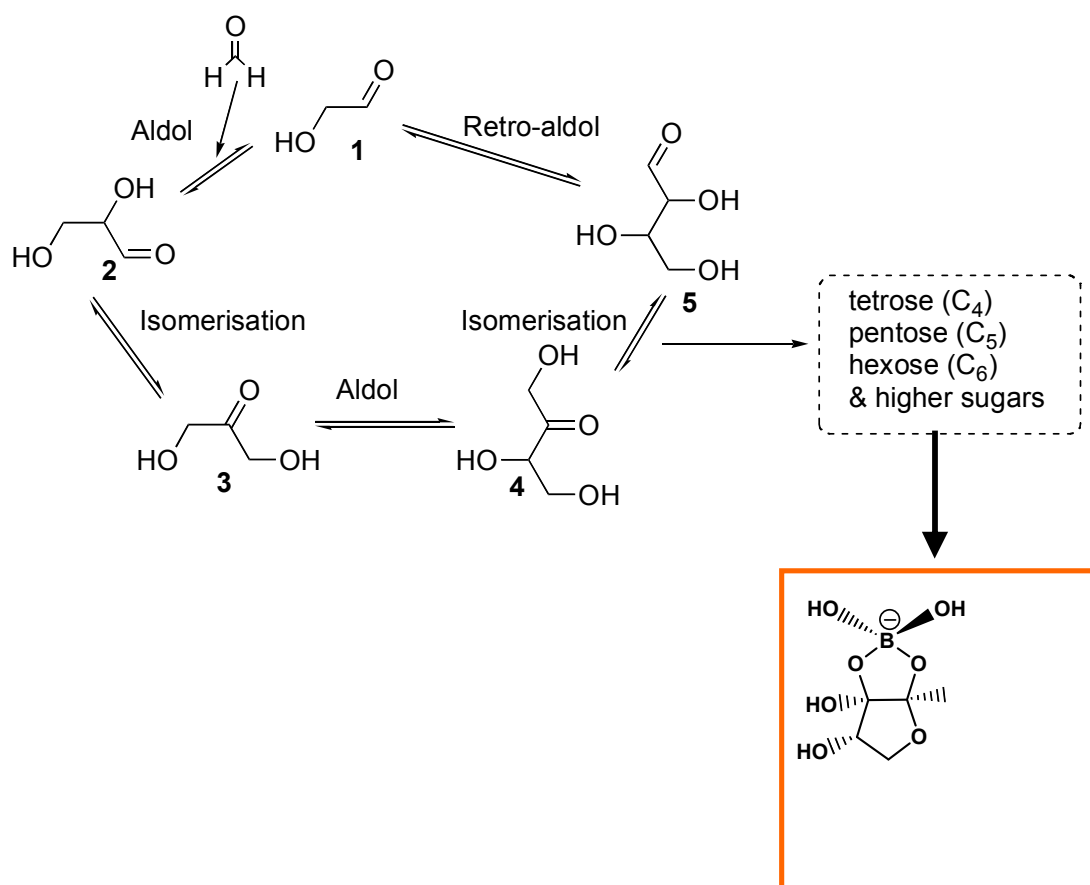


**Figure 5-5.** The formose reaction and its products. Formation of the AI-2 upon addition of borate in the reaction mixture.

Intriguingly, this evidence might support the perception that the formose reaction could have been a life-generating reaction since its products are

found to be active participants in the molecular language that bacteria commonly use. Also, the fact that the AI-2 has been found in more than one bacterial species quorum sensing network implies that a common reaction-ancestor could be the origin of all living organisms.

In future studies, we envision to incorporate the formose reaction inside the vesicles in order to act as a pseudo-metabolism. The reaction products can diffuse outside and enable communication events with bacterial species that can understand this language such as *V. harveyi*. Therefore, the bacteria will respond to the artificial signal of the CHELLs and switch on the gene expression triggered by the quorum sensing network. Consequently, the bacteria will regard the CHELLs as ones of their own. Conversely, production of bacterial AI-2 and diffusion of them inside the CHELLs should alter the equilibria established in the formose mixture. In essence, a dynamic combinatorial library is formed with the LuxP protein acting as the molecular template that will alter the chemical equilibria. Therefore, bidirectional information transport is established that impacts both bacterial metabolism and gene expression but also the pseudo-metabolic reactions taking place inside the CHELLS. Also, modulation of the quorum sensing could be mediated from the polymeric bilayer as the sugar rich coronae should scavenge the bacterial AI-2 as demonstrated in chapter four. Alternatively, incorporation of polyhydroxyl scavengers inside the vesicles could potentially regulate the diffusion/production rate of the formose products (again acting as a pseudo-dynamic combinatorial library template) as the latter are produced and therefore adjust the optimum rate of signaling molecules for cell-CHELL interactions.

Overall, we feel we have set up a basic platform giving us an idea of the mechanisms and the concepts required to understand the guiding principles of the artificial cellularity. We have constructed materials that can show a significant degree of interaction with “living matter” and that can mimic to

some extent the biological functions of natural cells. There remains a need to further develop these materials so that they embed increased sensitivity towards biological signals (for example by further exploitation of the sugar recognition subtlety) and resemble even more the structure and function of natural entities so that the communication established between the two parts is even more natural and truly bidirectional. Also, introduction of the principle of self-reproduction must take place regarding these synthetic vesicles if we want to start thinking of pseudo-evolution procedures. Ideally, this should be coupled with the pseudo-metabolic reactions in order to achieve some degree of self-sustainability.

For the immediate future, competition tests in the quorum sensing context can be conducted by simple experiments utilizing the vesicles synthesized in chapter 3. Also, incorporation of formose products or simpler autoinducer analogues and their release from the vesicles in presence of *Vibrio* species might elucidate whether we can set up a first communication arena where the CHELLS are capable of altering the quorum sense response of the bacteria. This would be a very first step not only towards achieving a primitive, albeit successful imitation game, but also to regard these materials as novel microreactors that could potentially prevent disease solely by dynamic intervention in biological processes instead of lethal action as common antibacterials exhibit.

## 5.2. References

1. Cronin, L., N. Krasnogor, B.G. Davis, C. Alexander, N. Robertson, J.H.G. Steinke, S.L.M. Schroeder, A.N. Khlobystov, G. Cooper, P.M. Gardner, P. Siepmann, B.J. Whitaker, and D. Marsh, *The imitation game - a computational chemical approach to recognizing life*. *Nature Biotechnology*, 2006. **24**(10): p. 1203-1206.

2. Turing, A.M., *Computing machinery and intelligence*. *Mind*, 1950. **59**: p. 433-460.
3. Andrianantoandro, E., S. Basu, D.K. Karig, and R. Weiss, *Synthetic biology: new engineering rules for an emerging discipline*. *Molecular Systems Biology*, 2006. **2**.
4. Bailey, J.A., J.M. Boncella, M.S. DeClue, P.A. Monnard, A. Shreve, S. Rasmussen, and H.J. Ziock, *Self-replicating chemical systems as protocells*. *Astrobiology*, 2007. **7**(3): p. 498-498.
5. Luisi, P.L., P. Stano, S. Rasi, and F. Mavelli, *A possible route to prebiotic vesicle reproduction*. *Artificial Life*, 2004. **10**(3): p. 297-308.
6. Takakura, K., T. Toyota, and T. Sugawara, *A novel system of self-reproducing giant vesicles*. *Journal of the American Chemical Society*, 2003. **125**(27): p. 8134-8140.
7. Mansy, S.S., J.P. Schrum, M. Krishnamurthy, S. Tobe, D.A. Treco, and J.W. Szostak, *Template-directed synthesis of a genetic polymer in a model protocell*. *Nature*, 2008. **454**(7200): p. 122-U10.
8. Rasmussen, S., L.H. Chen, D. Deamer, D.C. Krakauer, N.H. Packard, P.F. Stadler, and M.A. Bedau, *Transitions from nonliving to living matter*. *Science*, 2004. **303**(5660): p. 963-965.

## *List of Publications*

### **In Refereed journals**

J.P. Magnusson, A. Khan , G. Pasparakis, A. O. Saeed, W. Wang, and C. Alexander, *Ion-responsive “isothermal” block copolymers prepared in water*, *Journal of the American Chemical Society*, **130**, 10852 – 10853 (2008).

G. Pasparakis, and C. Alexander, *Sweet-talking block copolymer vesicles*, *Angewandte Chemie International Edition*, **47**, 4847- 4850 (2008).

George Pasparakis and Cameron Alexander, *Synthetic polymers for capture and detection of microorganisms*, *The Analyst*, **132**, 1075 – 1082 (2007).

G. Pasparakis, A. Cockayne, and C. Alexander, *Control of bacterial aggregation by thermoresponsive glycopolymers*, *Journal of the American Chemical Society*, **129**, 11014 - 11015 (2007).

### **Presentations**

G. Pasparakis, “ ‘Smart’ glycopolymers control bacterial aggregation”, *7th International Symposium on Polymer Therapeutics: From Laboratory to Clinical Practice*, Valencia, Spain, 27 May, 2008.

G. Pasparakis, “Reversible control of bacterial aggregation by thermoresponsive glycopolymers”, *RSC/SCI Macro Group Young Researchers’ Annual Meeting*, University of Nottingham , UK, 12 April, 2007.